

FINAL REPORT
on
DEVELOPMENT OF STRAIN GAGES FOR
USE TO 1311 K (1900 F)

Prepared for
NATIONAL AERONAUTICS AND SPACE ADMINISTRATION

July 10, 1974

by

M. M. Lemcoe

Contract NAS 1-12099

Langley Research Center
Hampton, Virginia



BATTELLE
Columbus Laboratories
505 King Avenue
Columbus, Ohio 43201

(NASA-CR-132485) DEVELOPMENT OF STRAIN
GAGES FOR USE TO 1311 K (1900 F) Final
Report (Batelle Columbus Labs., Ohio.)
98 p HC \$4.00 CSCI 14B

N74-32898

G3/14 Unclas
48460

FINAL REPORT

on

DEVELOPMENT OF STRAIN GAGES FOR
USE TO 1311 K (1900 F)

Prepared for

NATIONAL AERONAUTICS AND SPACE ADMINISTRATION

July 10, 1974

by

M. M. Lemcoe

Contract NAS1-12099

Langley Research Center
Hampton, Virginia

BATTELLE
Columbus Laboratories
505 King Avenue
Columbus, Ohio 43201

ABSTRACT

A high temperature electric resistance strain gage system was developed and evaluated to 1366 K (2000 F) for periods of at least one hour. Wire fabricated from a special high temperature strain gage alloy (BCL-3), developed at the Battelle-Columbus Laboratories, was used to fabricate the gages. Various joining techniques (NASA butt welding, pulse arc, plasma needle arc, and DC parallel gap welding) were investigated for joining gage filaments to each other, gage filaments to lead-tab ribbons, and lead-tab ribbons to lead wires. The effectiveness of a "clad-wire concept" as a means of minimizing apparent strain of BCL-3 strain gages was investigated by sputtering platinum coatings of varying thicknesses on wire samples and establishing the optimum coating thickness--in terms of minimum resistivity changes with temperature. Finally, the moisture-proofing effectiveness of barrier coatings subjected to elevated temperatures was studied, and one commercial barrier coating (BLH Barrier H Waterproofing) was evaluated.

It was concluded, on the basis of the results from the program, that (a) the BCL-3 strain gage system should perform satisfactorily to at least 1311 K (1900 F) for at least one hour at maximum temperature, (b) of those joining processes investigated for BCL-3 gages, the NASA butt welding, DC parallel gap welding, and resistance spot-welding processes are considered the best processes for making gage filament to gage filament, gage filament to lead tab, and lead tab to lead wire joints, respectively, (c) the clad wire concept offers a viable means of reducing apparent strain, while at the same time providing protection against oxidation, and (d) because of the severity of the stress and temperature requirements, only limited moisture protection can be expected from commercial strain gage barrier coatings, after their exposure to temperatures exceeding 589 K (600 F).

TABLE OF CONTENTS

	<u>Page</u>
SUMMARY.	1
INTRODUCTION	2
EXPERIMENTAL DEVELOPMENT, EVALUATION, AND RESULTS.	3
1. Gage Fabrication and Specimen Preparation	3
1.1 General	3
1.2 Materials	3
1.2.1 Gages.	3
1.2.2 Specimens.	4
1.2.3 Lead-Wire Systems.	4
1.2.4 Precoatings.	4
1.2.5 Barrier Coatings	5
1.3 Gage Fabrication.	5
1.3.1 Gage Winding Fixture	5
1.3.2 Gage Geometry and Fabrication Procedure.	5
1.4 Specimen Preparation	5
1.4.1 Specimen Geometry and Gage Locations	5
1.4.2 Development and Application of Precoat System	6
1.4.2.1 General.	6
1.4.2.2 Nickel Aluminide Precoat System	6
1.4.2.3 Graded Precoat Systems	7
1.4.3 Gage Attachment Procedures	7
1.4.4 Lead Wire Attachment Procedures.	8
1.5 Preparation of Joint Evaluation Specimens	8
1.5.1 General.	8
1.5.2 NASA Butt Weld Joints.	8
1.5.3 Pulse Arc Weld Joints.	9
1.5.4 Plasma Needle Arc Weld Joints.	9
1.5.5 Laser Weld Joints.	10
1.5.6 D. C. Parallel Gap Weld Joints	10
1.6 Preparation of Barrier Coating Specimens.	12

TABLE OF CONTENTS (Continued)

	<u>Page</u>
2. Description of Gage Evaluation Facilities	12
2.1 High Temperature Gage Evaluation Facilities	12
2.2 Joint Evaluation Equipment.	14
2.3 Barrier Coating Evaluation Equipment.	14
2.4 Dynamic Evaluation Equipment.	15
2.4.1 Thermal Shock.	15
2.4.2 Mechanical Shock	16
3. Gage Evaluation	16
3.1 Approach	16
3.2 Static Evaluation Procedure	17
3.3 Dynamic Evaluation Procedure.	18
3.3.1 Thermal Shock.	18
3.3.2 Mechanical Shock	18
3.4 Test Matrix	19
4. Joint Evaluation.	19
4.1 Approach.	19
4.2 Evaluation Procedures	20
4.2.1 Mechanical Strength.	20
4.2.2 Resistivity Characteristics.	20
5. Barrier Coating Evaluation.	20
5.1 Approach.	20
5.2 Evaluation Procedures	21
6. Clad-Wire Concept Evaluation.	22
6.1 Approach.	22
7. Results	23
7.1 Static Gage Evaluations	23
7.1.1 General.	23
7.1.2 Gage Factor and Linearity.	23
7.1.3 Apparent Strain.	25
7.1.4 Drift Characteristics.	27
7.1.5 Zero-Shift	30
7.1.6 Resistance to Ground	33

TABLE OF CONTENTS (Continued)

	<u>Page</u>
7.1.7 Thermal and Mechanical Shock	34
7.1.8 Performance History.	34
7.2 Joint Evaluations	36
7.3 Barrier Coating Evaluation.	39
7.4 Coated-Wire Evaluation.	41
CONCLUSIONS.	42
ACKNOWLEDGMENTS.	44
TABLES	45
FIGURES.	58
APPENDIX A - RESISTANCE TO GROUND MEASUREMENTS	86
REFERENCES	88

LIST OF TABLES

	<u>Page</u>
TABLE 1. HAYNES 25 SPECIMEN MATERIAL PROPERTIES	45
TABLE 2. TEST MATRIX.	46
TABLE 3. BARRIER COATING EVALUATION HISTORY	47
TABLE 4. SPECIMEN H-21R (AILTECH) GAGE FACTOR CHARACTERISTICS (ROOM TEMPERATURE)	48
TABLE 5. GAGE FACTOR SUMMARY.	49
TABLE 6. ZERO-SHIFTS.	50
TABLE 7. PERFORMANCE HISTORY.	52
TABLE 8. SUMMARY OF NASA BUTT-WELD, PULSE ARC, AND LASER JOINTS, MECHANICAL (TENSILE) STRENGTH EVALUATIONS.	53
TABLE 9. SUMMARY OF DC PARALLEL GAP JOINT MECHANICAL (TENSILE) STRENGTH EVALUATIONS	54
TABLE 10. NASA BUTT-WELD RESISTIVITY MEASUREMENTS (BCL-3 TO BCL-5 WIRE).	55
TABLE 11. NASA BUTT-WELD RESISTIVITY MEASUREMENTS (BCL-3 TO ALLOY 875 RIBBON).	56
TABLE 12. DC PARALLEL GAP WELD JOINTS, RESISTIVITY CHARACTERISTICS	57

LIST OF FIGURES

	<u>Page</u>
FIGURE 1. GAGE GEOMETRY.	58
FIGURE 2. STATIC CALIBRATION SPECIMEN GEOMETRY AND GAGE LOCATIONS. .	59
FIGURE 3. JOINT GEOMETRIES	60
FIGURE 4. OVERALL VIEW OF GAGE EVALUATION FACILITY	61
FIGURE 5. CLOSE-UP OF SPECIMEN IN EVALUATION FACILITY.	62
FIGURE 6. SPECIMEN H-21R (AILTECH), GAGE FACTOR, RT, 589 K (600 F), 922 K (1200 F)	63
FIGURE 7. SPECIMEN H-28, GAGE FACTOR, RT, 755 K (900 F), 1200 K (1700 F), 1255 K (1800 F).	64
FIGURE 8. SPECIMEN H-29, GAGE FACTOR, RT, 811 K (1000 F), 1311 K (1900 F), 1366 K (2000 F).	65
FIGURE 9. SPECIMEN H-32, GAGE FACTOR, RT, 811 K (1000 F), 1311 K (1900 F)	66
FIGURE 10. SPECIMEN H-21R (AILTECH GAGES) APPARENT STRAIN TO 922 K (1200 F)	67
FIGURE 11. SPECIMEN H-21R (AILTECH GAGES) APPARENT STRAIN TO 922 K (1200 F), 3 CYCLES	68
FIGURE 12. SPECIMEN H-26R2, APPARENT STRAIN TO 1366 K (2000 F). . . .	69
FIGURE 13. SPECIMEN H-28, APPARENT STRAIN TO 1200 K (1700 F).	70
FIGURE 14. SPECIMEN H-28, APPARENT STRAIN TO 1200 K (1700 F), 3 CYCLES	71
FIGURE 15. SPECIMEN H-28, APPARENT STRAIN TO 1311 K (1900 F), 3 CYCLES	72
FIGURE 16. SPECIMEN H-29, APPARENT STRAIN TO 1311 K (1900 F),	73
FIGURE 17. SPECIMEN H-29, APPARENT STRAIN TO 1311 K (1900 F), 2 CYCLES	74
FIGURE 18. SPECIMEN H-32, APPARENT STRAIN TO 1311 K (1900 F), 4 CYCLES	75
FIGURE 19. SPECIMEN H-32, APPARENT STRAIN TO 1366 K (2000 F), 3 CYCLES	76
FIGURE 20. SPECIMEN H-21R (AILTECH GAGES), DRIFT AT 922 K (1200 F). .	77
FIGURE 21. SPECIMEN H-25R2 (AILTECH GAGES), DRIFT AT 866 K (1100 F), 922 K (1200 F), 978 K (1300 F)	78

LIST OF FIGURES (Continued)

	<u>Page</u>
FIGURE 22. SPECIMEN H-28, DRIFT AT 1200 K (1700 F) AND 1297 K (1875 F)	79
FIGURE 23. SPECIMEN H-29, DRIFT AT 1311 K (1900 F)	80
FIGURE 24. SPECIMEN H-32, DRIFT AT 1311 K (1900 F)	81
FIGURE 25. SPECIMEN H-32, STRAIN-DEFLECTION LOOP UNDER REVERSED LOADING, ROOM TEMPERATURE.	82
FIGURE 26. SPECIMEN H-32, STRAIN-DEFLECTION LOOP UNDER REVERSED LOADING, 1311 K (1900 F)	83
FIGURE 27. HOPKINSON BAR, (GF) x MEASURED STRAIN VERSUS TRUE STRAIN, ROOM TEMPERATURE.	84
FIGURE 28. UNIT RESISTIVITY CHANGES VERSUS TEMPERATURE, COATED AND UNCOATED BCL-3 WIRE	85

DEVELOPMENT OF STRAIN GAGES FOR
USE TO 1311 K (1900 F)

By M. M. Lemcoe
Battelle-Columbus Laboratories

SUMMARY

Under prior contract NAS1-11277, a high temperature electric resistance strain gage system, utilizing BCL-3 strain gage alloy (Fe-25Cr-7.5Al), was developed at the Battelle-Columbus Laboratories. Although it was not possible to meet the desired NASA target temperature requirement of 1478 K (2200 F), a strain gage system was developed with a 1089 K (1500 F) capability, and a useful life considerably in excess of the 1/2 hour minimum life requirement. Excessive variability in apparent strain from gage to gage and separation of the Rokide substrate from the base material at temperatures above 1089 K (1500 F) were the primary reasons for not achieving a higher useful operating temperature limit. (For a more detailed discussion on this point, refer to Reference 1.)

Careful assessment of possible causes for the two above-mentioned deficiencies, and consideration of the otherwise superior performance of the BCL-3 strain gage system, indicated that the system had potential for use at still higher temperatures--perhaps approaching the 1478 K (2200 F) NASA target temperature, if the two deficiencies could be eliminated.

It was therefore the primary objective of this program to develop ways and means of eliminating the difficulties. This required, among other things, the development of improved attachment and joining techniques, and use of improved lead wire systems.

To eliminate separation of the Rokide substrate from the base material, a special "graded" precoating system was developed. This involved the evaluation of several different precoating materials combinations. Improved joining techniques and lead wire systems were also developed to eliminate the large gage to gage variations in apparent strain that previously occurred at temperatures above 1089 K (1500 F). New strain gage systems, incorporating these modifications and improvements were then developed.

Since the principal temperature range of interest was that between the upper limits established in the previous program and the maximum 1478 K (2200 F) NASA target temperature, the main effort in this program was directed toward development and evaluation of the performance of gage systems between 1200 K (1700 F) to 1366 K (2000 F). Evaluation procedures were utilized to determine such pertinent gage characteristics as linearity and gage sensitivity (hereinafter referred to as "gage factor" in the interest of brevity), apparent strain versus temperature, no-load drift, zero-shift, gage to gage and cycle to cycle variations, and resistance to ground versus

temperature characteristics, under static and dynamic (mechanical and thermal shock) conditions. Performance was also evaluated in terms of failure modes such as erratic gage behavior, "open" gages, or substrate failure.

This report contains, in graphical or tabular form, the pertinent results and conclusions obtained from the above mentioned development and evaluation efforts, and references to findings from previous studies. It also includes the pertinent findings obtained from the evaluation of several joining techniques (NASA butt, pulse arc, plasma needle arc, laser, and D.C. parallel gap welding) and the findings obtained from evaluation of barrier coatings for moisture-proofing gages and from the evaluation of the clad-wire concept for achievement of temperature compensation.

In summary, the primary objectives of this program were attained and a BCL-3 strain gage system has been developed for use to at least 1311 K (1900 F). The exact extent beyond 1311 K (1900 F) that useful strain information can be obtained is not known at this time, since this was essentially the limiting temperature for the Haynes 25 calibration bars used to perform the evaluations. It should be noted, however, that a limited evaluation was performed at 1366 K (2000 F) with promising results. Also, the preliminary data obtained from the clad-wire gage concept evaluation, clearly demonstrated that the concept provides a viable means for temperature compensating BCL-3 gage systems. Finally, results from this program also indicate good potential for extending the useful upper temperature limit of the Ailtech SG 400 series gages to at least 922 K (1200 F). At 978 K (1300 F) a sharp increase in drift rate was observed (approximately $-175 \mu\epsilon/\text{hr}$). The reason for this sharp increase is not known, since post-mortem examination was not performed. However, it may be due to migration of the gold on the gold shanks along the sensing portion of the BCL-3 gage filament, thereby decreasing its resistance. Should this be the case, the problem might be readily solved by plating the shanks with a metal having a much higher melting point such as platinum instead of gold. This should then permit a fuller achievement of the potential of the BCL-3 alloy.

INTRODUCTION

To obtain experimental data on the magnitudes of stresses (or strains) during flight, and to provide a check on the reliability of existing analytical methods for predicting these stresses, strain gage systems with operating temperatures in excess of 1033 K (1400 F) are essential. Further, monitoring of strains during each flight provides data for assessing cyclic or cumulative effects or remaining service life of the vehicle. These systems must, of course, be capable of field installation in remote locations on the vehicle, capable of faithfully recording strains under both static and transient conditions (including shock and vibration), be relatively insensitive to moisture, electric or magnetic fields, and not prohibitive, costwise, for strain measurements involving gages at a number of locations, which is frequently the case on space or aircraft vehicles.

Although there are commercially available electric resistance strain gages for reliable use to about 755 K (900 F) there are none that would meet

the substantially higher temperature requirements. Under the previous Contract NASI-11277, BCL-3 strain gage systems were developed with a maximum useful operating temperature in the neighborhood of 1089 K (1500 F), and a useful operating life of at least 1/2 hour. Although this represented a substantial increase in operating temperature, it still did not sufficiently approach the desired NASA target temperature of 1478 K (2200 F). Variability in apparent strain characteristics from gage to gage and separation of the Rokide substrate from the calibration bar were the primary reasons for not being able to make reliable strain measurements above 1089 K (1500 F).

Careful assessment of possible causes for the two above mentioned deficiencies (excessive apparent strain gage to gage variations and substrate separation) and consideration of the otherwise superior performance of the BCL-3 strain gage system, indicated that the system might be satisfactory at still higher temperatures--perhaps approaching the 1478 K (2200 F) NASA target temperature, if the two deficiencies could be eliminated.

It was therefore the primary objective of this program to develop ways and means of eliminating the difficulties. This, in turn, required the development of improved attachment and joining techniques, and use of improved lead wire systems. It was a secondary objective of this program to evaluate the clad-wire concept as a means to temperature compensate BCL-3 strain gage systems.

EXPERIMENTAL DEVELOPMENT, EVALUATION, AND RESULTS

1. Gage Fabrication and Specimen Preparation

1.1 General

During the course of this investigation, cantilever calibration specimens H-21R, H-22R, H-23R, H-24R, H-25R2, H-26R2, H-27R, H-28, H-29, and H-32 were prepared for various types of evaluations in the high temperature strain gage calibration facility. Specimens H-21R and H-25R2 were prepared for evaluation of the special type Ailtech SG 420 strain gages. Specimens H-22R, H-23R, H-24R, and H-27R were prepared for precoating evaluations. The other specimens were prepared for evaluation of BCL-3 strain gages having a gage length of 20.3 mm (0.8 in.) and a nominal resistance of 70 ohms. Other specimens prepared included sheet-type specimens, BC-1 through BC-3, for the moisture barrier coating study, a variety of joint type specimens for evaluation of various joining techniques, and a Hopkinson bar for evaluation of BCL-3 gages under mechanical shock.

1.2 Materials

1.2.1 Gages

The BCL-3 gages evaluated in this program were fabricated at the Battelle-Columbus Laboratories (BCL) from nominal 0.051 mm (2 mils) BCL-3 alloy

wire (Fe-25 Cr-7.5 Al) developed at BCL specifically for high temperature strain gages. The lead tabs were fabricated from 0.79 mm x 0.051 mm (1/32 in. x 0.002 in.) Hoskins Alloy 875 ribbon. The perforated gage carrier was made from Teflon impregnated glass fiber tape, and the gage backing from 0.79 mm (1/32 in.) thick Teflon sheet. (See Appendix A, Reference 1, for further details.)

The special Ailtech SG420 gages were fabricated for BCL by Ailtech, using nominal 0.025 mm (1 mil) diameter BCL-3 alloy wire for the strain filaments, which was supplied by BCL.

1.2.2 Specimens

The cantilever calibration specimens were machined from Haynes 25 plate, which was aged at 1283 K (1850 F) for one hour. The mechanical and chemical properties of the material are summarized in Table 1. It should be noted that the room temperature mechanical properties and chemical composition were obtained from the mill report, and that the elevated temperature properties were taken from the manufacturer's literature for sheet material, in the absence of any other elevated temperature information.

The specimens for the joint evaluation study were fabricated from 0.051 mm (2 mil) diameter BCL-3 wire, Hoskins Alloy 875 ribbon 0.794 mm (1/32 in.) x 0.051 mm (2 mils) thick, and 20 gage Hoskins Alloy 875.

The specimens for the barrier coating study were fabricated from 304 stainless steel sheet.

The specimen for the mechanical shock evaluation specimen was fabricated from SAE 4340 normalized aircraft quality bar stock, heat-treated to a tensile strength of approximately 1723 MN/m² (250 ksi).

1.2.3 Lead-Wire Systems

The high temperature portion of the lead wire system for the BCL-3 gages consisted of 20 gage, 3-conductor Hoskins Alloy 875 wire, MgO insulated, in a 4.77 mm (3/16 in.) diameter Inconel 600 sheath. This cable was custom-made to BCL specifications. The room temperature portion of the cable consisted of standard 3-conductor, PVC insulated, strain gage lead wire.

The lead wire for the barrier coating specimens consisted of 28 gage 3-conductor Oxalloy, MgO insulated, in a 1.83 mm (0.072 in.) Inconel 600 sheath.

1.2.4 Precoatings

The material for the first layer of the graded precoating system was powdered Nichrome. The material for the second layer of precoat consisted

of a 50-50 mixture of powdered Nichrome and powdered aluminum oxide. The earlier precoating used was nickel aluminide (Metco 450).

1.2.5 Barrier Coating

The material is a single component heat-curing resin, which is available under the trade name, "BLH Barrier H Waterproofing".

1.3 Gage Fabrication

1.3.1 Gage Winding Fixture

The gages evaluated in this program were produced with a fixture which was designed and fabricated at BCL for an earlier high temperature strain gage program. Special features incorporated in the design of the fixture included the capability for spot-welding the lead tab ribbons to the gage filament, without having to remove the gage from the fixture head (which insures precise control of gage resistance and constant wire tension), recessing pins, variable gage length, and precise pre-stressing of the gage filament, after winding, to maintain filament straightness.

Photographs and a detailed description of the fixture are contained in Appendix A of Reference 1.

1.3.2 Gage Geometry and Fabrication Procedures

The gage geometry for the BCL-3 gage is shown in Figure 1. Procedures for fabricating the gages, with the fixture mentioned in the above, are described in detail in Appendix A of Reference 1. Gages with a gage length less than 20.3 mm (0.8 in.) could have been fabricated with the same fixture; however, this would have resulted in a gage with a resistance correspondingly less than 70 ohms, unless a smaller diameter wire were used.

The special Ailtech SG420 weldable gage is a half-bridge gage and has geometry identical to the standard Ailtech SG420 gage with a nominal resistance of 120 ohms, and an effective gage length of approximately 18 mm (0.7 in.) according to the manufacturer. In fabricating these gages the manufacturer used 0.025 mm (1 mil) diameter BCL-3 vacuum annealed BCL-3 alloy wire, instead of the usual 92% Pt-8%W alloy. In all other respects, the construction of the special Ailtech 420 gages is similar to the standard Ailtech SG 420 gage. For further details on the standard gage, refer to the manufacturers' literature.

1.4 Specimen Preparation

1.4.1 Specimen Geometry and Gage Locations

The geometry of the Haynes 25 cantilever specimens and typical gage locations are shown in Figure 2. It should be noted that the holes at the shank end of the specimen are for four Inconel clamping bolts and the Inconel indexing pin, which is installed for precise specimen positioning

prior to insertion of the bolts and removed after tightening of the bolts.

The geometry of the joint evaluation specimens is shown in Figure 3. Refer to 1.2.2 for specimen dimensions.

The 304 stainless steel strip type specimens for the barrier coating study were 1.98 mm (.078 in.) thick, 25.4 mm (1 in.) wide, and 152 mm (6 in.) long. One BCL-3 gage was located in the center of the specimen on one face only. A thermocouple was also installed adjacent to the gage near the mid-length of the sensing portion of the gage.

The Hopkinson bar specimen consisted of a piece of 2.54 cm (1 in.) diameter SAE 4340 bar stock 107 cm (42 3/16 in.) long with two BCL-3 gages, 180 degrees apart, oriented in the longitudinal direction and located at the mid-length of the bar.

1.4.2 Development and Application of Precoat System

1.4.2.1 General

In the previous study (reported in Reference 1), Rokide was applied directly to the surface of the calibration bar. It was found that, regardless of the care exercised in preparing the specimen surface, or in applying the Rokide, separation of the substrate occurred when the temperature was in the neighborhood of 1089 to 1144 K (1500 to 1600 F). This separation was primarily due to oxidation and other degradation at the interface between the Rokide and the specimen surface, and the large thermal shearing stresses developed at the interface resulting from the combined effects of the thermal expansion differences between the Rokide and the Haynes 25 material and the high temperatures attained. As a consequence, special precoat systems described in 1.4.2.2 and 1.4.2.3 were developed to minimize, if not eliminate, failures due to substrate separation.

1.4.2.2 Nickel Aluminide Precoat System

Two Haynes 25 calibration bars (specimens H-22R and H-23R) were pre-coated with Nickel Aluminide (Metco 450 powder), which was plasma-sprayed in varying thicknesses of 0.08 mm (3 mils), 0.10 mm (4 mils) and 0.13 mm (5 mils) on both faces of both specimens. A 0.13 mm (5 mils) thick layer of Rokide was then flame-sprayed on top of the nickel aluminide precoat. Thermocouples were also installed at several locations to permit accurate monitoring of temperature over the specimen surface. An additional layer of Rokide 0.10 mm (4 mils) thick was sprayed on top of the Rokide on one face of Specimen H-23. This was done to simulate the thickness of the final coat of Rokide which bonds the gage to the Rokide substrate. The specimens were then placed in separate furnaces and Specimen H-22R was heated for 8 hours at 1255 K (1800 F) and Specimen H-23R for 5 hours at 1144 K (1600 F). The furnaces were then turned off and after cooling down, the specimens were examined. On Specimen H-22R, Rokide substrate separation occurred for all

but the thickest precoat, with no separation whatever between the precoat and the specimen. On Specimen H-23R there were no separations of any kind. Specimen H-22 was then heated for an additional 3-1/2 hours at the same soak temperature, and the specimen again cooled down. It was found that all substrates had failed. Since the failures had occurred at a temperature about 200 K (366 F) below the maximum NASA target temperature, and under thermal cycling only (i.e., without mechanical stress present), it was concluded that although definite benefit resulted from the use of the 0.13 mm (5 mil) thick nickel aluminide precoat, the benefit derived was not sufficient to satisfy the requirements for this program. This conclusion was borne out during room temperature mechanical precycling of Specimen H-23, after cooling down. On the third room temperature cycle to 2,000 $\mu\epsilon$, substrate failure occurred, again indicating the need for still greater bond strength.

1.4.2.3 Graded Precoat Systems

It was evident from the results described in 1.4.2.2 that a nickel aluminide precoat, alone would not provide sufficient bond strength, and that a different or modified precoat system would be required. It was therefore decided to investigate the performance of a "graded" multilayer system. It was known that Nichrome bonds strongly to cobalt base alloys such as Haynes 25, and that it provides excellent oxidation resistance. It was consequently decided that the first precoat layer should be Nichrome. Then, to minimize effects due to differences of thermal expansion coefficients of the ceramic material (Rokide) and the metallic materials (Nichrome precoat and Haynes 25 bar), it was decided that an intermediate or transitional layer comprised of 50% nichrome and 50% alumina should be interposed between the Rokide and the Nichrome.

Two specimens, H-24R and H-27R, were then prepared with a graded precoat system. The first layer consisted of a plasma-sprayed layer of Nichrome 0.10 mm (4 mils) thick. The second layer consisted of a plasma-sprayed layer of a 50-50 mixture of alumina and Nichrome, also 0.10 mm (4 mils) thick. The final layer consisted of a 0.23 mm (9 mil) thick flame-sprayed layer of Rokide which simulated the Rokide substrate and final Rokide coat. These specimens were subjected to thermal soaking at 1311 K (1900 F) for periods up to 7-1/4 hours and mechanical precycling to 2000 $\mu\epsilon$. It was observed that their performance was definitely superior to that of the specimens with the nickel aluminide precoat. Accordingly, all subsequent Haynes 25 gage calibration specimens were precoated with the above mentioned graded precoat system, prior to attachment of gages with the Rokide process.

1.4.3 Gage Attachment Procedures

Gages were bonded to the calibration bars by means of the Rokide flame-spray process, using high purity aluminum oxide rod. Prior to application of the Rokide, the graded precoating described in 1.4.2.3 was applied to the surface of the bar. In the previous program (reported on in Reference 1), it was found that at temperatures above 1809 K (1500 F), a Rokide substrate thickness of 0.13 mm (5 mils) was necessary to minimize oxidation at

interface resulting from permeation of air through the relatively porous Rokide. An 0.10 mm (4 mil) thick Rokide layer was therefore applied to bond the gage to the Rokide substrate. For a detailed description of the Rokide procedures used, refer to Appendix B of Reference 1.

1.4.4 Lead Wire Attachment Procedures

The 20 gage 3-conductor Hoskins Alloy 875 lead wire was attached to the Hoskins Alloy 875 lead tabs by means of resistance spot-welding. To facilitate joining, the ends of the conductors were flattened by an amount sufficient to provide a flat surface for the ribbon. It was found that a 7 to 8 watt-second setting and moderate pressure produced satisfactory joints.

The welding equipment consisted of a Unitek Model 1-065-03 resistance spot welder, Model 34066 hand piece with a Model 13-012-04-02 electrode.

1.5 Preparation of Joint Evaluation Specimens

1.5.1 General

For the preliminary studies of the 5 joining techniques (NASA butt, pulse arc, plasma needle arc, laser, and D.C. parallel gap welding) joint specimens were prepared at BCL for the pulse arc, plasma needle arc and D.C. parallel gap welding techniques. Preparation of the NASA butt welded joints was done at NASA Langley, and preparation of the laser joints was done at the Mound Laboratory, Miamisburg, Ohio. Figure 3 shows the geometries of the basic joint types prepared for evaluation of each of the 5 joining techniques. It should be noted that the "tapered" conductor joint concept shown in Figure 3C, if successful, would have eliminated the need for the Nichrome lead tab ribbons and the related spot-weld joints.

1.5.2 NASA Butt Weld Joints

Figure 3a shows the geometry of the NASA wire butt joint and wire to ribbon butt joint. As mentioned earlier, these joints were prepared at NASA Langley, using a special butt welder developed at NASA for joining fine thermocouple wires as fine as 0.025 mm (0.001 in.) diameter. Prior to welding, the parts were deburred and cleaned. The welder consists of a capacitor discharge power supply, a parallel gap weld head with adjustable electrode gap and vertical force, bow shaped electrodes, a copper weld base made in two sections and separated by a thin insulator, an inert gas tube, and a binocular microscope to view and position the work. The bow-shaped electrodes complete the electric circuit and provide a unique mechanical motion which bring the two ends of the wires together and keeps the wires continuously butted together as the weld is completed. Sufficient 0.051 mm (2 mil) diameter BCL-3 and BCL-5 wire and Hoskins Alloy 875 ribbon 0.794 mm (1/32 in.) x 0.051 mm (2 mils) were supplied to NASA to provide for fabrication of all joint specimens required for the joint evaluation described in 4.0. The wire and ribbon were cut into pieces each approximately

10.16 cm (4 in.) long, prior to butt welding the pieces together. For a more complete description of the welder, refer to Reference 2.

Geometry 3a(1) is representative of the gage filament to gage filament joint for a temperature compensated composite gage design, fabricated of two materials having coefficients of resistivity of opposite signs. Butt joint geometry 3a(2) provides another way of making the gage filament to lead tab joint.

1.5.3 Pulse Arc Weld Joints

The feasibility of fabricating joints of the three geometries shown in Figures 3b and 3c was investigated with the pulsed-arc technique. Of these, only configuration 3c was found to be practical from the standpoint of gage fabrication. Consequently, it was the only geometry for which joint evaluation specimens were prepared.

The tapered Hoskins Alloy 875 wire shown in Figure 3c in reality represents a portion of each 20 gage conductor in the 3-conductor lead wire cable. The taper is produced by placing the wire in an electropolishing bath and gradually removing the wire from the bath. The degree of taper is controlled by the rate of removal from the bath. Wire taken from 3-conductor cable was cut into pieces approximately 15.4 cm (6 in.) long to provide the material for making the tapered wires. Approximately 10.16 cm (4 in.) of each piece were placed in the electropolishing bath. Each piece was tapered over this distance to produce a tip approximately 0.076 mm (3 mils) diameter. A BCL-3 wire approximately (6 in.) long was then wound around the tapered tip (several turns) and the assembly placed in the chuck (pin-vise) of the pulse arc welder. The assembly was then cleaned in Freon and welded. The welder consisted of a Cannon Model 100-Percussive Arc Welder power supply, 100 amp gas cooled Visuweld Torch with an 0.0254 cm (.010 in.) diameter 2% thoriaed tungsten electrode, and foot switch. In operation, a high energy electrical pulse arc melts the joint materials and produces a "ball" of fused material at the very tip of the specimen.

The torch was positioned directly over the axis of the specimen, with a 0.51 mm (20 mil) gap between the tip of the electrode and the tip of the tapered wire. Argon gas at a flow rate of 7.86×10^{-5} to 11.8×10^{-5} m³/sec (10 to 15 ft³/sec) was fed into the torch to provide an inert cover gas for the specimen.

Difficulties were encountered in getting the equipment to fire in a predictable manner, in spite of numerous attempts to establish a proper weld schedule by varying the equipment settings over a wide range. Nevertheless, it was possible to make 6 joints for evaluation.

1.5.4 Plasma Needle Arc Weld Joints

Because of difficulties experienced with the pulsed-arc technique, the feasibility of fabricating these joints with the plasma needle-arc technique was investigated. The equipment consisted of a Linde Plasma Needle Arc

Welder, a Linde PT 10 plasma torch with a 1.02 mm (.040 in.) diameter tungsten electrode, cooling pump, and an argon inert atmosphere chamber. The torch was positioned directly over the axis of the specimen which was held vertically in a fixture. Because of the relatively intense heat of the plasma stream, a reflective shield was provided over the tip of the specimen. This shield consisted of a 0.79 mm x 1.59 mm (1/32 in. x 1/16 in.) washer cut from 0.05 mm (.002 in.) thick Hoskins Alloy 875 ribbon. The washer was pierced to provide a 0.10 mm (4 mil) diameter hole in the center of the washer.

The specimen was assembled by threading the 0.05 mm (2 mil) diameter BCL-3 wire through the hole and then placing the wire washer onto the tapered alloy 875 wire. The BCL-3 wire was then looped several times around the taper directly beneath the shield. The assembly was then cleaned with Freon. The assembly was then welded. The distance between the torch and the reflective shield was approximately 16 mm (5/8 in.). A 16% setting on the low range of the welder was used to make the joints. The plasma stream melted the shield and tip of the taper to produce a ball of metal which enveloped the BCL-3 wire. Twelve joint specimens were fabricated in this manner.

1.5.5 Laser Weld Joints

Twelve laser joints of the geometry shown in Figure 3c were fabricated with a Korad Model KWD Laser Welder-Driller. It should be noted that it was not necessary to use a reflective shield with this technique. The BCL-3 wire was merely looped several times around the tip of the tapered wire. The joining was done in an air environment. It was found that a low power setting and a 7 ms pulse duration was sufficient to melt the tip of the taper and produce a "ball" of metal, which enveloped the BCL-3 wire.

1.5.6 DC Parallel Gap Weld Joints

In the previous program, the gage filament to lead tab joints were made by this technique, with the electrodes positioned parallel to the strain filament, as shown in Figure 3d (1). Also, the electrodes then used were copper and required an electrode force in the neighborhood of 31.1 N (7 lb.) to produce a satisfactory weld with the air-annealed wire. This relatively large electrode force resulted in high contact pressure, which caused undue wear and "mushrooming" of the electrode tips, and thus required frequent dressing of the electrodes. Even then it was difficult to obtain consistent welds for more than several gages in succession.

An evaluation was therefore conducted to determine what improvement, if any, would result from (a) use of a perpendicular orientation of the electrodes with respect to the gage filament, as shown in Figure 3d (2), (b) use of molybdenum rather than copper electrodes and (c) use of as-drawn rather than air-annealed wire, which has an oxide protective coating. This involved the evaluation of 6 different wire condition-electrode orientation-electrode material combinations. These combinations were:

<u>Joint Type</u>	<u>BCL-3 Wire Condition</u>	<u>Joint Geometry*</u>	<u>Electrode Material</u>
1	Air Annealed	1	Mo
2	Air Annealed	3	Cu**
3	As Drawn	2	Mo
4	Air Annealed	3	Mo
5	As Drawn	3	Mo
6	As Drawn	2	Mo

* Number refers to specific geometry in Figure 3d.

** RWMA, Class II electrodes.

Approximately 12 joint specimens of each joint type were prepared for room temperature tensile evaluations. In addition, a like number of joints specimens of each joint type were prepared for evaluation of joint resistivity characteristics at elevated temperatures. Refer to 1.2.2 for wire and ribbon dimensions.

The Hoskins Alloy 875 ribbons used in the fabrication of the joints with folded ribbons were prepared in accordance with the same procedure outlined in Section A3.2 of Reference 1 for the folded Nichrome V ribbons. For the unfolded ribbons (Joint Geometry 3), the procedure was the same except that the portion of the procedure relating to folding is omitted.

The following weld schedules were established for fabrication of each of the 6 joint types.

<u>Joint Type</u>	<u>Electrode Force</u>		<u>Volts</u>	<u>Dwell Time</u> m sec	<u>Environment</u>
	<u>N</u>	<u>lb.</u>			
1	31.1	7	0.9	100	Air
2	22.2	5	0.9	100	Air
3	31.1	7	0.9	25	Argon
4	31.1	7	1.0	10	Argon
5	31.1	7	0.95	15	Argon
6	31.1	7	1.45	2	Argon

The following equipment was used to fabricate the joint evaluation specimens:

- (1) Hughes constant voltage welding power supply, Model No. MCW-550
- (2) Hughes parallel gap weld head Model No. VTA-66
- (3) Hughes Type MCW electrodes, Catalog No. ESQ-1525-02 (Cu)
- (4) Hughes Type MCW electrodes, Catalog No. ESQ-1525-00 (Mo)
- (5) Bausch and Lomb microscope, Hughes Model No. MCW-552

1.6 Preparation of Barrier Coating Specimens

Three specimens were prepared by shearing specimens 25.4 mm (1 in.) wide, 152 mm (6 in.) long, from 1.98 mm (0.078 in.) thick, Type 304 stainless steel sheet. BCL-3 strain gages were installed in the center of one face of each specimen, using the Rokide flame-spray process. The Rokide substrate thickness was 0.13 mm (5 mils). The thickness of the final Rokide coating was 0.10 mm (4 mils). No precoating was applied, since it was considered unnecessary for the purposes of this evaluation. (For detailed information on the installation procedure, refer to Appendix B of Reference 1.) A Chromel-Alumel thermocouple was installed immediately adjacent to the mid-length of each gage.

After completion of gage and thermocouple installation, "BLH Barrier H Waterproofing" was applied to each assembly, using the manufacturers instruction as a guide. Specifically, two coatings of the waterproofing were applied to each specimen. The specimens were cured in accordance with the following schedule:

1 hour at (150 F)
1 hour at (200 F)
1 hour at (350 F)
1 hour at (450 F)
16 hours at (500 F)

2. Description of Gage Evaluation Facilities

2.1 High Temperature Evaluation Facilities

Strain gage evaluations were performed in a special high temperature facility developed at BCL. Figure 4 is an overall view of the facility. Figure 5 is a close-up of a calibration specimen (instrumented with numerous thermocouples) installed in the facility for the purpose of checking uniformity of furnace temperature. The loading mandrels (in the no-load position), deflection dial gage extensions, and supporting truss and box-beam structure for holding the cantilever specimen are also clearly shown. The furnace is a 3-zone, split type furnace, with a 12.7 cm (5 in.) bore and heated length of approximately 61 cm (24 in.). The furnace is capable of continuous operation for temperatures up to 1478 K (2200 F). A pulley-system is used to facilitate positioning of the upper half of the furnace.

The fixture basically consists of an exterior low carbon steel box frame mounted on legs with leveling screws, the cantilever box beam assembly, deflection gage support structure, deflection gages, and loading mandrels.

The exterior box frame was designed to resist the mandrel loads and moment induced at the root-end of the box beam, with a minimum amount of deflection in the frame.

The box beam, which was fabricated as a weldment from Inconel 600, was heavily reinforced with an interior web plate to provide additional stiffness. The outer dimensions of the box were the maximum permissible in terms of the furnace bore. The box beam was clamped to the support structure by means of six Inconel bolts, four of which go through the specimen shank. To minimize the flow of heat from the box beam into the cooler support structure, high strength Lucalox thermal insulation spacer blocks were used between the support structure and the side faces of the box beam. A mullite thermal insulation block was also provided on the underside of the box beam to thermally isolate it from the support structure.

The deflection gages were protected from the heat by thermally isolating the deflection gage yoke from the deflection gage support truss with mullite wafers. Further protection of the gages and external lead wire was provided by plugging the furnace ends with Refrasil insulation.

The deflection gage truss, fabricated from Inconel X-750 was welded to the end of the box beam. Consequently, the deflections measured by the dial gages represent the relative deflection on the beam at the point of contact with the dial gage with respect to the shank of the specimen. The deflection measurement is therefore independent of deformation in the box beam, itself, which is relatively small in any event.

With loading mandrels on each side of the specimen, it was possible to subject a gage to reverse strain cycles, i.e., 0, +, 0, -, 0, or the opposite sequence, 0, -, 0, +, 0, without removing and repositioning the specimen.

The fixture was calibrated over a $\pm 2000 \mu\epsilon$ range by accurately measuring dial deflection versus specimen strain-over the full deflection range-with a specimen instrumented with four room-temperature select foil gages of known gage factor and accuracy.

The temperature control system consisted of a solid-state temperature programmer and temperature controller, and a solid-state SCR power controller.

Specimen temperature was monitored by means of Type S (Pt/Pt - 10% Rh) thermocouples. The thermocouples were attached to the specimen midway between each gage, with one thermocouple so located on each face of the specimen.

The temperature programmer expedited evaluation of the gage apparent strain characteristics. The predetermined temperature-time history for each test series was drawn on the electrically conducting program chart with a stylus. The temperature control system then imposed this temperature-time history on the specimen with a minimum amount of temperature deviation or over-shoot during heating. It also should be pointed out that the temperature controller incorporated circuitry to provide proportional band, rate time, and reset action, which also minimized temperature over-shoot during heating.

To expedite evaluation, a simple forced convection air-cooling system was later incorporated into the box frame to keep the frame and dial gage gages cool.

A conventional strain indicator and 10 channel switch and balance unit were used to measure gage factor and linearity characteristics, in a 1/4 bridge hook-up with a 3-lead wire system to minimize lead wire errors. A precision decade box was used in the dummy leg of the bridge, and in series with the active gage when required. A multichannel data acquisition system was also used to obtain the apparent strain and drift data.

Temperatures were determined with a millivolt potentiometer, whose reference junction temperature was measured by means of a precision laboratory thermometer. Resistance and resistance to ground measurements were made with a vacuum tube voltmeter, or megger.

Specimen deflection was measured by means of precision mechanical dial gages, having a least count of 0.0254 mm (0.001 in.). All instruments were calibrated with standards traceable to NBS.

2.2 Joint Evaluation Equipment

Elevated temperature resistivity properties of the joint specimens were determined in a miniature split-type electric resistance furnace having a bore of 3.81 cm (1-1/2 in.) diameter and a heated length of approximately 30.5 cm (12 in.). The furnace can accommodate up to 12 wire specimens at a time. Low-contact resistance binding post type terminal strips, on each side of the furnace, provided a means for connection of the leads of the resistance measuring equipment.

Furnace temperature was regulated by means of an L and N temperature controller with proportional, reset, rate, and approach action. Furnace temperature was sensed by means of a centrally located Type S thermocouple. Although there was some fall-off in furnace temperature near the ends of the furnace, it is believed the manner in which the results were analyzed minimized any uncertainties due to this temperature drop.

Resistance measurements were made with a precision Wheatstone or Kelvin bridge. Readings were, in general rounded off to the nearest 1/100 of an ohm.

For the mechanical strength measurements, miniature precision spring-type dynamometers were used for load application.

2.3 Barrier Coating Evaluation Equipment

The equipment used to perform the barrier coating evaluation primarily consisted of a constant humidity chamber, three loading capsules, tubular resistance heating furnace, and temperature controller and a megger for monitoring resistance to ground.

The constant humidity chamber consisted of a large dessicator containing a saturated solution of $\text{CaSO}_4 \cdot 5 \text{H}_2\text{O}$ which produced a 98% constant humidity environment. A special rubber gasket was fabricated to provide a gap between the lid and body of the dessicator for exit of the lead wires and to also serve as a seal. The dessicator was large enough to readily accomodate the three loading capsules.

The loading capsules were designed to provide a "3-point" central loading to the strip-type flexural specimens described in 1.4.1 and 1.6. The body of the capsule, which was sized to permit ready installation of three capsules in tandem within the heated zone of the furnace, consisted of a section of stainless steel tubing with a wall thickness of .381 cm (.150 in.), O.D. of 6.01 cm (2.367 in.), and a length of 15.24 cm (6 in.). Holes were than drilled at each end for insertion of pins, which served as end supports. A radial hole was also drilled in the center of the body to provide for the loading screw which was adjusted to provide the required strain in the beam. The body was ample enough to resist the screw and pin loads at temperature=without creep deformation.

The furnace was a 3-zone tubular resistance type furnace having a bore diameter of 8.89 cm (3-1/2 in.) and heated length of approximately 61 cm (24 in.). Uniformity of temperature along the length of the furnace was obtained by initial adjustment of the power-stats for each zone. Overall temperature control was provided by a centrally located control thermocouple which fed into a proportional band temperature controller.

2.4 Dynamic Evaluation Equipment

2.4.1 Thermal Shock

After completion of the static evaluations, Specimens H-25R2 and H-28 were subjected to repeated thermal shocks.

The equipment used consisted of a 10 KVA step-down transformer, phaser and solid state power controller system, which provided between 800 to 1000 amps for direct resistance heating through the specimen. The cables were attached to the specimens with specially machined copper clamps. The system was programmed to provide a 33.33 to 38.89 K/sec (60 to 70 F/sec) ramp in temperature. Prior to commencement of the evaluation, dummy specimens with five fast response Type K longitudinal and transverse thermocouples were used to verify uniformity of temperature over the heated portion of the specimen. To achieve uniformity of temperature, it was necessary to use a silver conducting paste beneath the clamp. A multichannel data acquisition system was used to record temperatures at two second intervals over a cycle period of 10 minutes and 40 seconds. The maximum temperature of 1311 K (1900 F) was reached in less than 1/2 minute. The remainder of the cyclic period represented the time required for cool-down from the maximum temperature.

Each specimen was cycled a minimum of 25 times. The specimen was periodically inspected for any signs of bond failure.

2.4.2 Mechanical Shock

A modified Hopkinson bar apparatus was used to assess the ability of the gage attachment system (precoats, substrate, bond-coats) to withstand severe mechanical shock, utilizing the gaged Hopkinson bar described in 1.4.1.

The instrumented bar was supported in a horizontal position between two nylon slide bearings. The bar was subjected to the longitudinal impact from a striker bar which was actuated by a high pressure gas system, comprised of a high pressure accumulator and pressure release valve (fast acting solenoid or rupture disc).

In operation, the striker bar is accelerated to the desired and measured velocity by the gas pressure in the striker bar cylinder. It strikes the end of the Hopkinson bar and creates a relatively square compression stress wave which travels to the opposite end of the bar and returns as a tensile wave. The striker bar was 40.64 cm (16 in.) long. The end of the Hopkinson bar opposite the impacted end was allowed approximately 1.25 cm (1/2 in.) free travel, before it impacted with a momentum absorber. During this free flight, the input stress wave made at least 4 round trips in the Hopkinson bar, each round trip comprised of a full compression and full tension wave. Thus, for each "shot" the gage installation was subject to 4 severe compressive and 4 tensile shocks.

An optical gate, in conjunction with a pulse-forming circuit and electronic timer was used to measure the velocity of the striker bar, just prior to impact. (With this velocity it was then possible to calculate the true strain in the bar by dividing the stress derived from the equation in 3.3.2 by Young's modulus of elasticity.)

The output from the gages was fed into the amplifiers of a high sensitivity dual beam oscilloscope, and the wave form was recorded on film.

3. Gage Evaluation

3.1 Approach

In the previous program, gage evaluation was limited, with few exceptions, to a maximum temperature in the neighborhood of 1089 to 1144 K (1500 to 1600 F) primarily because of substrate failure. To determine enhancement of performance (with respect to maximum operating temperature) resulting from improved gage attachment procedures and joining procedures, etc., the main thrust of the evaluation was directed toward evaluation of performance at maximum temperatures above 1089 K (1500 F). Also, in the previous program, the evaluations were performed only under static or quasi-static conditions. In this program, gage performance, under mechanical and thermal shock conditions, was included as a part of the total evaluation effort.

3.2 Static Evaluation Procedure

Prior to beginning an elevated temperature evaluation, it was necessary to establish the maximum evaluation temperature for that particular evaluation sequence (run). This was done on the basis of gage performance from a previous test(s), or on anticipated gage performance. If erratic behavior (or gage failure) did not occur during the run, the maximum run temperature (M.R.T.) was generally increased by 55.5 K (100 F), and the run repeated. This process was continued until erratic behavior (or gage failure) occurred. This permitted obtaining a maximum amount of information from each specimen. The evaluation procedure used, unless otherwise indicated, was comprised of the following steps:

- (1) Measure and record gage assembly resistance and resistance to ground at room temperature (R.T.) from ends of lead wire, and replace or repair obviously bad gages or joints.
- (2) Prestabilize the gages by soaking for 4 hours, unless otherwise instructed, at a temperature 13.89 K (25 F) higher than the maximum run temperature (M.R.T.).
- (3) Thermally precycle to M.R.T. three times. Record gage output, at R.T. and M.R.T. only, and resistance to ground.
- (4) Hold at M.R.T. for 30 minutes, and then precycle, mechanically, three times to 2000 $\mu\epsilon$, unless otherwise instructed and record gage output at zero and maximum deflection, and resistance to ground.
- (5) With specimen at M.R.T., go up in a minimum of 4 tensile increments to 2000 $\mu\epsilon$, unless otherwise indicated, and back down to zero deflection. Record gage output at each level going up and coming down. Repeat two additional times. Repeat at mid temperature and room temperature unless otherwise instructed.
- (6) Determine apparent strain versus temperature from room temperature to M.R.T., every 138.8 K (250 F) going up and coming down to room temperature. Allow a minimum of 30 minutes at each temperature level to insure isothermal conditions. Repeat procedure two additional times.
- (7) Hold temperature at M.R.T., and periodically record drift (under no mechanical stress) as a function of time, for a minimum of 4 hours, unless otherwise instructed.
- (8) Remove from furnace after cooling and install specimen in thermal shock fixture. Heat at rate of 16.67 K/sec (30 F/sec) to M.R.T. (unless otherwise instructed) and cool to room temperature with forced air-cooling. Repeat for specified number of cycles.

(9) Replace bar in calibration facility and repeat Step 5.

NOTE: Perform Steps (8) and (9) only if requested.

It should be noted that where excessive permanent set occurred in the calibration bar due to the high temperature and strain level, Step 5 was modified. The calibration bar would then be loaded alternately in tension and compression (generally to a lesser strain level) to minimize permanent set in the calibration bar which, otherwise, would be cumulative.

(Unfortunately, there are no known high temperature wrought materials available to fabricate calibration bars which can withstand the combined effects of the 2000 $\mu\epsilon$ strain level at the higher temperatures involved in this program without yielding. Cast material such as IN 100 (ASM 5397) would be required. At 1366 K (2000 F), for example, it has a yield strength at 0.2% offset of approximately 241 MN/m² (35 ksi); Haynes 25 has only about 82.7 MN/m² (12 ksi). However, the material is in the difficult to work category.

3.3 Dynamic Evaluation Procedure

3.3.1 Thermal Shock

To assess the ability of the layered precoat/Rokide substrate/gage/Rokide system to withstand severe thermal shock, specimens were subjected to repeated thermal shocks at a heating rate of 39 K/sec. (70 F/sec.), to maximum stated evaluation temperatures. This was accomplished by direct resistance heating through the specimen, utilizing the equipment described in 2.4.1. These shocks were applied, after completion of the static evaluation procedure described in 3.2. Upon completion of application of the thermal shocks, the gage installation was carefully examined for indications of bond failure or other damaging effects to the gage/leadwire system.

3.3.2 Mechanical Shock

To assess the ability of the layered precoat/Rokide substrate/gage/Rokide system to withstand severe mechanical shock, two BCL-3 strain gages were Rokided to a precoated Hopkinson cylindrical bar described in 1.4.1. and subjected to severe mechanical shock in the Hopkinson bar apparatus described in 2.4.2. These evaluations were performed at room temperature. A total of 13 increasingly severe shocks (impacts) were applied to the bar and the dynamic gage response noted during the application of each shock. After application of each shock each gage installation was carefully examined for signs of bond failure or other damage.

Stress levels in the impacted Hopkinson bar ranged from 119.79 MN/m² (17,375 psi) to 448.07 MN/m² (64,988 psi). These values were calculated from the relation

$$\sigma = 1/2 \rho C_B V$$

where

$$\begin{aligned}\rho &= \text{Bar density} \\ C_B &= \text{Bar sonic velocity} = \sqrt{\frac{E}{\rho}} \\ E^B &= \text{Young's modulus} \\ V &= \text{Striker bar velocity}\end{aligned}$$

The strain levels in the bar which ranged from 571 $\mu\epsilon$ to 2353 $\mu\epsilon$ were readily determined by dividing the stresses by Young's modulus 0.2098 MN/m² (30.43 x 10⁶ psi).

3.4 Test Matrix

Table 2 is a matrix of the actual evaluation steps to which each specimen was subjected. The step numbers in the table correspond to those steps in the evaluation procedure described in 3.2. It is noted that each specimen was not subjected to the complete evaluation procedure. In the case of the Ailtech gages, Specimen H-25R2 was evaluated for the specific purpose of determining the upper temperature at which the gage would become unstable. Consequently, only a drift evaluation (Step 7) was performed at progressively increasing temperatures to the temperature at which excessive drift occurred. This information provided a basis for establishing the maximum temperature at which meaningful data could be obtained during the more comprehensive evaluation of the Ailtech gages on Specimen H-21R.

Likewise, in certain instances, a step(s) was eliminated from the evaluation procedure, if meaningful data could not be obtained from that step. For example, at the higher temperatures, in some instances, Step 5 (gage factor) was eliminated or conducted to a reduced maximum strain level (2000 $\mu\epsilon$ strain in calibration bar), if excessive permanent set resulting from yielding in the bar prevented obtaining meaningful data. This philosophy permitted obtaining the maximum amount of useful technical information from each specimen.

4. Joint Evaluation

4.1 Approach

Because of the high operating temperatures of the BCL gages, their joints can be subjected to severe oxidation in air environments, as well as mechanical and thermal stresses. Although the gage filaments and lead tab ribbons are fabricated from high temperature, oxidation resistant materials (BCL-3 alloy and Hoskins Alloy 875), the effects of joint degradation on gage performance was still of concern.

DC parallel gap welding has been used to join the lead tab ribbons to the gage filaments for some time and with some degree of success. The technique's main virtue is the ease with which the lead tab to gage

filament joint can be made. Also no elaborate equipment or fixturing is required. On the other hand, visual inspection of the joints (Configurations 1, 2, Figure 3d) is not possible, and consistency of joint quality was difficult to maintain; also the technique is not feasible for making gage filament to gage filament butt-welded joints, which would be required in composite gages. Thus, there was a need to reduce joint failures or gage to gage variations with an improved joint design. Consequently, a preliminary study of five joining techniques was undertaken as a part of this program; namely, the NASA butt-weld, pulse arc, plasma needle arc, laser, and DC parallel gap welding techniques.

The scope of the study was limited to an assessment of electrical resistivity and room temperature mechanical strength characteristics of the joint specimens described in 1.5. Once it had been established that the DC parallel gap welding technique was the most viable of the 5 techniques for making the gage filament to lead tab joints, the remaining effort in this study was devoted to improving the DC parallel gap technique.

4.2 Evaluation Procedures

4.2.1 Mechanical Strength

The joint specimens, prepared in accordance with the procedures described in 1.5, were evaluated with respect to breaking strength by subjecting them to a gradually increasing tensile load applied along the axis of the wire, while held in a special fixture. Calibrated miniature load dynamometers were employed to apply the load. The location of the break was noted and recorded.

4.2.2 Resistivity Characterisitcs

The resistivity characteristics were determined on the basis of measurements of unit change in joint specimen resistance ($\Delta R/R$) and drift rate ($\Delta R/R t$) at 1144 K (1600 F) and 1311 K (1900 F) in an air environment, utilizing the equipment described in 2.2. The differences in joint specimen room temperature resistance, before and after the 1144 K (1600 F) soak were also determined. To expedite measurements, the full capacity of the furnace (12 specimens) was used, whenever possible.

5. Barrier Coating Evaluation

5.1 Approach

A careful survey of commercially available barrier and other coatings failed to uncover compatible coatings which would provide a protective barrier against moisture penetration upon cool-down from temperatures above about 589 K (600 F), after being subjected to deformations of 2000 $\mu\epsilon$, or greater at temperature.

Ceramic coatings, impervious to moisture, are available which can readily withstand temperatures up to 1366 K (2000 F); however, they do not possess sufficient ductility to permit straining to at least 2000 $\mu\epsilon$, without cracking.

Metallic coatings are also available which can withstand both the strain and temperature; however, they would have to be deposited by processes such as physical vapor deposition which are impractical for field use. Also, there is a possibility that the metallic particles would penetrate the Rokide and cause electrical problems such as shorting or low resistance to ground. Thus, a two-layer system would be required. The first layer would have to be non-conductive, electrically, and seal the Rokide against penetration of metallic particles during application of the next layer, which would be metallic.

There are glass-base coatings which have been developed for insulating copper wire used for specific applications. These coatings become relatively plastic at elevated temperatures and can accommodate large strains. They are applied as a slurry and fused at a temperature in the neighborhood of 1367 K (2000 F). They might be applied in the field, by flame-spraying provided the structure and gage could tolerate the heat generated during application of the coating. It is also possible that the maximum temperature of the structure and gage might be substantially below the fusion temperature, because of the rapid cooling associated with the flame-spray process. However, some effort, beyond the scope of this program, would be required in the formulation of the barrier coating and development of a viable field installation procedure.

In light of the above findings, evaluation in this program was limited to "BLH Barrier H Waterproofing", which is specifically formulated for Rokide and ceramic installations and has the highest operating temperature limit of any of the commercially available coatings.

According to the manufacturer's literature, the BLH Barrier H coating "can be exposed to temperatures under 650 F for terms of more than 24 hours and to 800 F for terms of up to 6 hours. It will retain its moisture resistance after such temperature excursions". No mention is made of the effects of strain on these upper temperature limits or exposure times.

It was therefore considered necessary to formulate an evaluation procedure and perform evaluation-assessing for upper temperature and time limits, below which coating effectiveness would be retained after exposure to the combined effects of strain and temperature.

5.2 Evaluation Procedures

Evaluation of the BLH Barrier H coating was performed by simultaneously subjecting three flexural specimens with barrier-coated strain gages to a prescribed humidity-strain-temperature history and observing the changes in resistance to ground as a function of time. (Refer to 1.4.1 and 1.6 for

details relating to specimen geometry and specimen preparation.) In formulating the evaluation procedure, it was recognized that zero-shifts may also provide an indication of moisture penetration. However, it was established that, in this instance, correlation of moisture penetration with zero-shift would be unfeasible, because of the difficulties associated with separating zero-shifts due to moisture from those due to exposure at temperature. Consequently, evaluation of the effectiveness of the barrier coating was assessed primarily in terms of changes in resistance to ground.

The specimens were loaded to produce 0, 1000, and 1500 $\mu\epsilon$ in Specimens BC-1, BC-2, and BC-3, respectively. This was accomplished by adjustment of the loading screws. Once adjusted, the capsule could be moved from humidity chamber to the furnace for elevated temperature exposure, or elsewhere, without disturbing the loading or induced strain. Table 3 delineates the strain-temperature-humidity-time history to which the three barrier coating specimens were subjected during the 911.6 hour period of evaluation. Resistance to ground measurements were taken with a megger, during each incremental step of the evaluation procedure.

6. Clad-Wire Concept Evaluation

6.1 Approach

Prior feasibility studies indicated that the co-extrusion process provided a viable method for cladding Fe-Cr-Al wire with platinum. It was demonstrated that it was possible to obtain a strong metallurgical bond between the wire and the cladding, and to co-extrude the combination to strain gage wire size. The cladding provides an oxidation resistant coating, as well as a possible means of temperature compensating BCL-3 alloy which has a negative temperature coefficient of resistivity to at least 1033 K (1400 F). However, determination of the initial thickness of platinum (prior to co-extrusion) to provide proper temperature compensation over a specified temperature range is by no means straight-forward, and was considered impractical from a cost standpoint.

It was therefore concluded that the most feasible way to determine cladding thickness and to illustrate the temperature compensation effectiveness of the clad-wire concept, was via the sputtering technique. Measurement of unit change in resistance of coated and uncoated wire as a function of temperature to 1089 K (1500 F) provided the necessary data for establishment of sputtering times. BCL-3 wire, air-annealed at 1033 K (1400 F), was used for the study. For one run, the wire was sputtered for 10 minutes on each side. On another run, the wire was sputtered for 20 minutes on each side. The coated wire was then annealed in air at 1033 K (1400 F). Resistivity measurements were then taken at eight different temperatures to establish resistivity curves. It was found that a sputtering time of 10 minutes, provided sufficient deposition of platinum to adequately flatten out the resistivity curve and also vividly illustrate the effectiveness of the clad wire concept for adjusting the resistivity curve.

7. Results

7.1 Static Gage Evaluations

7.1.1 General

The results of the gage evaluation are presented, herein, in terms of gage factor and linearity, apparent strain, drift, zero-shift, resistance to ground, and performance history. Unless otherwise stated, the above characteristics were obtained for a gage factor setting of 2.00. The true value of strain for any other gage factor may be readily obtained from the relation

$$\epsilon_T = \epsilon_M \frac{GFS}{GF}$$

where

ϵ_M = measured strain for a gage factor setting (GFS) = 2.00

GF = true gage factor obtained from gage factor versus temperature curve or other information.

7.1.2 Gage Factor and Linearity

Figures 6 through 9 are plots of true strain versus measured strain at various temperatures for Specimens H-21R, H-28, H-29, and H-32. The plots were constructed by fairing straight lines through as many data points as possible. Figure 6 is a plot for the four Ailtech gages on Specimen H-21R. It is noted that (a) with the exception of the room temperature run for Gages 1 and 2, the response was linear throughout the strain range up to the maximum temperature of 922 K (1200 F), (b) the responses of the two gages in tension (Gages 1 and 2) were virtually identical, as well as the responses of the two gages in compression (Gages 3 and 4), (c) the sensitivities in tension and compression were essentially the same, and (d) with the exception of the room temperature run for Gages 1 and 2, gage sensitivity increased with temperature.

The reason for the non-linearity exhibited by Gages 1 and 2 during the room temperature run is not known. Although there was a very slight amount of permanent set in the calibration bar, it could not explain the behavior, since the responses of Gages 3 and 4 were linear. Likewise, any other external effects that could cause non-linearities would affect all four gages. Table 4 is a summary of the data for Cycles 2 and 3. (Figure 6 was plotted from the Cycle 2 data.) An inspection of Table 6 reveals that (a) in spite of the non-linearity, zero shifts for any gage do not exceed $7 \mu\epsilon$ the zero shift for Gages 1 or 2 not exceeding $3 \mu\epsilon$, (b) the repeatability from cycle to cycle is also excellent, even for Gages 1 and 2 which exhibited the non-linearity.

Figure 7 is a similar plot for the four BCL-3 gages on Specimen H-28. It is observed that (a) the responses in tension and compression are quite linear at all temperatures and strain levels, except for the data points in tension at the highest strain level for the two highest temperatures, where there is a maximum deviation from linearity of about 6%, (b) the responses of the gages in tension are virtually identical; likewise for the gages in compression, (c) there is the usual decrease in gage sensitivity (gage factor) with increasing temperature.

Figure 8 is a similar plot for the four BCL gages on Specimen H-29. It is noted that the responses are, in general, like those for the gages on Specimen H-28. However, the gage sensitivity in compression at 1366 K (2000 F) is slightly higher than that at 1311 K (1900 F), which is atypical in terms of the other gages. This atypical behavior may, in reality, be due to data scatter, since the response at 1366 K (2000 F) is for Gage 4 only. It is also noted that, as with Specimen H-28, there is generally a slightly larger strain output exhibited at the highest strain levels. (Possible reasons for this non-linearity will be discussed later.) At 2000 $\mu\epsilon$, at 1311 K (1900 F) the permanent set in the calibration bar at the dial gage location was approximately 0.5 cm (0.2 in.). This amount of permanent set would have occurred with each successive cycle of loading to 2000 $\mu\epsilon$. To avoid a total permanent set greater than 0.5 cm (0.2 in.), the evaluation was consequently performed by subjecting the specimen to reversed loading cycles.

Figure 9 is a similar plot for the BCL-3 gages on Specimen H-32. It is noted that at 1311 K (1900 F), the response becomes highly non-linear when the strain level exceeds 800 $\mu\epsilon$, even under reversed loading. This was the strain level at which a permanent set was first observed in this specimen.

During evaluation, the precise strain in the specimen (calibration bar) can be determined on the basis of dial gage deflection readings, only if the bar geometry and strain distribution (throughout its volume) are identical to that of the calibration bar used to calibrate the calibration facility. The first condition (geometry) was met using bars that were the same size, within very close tolerances. The second condition (equality of strain distribution) requires that (a) the bar be essentially straight, (b) that there be no shift in location of the neutral axis during loading, (c) that there be none other than transverse loads applied to the calibration bar.

Unfortunately, because of the excessive yielding in the specimen, the specimen developed a permanent "bow" which, resulted in a small longitudinal component of load, in addition to the transverse load. (The loading mandrel was no longer perpendicular to the specimen; hence the longitudinal component.) Instead of behaving like a simple cantilever beam, the specimen therefore behaved somewhat as a beam-column with initial curvature, or as a mildly curved beam, in which case the neutral axis is no longer at the centroidal location (mid-thickness in this instance) and the strain distribution through the thickness of the specimen is hyperbolic rather than linear. Also, it can be shown for the case of a beam-column, a small initial curvature greatly

increases (magnifies) the effect of the longitudinal forces on the total deflection, and hence alters--in a non-linear manner--the distribution of strain throughout the volume of the specimen.

It is believed that the non-linearity and increased strain output at the higher strain levels are due, at least in part, to a combination of the above mentioned non-linear effects and/or alterations of the location of the neutral axis. Yielding in the BCL-3 strain filament at the highest temperature and strain levels may also have been a factor.

Table 5 contains the average gage factors for the gages on Specimens H-21R, H-28, H-29, and H-32. Values for tension and compression are presented, over a range in temperature from room temperature to 1366 K (2000 F).

It is noted that (a) the Ailtech gages have a somewhat lower gage factor than those of the BCL-3 gages, (b) there is a gradual decrease in gage factor with temperature for all gages, except the Ailtech gages, which have a somewhat lower gage factor in tension and compression at the intermediate and lowest temperatures, respectively, (c) although there is a consistent decrease in gage factor with temperature for BCL gages on a given specimen, there are some specimen to specimen variations for a given temperature. These variations are believed due to limited number of samples averaged (generally two in tension and two in compression), and possible shifts in neutral axis and non-linearities as mentioned above.

7.1.3 Apparent Strain

Figures 10 through 19 are the plots of apparent strain versus temperature for the gages on Specimens H-21R, H-26R2, H-28, H-29, and H-32. These plots show gage-to-gage or cycle-to-cycle variations. Where cycles are shown, the curve represents the average for the gages on the specimen.

Figure 10 is a plot for the four Ailtech half-bridge gages on Specimen H-21R. It should be pointed out that these plots show basic gage characteristics; no temperature compensation resistor was used to minimize apparent strain. It is noted that (a) the apparent strain becomes increasingly negative with increasing temperature, reaching a value of $-2300 \mu\epsilon$ at 911 K (1180 F), (b) the scatter from gage to gage is approximately $100 \mu\epsilon$ at the lower temperatures and increases to about $220 \mu\epsilon$ at the maximum temperature.

Figure 11 shows the variation in apparent strain during heat-up for three consecutive cycles for the gages on Specimen H-21R. It is noted that (a) all three cycles converged at the maximum temperature, a characteristic which is attributed to the BCL-3 alloy, (b) the maximum spread from cycle to cycle is about $100 \mu\epsilon$, the maximum being at the lowest temperature, (c) the second and third cycles are identical and (d) the zero-shift between the first and second cycles is $-100 \mu\epsilon$, and zero between the second and third cycles.

Figure 12 shows both the heating up and cooling down portions of the cycle for the gages on Specimen H-26R2 which was prepared and evaluated up to a maximum temperature of 1366 K (2000 F) to illustrate a very important characteristic of the BCL-3 alloy; namely, its ability, during the up-portion of the cycle, to retrace the down portion of the previous cycle within very close limits. (It is the characteristic of the alloy which causes consecutive cycles to converge at the maximum temperature.)

Point 1 represents the beginning of a heat-up cycle; Point 2 represents the terminal point of that cycle. Point 3 represents the terminal point, after cool down, and the beginning of the next heat-up cycle. (The first heat-up cycle is not plotted.) Point 4 represents the terminal point after cool-down. It is observed that even up to temperatures of 1366 K (2000 F), the heating up cycle is essentially identical to the previous cool down cycle, in spite of a zero-shift of about 4000 $\mu\epsilon$, during the first cycle, and about -3000 $\mu\epsilon$ during the next cycle. This same characteristic was observed in the previous study (reported in Reference 1) which was conducted at somewhat lower temperatures. The significance of the retracing characteristics, in terms of enhancing the accuracy of strain measurement is discussed in Reference 1 and will be discussed again later in this report.

Figure 13 is an apparent strain plot to 1200 K (1700 F) for the four gages on Specimen H-28. It is observed that (a) the spread between gages is relatively small at the lower temperatures and increases with temperature to a maximum of about 1500 $\mu\epsilon$ at the maximum temperature, (b) the apparent strain is everywhere positive and increases in a more-or-less uniform rate with some leveling off as the maximum value of about 39,000 $\mu\epsilon$ is approached.

Figure 14 shows the variation in apparent strain, during heat-up to 1200 K (1700 F), for three consecutive cycles for the same gages on Specimen H-28. It is noted that (a) all three curves characteristically converge at the maximum temperature, (b) the curves are relatively close together at temperatures between 644 K (700 F) and 755 K (900 F) and are virtually identical above 755 K (900 F) to the maximum temperature, and (c) the maximum spread between cycles occurs at the lowest temperature and is about 1600 $\mu\epsilon$. The zero-shifts associated with Cycles 1, 2, and 3 are 600 $\mu\epsilon$, 1000 $\mu\epsilon$, and 1000 $\mu\epsilon$, respectively.

Figure 15 shows the variation in apparent strain, during heat-up to 1311 K (1900 F), for three consecutive cycles for the gages on Specimen H-28. It is observed that (a) the curves tend to level off as they converge at the highest temperature, and (b) the curves for the second and third cycles are relatively close together to 700 K (800 F), and above that temperature they are identical to the maximum temperature. The zero-shifts associated with Cycles 1, 2, and 3 are -5500 $\mu\epsilon$, -1500 $\mu\epsilon$, and -500 $\mu\epsilon$, the zero-shift becoming progressively smaller with each cycle.

Figure 16 is an apparent strain plot to 1311 K (1900 F) for the four gages on Specimen H-29. It is noted that (a) the gage to gage scatter increases

from virtually nothing at the lower temperatures to a maximum of about 2000 $\mu\epsilon$ at the highest temperature where the apparent strain is about 56,500 $\mu\epsilon$.

Figure 17 is an apparent strain plot of the gages on Specimen H-29 for two consecutive cycles to 1311 K (1900 F). It is observed that (a) the curves are virtually identical from 478 K (400 F) to the maximum temperature, and (b) the maximum spread between the two curves is about 2000 $\mu\epsilon$, and (c) the zero shifts for the first and second cycles are about -1100 and -2300 $\mu\epsilon$, respectively.

Figure 18 is an apparent strain plot to 1311 K (1900 F) of the gages on Specimen H-32 for three consecutive cycles. The data points are averages of the individual gage readings. A careful inspection shows that the heat-up portion of the cycles are identical to the cool down portion of the previous cycles for all three cycles. This same type of behavior is depicted in Figure 12. It is further observed that above 700 K (800 F) the curves are virtually identical for all three cycles, and that all curves characteristically converge at the maximum temperature, where the apparent strain is about 53,500 $\mu\epsilon$. This behavior has particular significance in those applications where strain measurements may be taken at elevated temperatures that lie within a temperature range of 700 K (800 F) to 1311 K (1900 F). If the readout equipment were balanced at 700 K (800 F), the apparent strain error due to possible cycle to cycle variations would then be virtually zero at all temperatures up to the maximum temperatures. Measurement accuracy would thus be considerably enhanced. The zero-shifts for Cycles 1, 2, and 3 were -1500 $\mu\epsilon$, -1200 $\mu\epsilon$, and -1200 $\mu\epsilon$, respectively.

Figure 19 is an apparent strain plot to 1366 K (2000 F) of the gages on Specimen H-32 for three consecutive cycles. The behavior is quite similar to that illustrated in Figure 18, except that the apparent strain (77,000 $\mu\epsilon$ at 1366 K) and spread between cycles is larger. The zero-shifts are also somewhat larger. For example, the zero-shift for the first cycle was -1500 $\mu\epsilon$ instead of -1200 $\mu\epsilon$.

7.1.4 Drift Characteristics

Figures 20 through 24 are plots of drift versus time for the gages on Specimens H-21R, H-25R2, H-28, H-29, and H-32. The solid line represents the average of the data points.

Figure 20 is a four hour drift versus time plot at 922 K (1200 F) for the gages on Specimen H-21R. The envelope represents the upper and lower bounds of the data points. It is noted that (a) the scatter is large in terms of the average values, and (b) that the drift rate, which is largest at the beginning, decreases after about one hour and tends to be rather uniform thereafter. The minimum drift rate was exhibited by Gage 4, whose initial drift rate and average drift rate were -140 $\mu\epsilon$ /hr. and -41 $\mu\epsilon$ /hr., respectively. The maximum initial drift rate was exhibited by Gage 3, the

value being $-550 \mu\epsilon/\text{hr}$. The maximum average drift rate over the four hour period was exhibited by Gage 2, the value being $-96 \mu\epsilon/\text{hr}$.

The reasons for not evaluating these gages at a higher temperature are mentioned in the following discussion relating to Specimen H-25R2.

Figure 21 is a four hour drift versus time plot at 866 K (1100 F), 922 K (1200 F) and 978 K (1300 F) for a single gage on Specimen H-25R2. This specimen, which was one of five special gages with BCL-3 filaments purchased from Ailtech, was prepared to obtain preliminary information as to the maximum temperature to which the remaining four gages should be subjected during evaluation. Accordingly, drift evaluations were performed at the above mentioned progressively increasing temperatures to determine the maximum temperature at which useful data could be obtained.

It is evident from Figure 21 that the gage exhibited excellent stability with respect to drift at 866 K (1100 F) and 922 K (1200 F), the drift strain never exceeding $20 \mu\epsilon$ at any time during the four hour evaluation. (It should be pointed out that this specimen had not been subjected to any prior prestabilization.) The maximum initial drift rate and average drift rates over a four hour period were $-44 \mu\epsilon/\text{hr}$. and $+5 \mu\epsilon/\text{hr}$., respectively, which are considered excellent at these temperatures.

Between 922 K (1200 F) and 978 K (1300 F) it is evident from Figure 21 that a drastic change in drift rate occurred. The reasons for this change are not known, but it is postulated that it may be associated with the migration of gold (used to form the shank of the gage) along or into the surface of the BCL-3 gage filament. This, of course, would result in a considerable decrease in gage resistance and manifest itself as a negative drift. If this were the case, the problem could readily be eliminated by using a different plating material such as platinum which has a much higher melting point.

There was also the possibility that the excessive drift behavior might have been due to the fact that the gage was not subjected to a prior prestabilization. To investigate this possibility, Specimen H-25R2 was subjected to a five hour prestabilization at 1033 K (1400 F), after completion of the drift evaluation at 978 K (1300 F). The specimen was then re-evaluated at 922 K (1200 F) to determine if there were any benefits from the prestabilization.

The following data were obtained:

Elapsed Time, hr.	Drift, $\mu\epsilon$
0	0
1	-128
2	-375
3	-545
4	-670

These figures correspond to an initial drift rate of $-128 \mu\epsilon/\text{hr.}$ and an average drift rate of $-167 \mu\epsilon/\text{hr.}$ over the four hour period. Since these rates are considerably higher than those previously measured ($-44 \mu\epsilon/\text{hr.}$ and $+5 \mu\epsilon/\text{hr.}$, respectively), it was concluded that migration, rather than lack of prior prestabilization, was responsible for the excessive drift.

In light of the above performance, it was therefore concluded that the four Ailtech gages on Specimen H-21R should not be evaluated at temperatures exceeding 922 K (1200 F).

Figure 22 shows the 1200 K (1700 F) and 1297 K (1875 F) drift behavior of the four BCL-3 gages on Specimen H-28. It is observed that there is little scatter from gage to gage and that at 1297 K (1875 F), while not considered excessive for that temperature, it is substantially larger than at 1200 K (1700 F). The initial and average drift rates for the 1200 K (1700 F) run were $-25 \mu\epsilon/\text{hr.}$ and $-12.5 \mu\epsilon/\text{hr.}$, respectively. The corresponding values for the 1297 K (1875 F) run were $-205 \mu\epsilon/\text{hr.}$ and $-86.8 \mu\epsilon/\text{hr.}$, respectively. Since the initial values represent an instantaneous rate, which decreases rapidly, none of the above rates is considered excessive for tests of several hours duration.

Figure 23 shows the 1311 K (1900 F) drift behavior of the four BCL-3 gages on Specimen H-29. It is evident that the gage to gage scatter is greater than that displayed by the above gages on Specimen H-28 that were evaluated at 1297 K (1875 F). The following is a tabulation of the initial and average drift rates for each of the four gages:

Gage	Initial Drift Rate ($\mu\epsilon/\text{hr.}$)	Average Drift Rate ($\mu\epsilon/\text{hr.}$) over 4 hrs.
1	-65	-107.5
2	-90	-117.5
3	-25	-81.3
4	-75	-105.0
	Av = -63.8	Av = -102.8

It is evident that, except for Gage 3, there is not a great amount of scatter in drift rate from gage to gage.

Figure 24 shows the 1311 K (1900 F) drift behavior of the four BCL-3 gages on Specimen H-32. The scatter, though acceptable, is somewhat greater than that exhibited by the gages on Specimen H-28, which were evaluated at nearly the same temperature 1297 K (1875 F). The initial and average drift rates for the two gages on this specimen were:

<u>Gage</u>	<u>Initial Drift Rate</u> <u>($\mu\epsilon$/hr.)</u>	<u>Average Drift Rate</u> <u>($\mu\epsilon$/hr.) over 4 hrs.</u>
1	-269	-172.5
3	-78	-150

7.1.5 Zero-Shift

Gage "zero-shift" (sometimes referred to as zero-offset) is generally attributed to changes in the gage system itself; these changes may be mechanical and/or electrical in nature. However, when yielding occurs in the material to which the gage is attached, it becomes difficult to determine how much of the zero-shift is due to the gage and how much is due to yielding in the material.

The Haynes 25 (L-605) material used to fabricate the calibration specimens employed in this program is a cobalt-base alloy considered to have excellent high temperature strength and oxidation resistance. Nevertheless, because of the very high temperatures which were later required to determine the full potential of the BCL strain gage system, it became necessary to subject the gaged specimens to temperatures as high as 1366 K (2000 F). At this temperature, the yield strength (0.2% offset) of Haynes 25 is only about 16% of its room temperature strength of 67,050 psi, or about 12,000 psi. Using a published value for Young's modulus of 42.0×10^3 MN/m² (6.1×10^6 psi) this would correspond (on a linear basis) to a yield strain of 1967 $\mu\epsilon$ which is comparable to the room temperature yield strain of 1960 $\mu\epsilon$. Since a permanent set of over 5.08 mm (0.2 in.) was actually observed in the calibration bar, under a strain of 1883 $\mu\epsilon$ at 1366 K (2000 F), it is evident that the proportional or elastic limit of this material is substantially less than its yield strength as defined by the 0.2% offset.

Figure 25 shows the strain-deflection loop generated under reversed loading at room temperature for Gage 2 on Specimen H-32. The loop was generated by subjecting the Specimen to a deflection of 322 mils in one direction and then unloading. After unloading, a permanent set in the bar of 34.5 mils from the unbent position in the direction of loading was observed. The load direction was then reversed and the specimen subjected to a deflection of 322 mils from the bent position. (It should be noted that 322 mils corresponds to approximately 2000 $\mu\epsilon$.) The specimen was then unloaded and the permanent set and final position of the bar observed. It is noted that (a) only over certain portions of the loop is the strain-deflection relationship linear, (b) because of permanent set in the bar, it was not possible to subject the bar to 322 mils in each direction. In the negative direction it was only possible to subject the bar to -287.5 mils, instead of 322 mils, (c) there was a zero shift of about -500 $\mu\epsilon$ upon unloading from the positive direction, and (d) in spite of the permanent set in the specimen and subsequent zero shift, the specimen returned almost exactly to its initial (unbent) position within 0.3 mils (see inset), and the gage registered a final reading which was within 5 $\mu\epsilon$ of its initial "zero" reading.

Figure 26 shows the strain-deflection loop generated under reversed loading at 1311 K (1900 F) for Gage 2 on Specimen H-32. The specimen was loaded to 322 mils in the positive direction and unloaded, as before. The permanent set was 204 mils, instead of 34.5 mils (at room temperature). The specimen was then loaded in the reverse direction 322 mils from its unloaded (bent) position. The specimen was then unloaded and the deflection and gage reading observed. It is noted that (a) the size of the loop is smaller than before, (b) non-linearity still exists over some portions of the loop, (c) because of the relatively large permanent set in the bar, the deflection in the negative direction was only 118 mils from the unbent (initial) position. This reduced the total deflection range from 609.5 mils to 440 mils, and (d) in spite of the permanent set in the specimen and subsequent zero-shifts, the specimen returned almost exactly to its initial (unbent) position within 4 mils (see inset), and the gage registered a final reading which was within $-1 \mu\epsilon$ of its initial "zero" reading. This type of response at elevated temperature, and the above mentioned similar type response at room temperature, vividly illustrates that a gage can perform in a repeatable or predictable manner, even when non-linearity and zero-shifts are exhibited. It also illustrates, however, that the magnitudes of the zero-shifts are strongly influenced by the sequence of loading when yielding in the specimen occurs. For example, if the specimen had been loaded in one direction only and then unloaded (see Figure 25), the zero-shift would have been $-250 \mu\epsilon$. If the specimen were "forced" to its initial (unbent) position from its unloaded position, the zero-shift would have then changed from $-250 \mu\epsilon$ to $-500 \mu\epsilon$. If the specimen were then loaded in the same direction to -287.5 mil and then unloaded, the zero-shift would then be only $5 \mu\epsilon$.

It is therefore evident that assessment of gage performance, in terms of zero-shifts, can get rather involved when yielding in the specimen occurs, since the magnitude of the zero-shift is highly load-path dependent.

Table 6 is a summary of the zero-shifts associated with the gage-factor evaluation portion of this study. (For information on the zero-shifts associated with the apparent strain evaluation, refer to 7.1.3.) The table entries are self-explanatory, except for the correction factors, which were obtained by multiplying the measured permanent set (after removal of the load) by the calibration factor, which represents the number of microstrains induced in the specimen per mil of deflection. This correction factor would therefore represent the strain induced in the specimen, if it were deflected an amount equal to the permanent set at the deflection dial gage location. If the zero-shift were due solely to the permanent set in the specimen, the zero-shift and correction factor magnitudes would then be equal. Thus, any differences in magnitudes between them represent zero-shifts attributable to causes other than permanent set in the bar, such as residual strains resulting from yielding at and near both faces of the specimen, or possible yielding in the gage system, itself. The following general observations may be made:

- (1) Zero-shift characteristics are strongly influenced by the manner of loading. Under reversed loading, the zero-shifts

exhibit a periodicity which is due primarily to the plastic deformation in the specimen. This periodicity is clearly depicted in the behavior of Specimens H-29 and H-32 under reversed loading. For example, on Specimen H-32, Gage 1, 1311 K (1900 F) run, zero-shifts of +1252 $\mu\epsilon$, +32 $\mu\epsilon$, +1165 $\mu\epsilon$, -14 $\mu\epsilon$, +1204 $\mu\epsilon$, +9 $\mu\epsilon$, occurred when the specimen was subjected to three completely reversed cycles comprised of the half-cycles, 1(T), 1(C), 2(T), 2(C), 3(T), 3(C). The other gages on Specimen H-32 responded similarly. It is noted that the "odd" half-cycles 1(T), 2(T), and 3(T) produce maximum zero shifts of +1252 $\mu\epsilon$, +1165 $\mu\epsilon$, and +1204 $\mu\epsilon$, whereas the "even" half-cycles produce minimum zero-shifts of +32 $\mu\epsilon$, -14 $\mu\epsilon$, +9 $\mu\epsilon$. This type of periodicity was also exhibited by the other specimens which were subjected to reversed loadings. The explanation for this periodicity, in terms of the deflection-strain cycle, is graphically presented in Figures 25 and Figures 26. On the other hand, those specimens which were subjected to non-reversed loadings did not exhibit periodicity; rather they tended to have zero-shifts which generally changed little from cycle to cycle, resulted in increased total permanent set.

- (2) All other factors equal, the higher the strain level, the larger will be the zero-shift. (This was, in fact, the reason the strain levels for Specimen H-28 and H-29 had to be reduced in some instances.)
- (3) All other factors equal, the higher the temperature, the larger the zero-shifts.
- (4) The larger the specimen permanent set, the larger will be the zero-shifts. For example, on Specimen H-32, room temperature run, the specimen permanent set was between 33.3 and 34.9 mils, with zero-shifts not exceeding 279 $\mu\epsilon$. On this same specimen, for the 1311 K (1900 F) run, the permanent set in the specimen varied from 202 to 222 mils, with corresponding zero-shifts as high as 1252 $\mu\epsilon$.
- (5) Where appreciable permanent set occurred (>30 mils), the magnitude of the correction factors and zero-shifts for non-reversed loadings were often of the same general magnitudes, indicating that permanent set was the primary cause of zero-shift. For example, for the specimen H-28 room temperature run, the application of the correction factor reduces the zero-shifts for Gages 1 and 2 from +220 and +213 to +8 and +2, respectively. In the case of reversed loadings, the magnitudes of the correction factors and the maximums of the zero-shifts were also often of the same general magnitude. For example, for Specimen H-32, room temperature run, for Cycles 1(T), 2(T), and 3(T) the permanent sets and corresponding zero-shifts for Gages 1 through 4 were:

Permanent set (mils)

Zero-shifts, $\mu\epsilon$

227	-254, -259, +273, +265
223	-252, -258, +279, +272
225	-247, -251, +281, +273

- (6) Under repetitive cycling (reversed or non-reversed), the zero-shift readings are, in general, quite repeatable, particularly for the second and third cycles, as evidenced from the above three sets of readings, and, for example, the three 1311 K (1900 F) tensile cycles for Specimen H-29, which read +291 $\mu\epsilon$, +216 $\mu\epsilon$, and +215 $\mu\epsilon$.

7.1.6 Resistance to Ground

Table A-1, Appendix A, summarizes the resistance to ground values obtained with a VTVM (or Megger) for each specimen, at various steps in the evaluation. The thicknesses of the precoats and substrates are:

<u>Specimen</u>	<u>Nichrome Precoat, Mils</u>	<u>50% Nichrome- 50% Alumina Precoat, Mils</u>	<u>Rokide Substrate Thickness, Mils</u>
H-26R2	3	3	3
H-28	3	3	5
H-29	3	3	5
H-32	3	3	5

Inspection of the resistance to ground values in Table A-1 shows excellent and consistent resistance values for Specimen H-21R at the maximum evaluation temperature of 936 K (1225 F). Specimens H-26R2, H-28, and H-32 showed infinite resistance at room temperature. (To expedite evaluation, measurements of room temperature resistances for the other specimens were not taken; nor were measurements taken at every evaluation temperature for every specimen.)

An inspection of the values at elevated temperatures shows no particular trend from specimen to specimen or, in some instances, from gage to gage in the same specimen. For example, on Specimen H-28, at 1316 K (1909 F), the resistance of the four gages varied from 70 K ohms to more than 600 K ohms. In general, however, the gage to gage variations observed are not considered unusual.

It is also noted that some of the highest resistance values measured occurred at the highest temperatures. Specimens H-26R2 and H-32 for example, had resistances to ground at a nominal temperature of 1366 K (2000 F) of at least two megohms, in contrast to values between 60 K ohms and 600 K ohms at a nominal temperature of 1311 K (1900 F). There also appears to be no particular trend with respect to prior exposure history on resistance to ground, i.e., with respect to degradation with time at temperature. Also, the gages on Specimen H-26R which had the thinner three mil thick Rokide substrate performed as well, or better, than some of the specimens with a five mil thick substrate. It should be pointed out that, in the previous program, it was established that a five mil thick substrate was required to provide increased resistance to oxidation at the interface of the substrate and base material.

At that time no precoats were used and it is possible that a five mil substrate would be no longer required, since protection of the interface against oxidation is now provided by the precoat system. A question consequently arises as to whether the substrate thickness could be reduced to three mils if applied over the two precoat layers. It is believed that there is not sufficient data, at this time, to warrant such a change.

Since no degrading effects on gage performance were observed during the study that could be attributed to low resistance to ground problems, it is presumed that the present system for bonding and electrically insulating the gages is adequate.

No explanation can be offered as to the lack of a particular trend in the resistance values, as above discussed, except to say that it is difficult at best to make precise resistance to ground measurements, even at lower temperatures. Also, it is conceivable that resistance to ground variations in the MgO insulated lead wire systems used, might account for some of the gage to gage and possibly some of the specimen to specimen variations.

7.1.7 Thermal and Mechanical Shock

Specimen H-28 was subjected to 25 severe thermal shocks at a heating rate of 39 K/sec. (70 F/sec.) utilizing the evaluation procedure outlined in 3.3.1. It was the purpose of this evaluation to determine whether the precoat Rokide substrate/Rokide final coat system could withstand severe thermal shock. No signs of failure were observed between the precoat and the specimen or between the precoat and the Rokide substrate, or between the substrate and the Rokide final coat. Temperature range during shocking was from 373 K to 1311 K (212 F to 1900 F).

A special specimen (Hopkinson bar) was subjected to severe mechanical impact, utilizing the evaluation procedure outlined in 3.3.2. Figure 27 is a plot of gage factor x measured strain versus true strain at room temperature. It is noted that the gages exhibited excellent linearity and that the differences between the two gages were not large.

There were no indications of bond failure resulting from the application of the 13 increasingly severe mechanical shocks (impacts) which produced strains in the specimen ranging from 571 $\mu\epsilon$ to 2353 $\mu\epsilon$. After removal of the specimen from the Hopkinson apparatus, gage resistance and resistance to ground were measured. There was no measureable change in gage resistance for either gage in spite of the severe multiple impacts and relatively large strain range. Excellent resistance to ground was still maintained; one gage read infinity, and the other gage 200 Megohms, after completion of the evaluation.

7.1.8 Performance History

Table 7 summarizes--on a fail or no-fail basis--the gage performance of gages subjected to the evaluation sequences delineated in Table 6. It is

noted that (a) no failure occurred with any of the four Ailtech gages on Specimen H-21R, which were evaluated to a maximum temperature of 922 K (1200 F), (b) no deterioration in the bonding system, of sufficient magnitude to preclude further evaluation, occurred in any of the remaining specimens, except Specimen H-26R2, which experienced a partial bond failure at 1366 K (2000 F) and Specimen H-32 which experienced a partial substrate separation after the room temperature evaluation of the 1366 K (2000 F) run, (c) virtually all other failures were associated with breaks or cracks in the lead-tabs during evaluation at elevated temperature. A review of the circumstances surrounding these failures indicates that the lead-tab ribbon failures were due to a combination of embrittlement of the lead-tab ribbon from oxidization due to the severe exposure and to tensile loads on lead-tab ribbons due to differential thermal expansion between the 20 ga, 3-conductor Hoskins Alloy 875 lead wire cable and the specimen support structure (box beam). (It should be noted that the box beam undergoes a longitudinal expansion of approximately 9.5 mm (3/8 in.) during heat-up from room temperature to 1311 K (1900 F). Although "flexibility loops" were incorporated in the lead tab ribbons, it is believed that sufficient load was generated by the large amount of thermal expansion to cause failure of the embrittled ribbon. It is also believed that some of the embrittlement may have been due to the manner in which the lead-tabs were cleaned, prior to resistance welding. The surface oxide film was removed by an abrading process, which may have reduced the ductility of the ribbon due to work hardening or other factors. Also the cross-sectional area was reduced by the abrading process. In future work, it is proposed to remove the oxide by means of chemical etching and neutralizing. Substitution of ribbon of a different material such as Nichrome is not proposed, since this would introduce a dissimilarity of materials. Further, in nominal use, exposure at temperature will be for considerably less periods of time (≈ 1 hr.), and it is doubtful that the oxidation would be sufficient to cause lead tab failure, if adequate flexibility loops are provided.

The above comments apply to gage performance, under static evaluations conditions, with the exception of Specimen H-28, which was also subjected to the thermal shock history specified in 7.1.7. No failures due to thermal shocking occurred to the gages on this specimen or to the two gages on the Hopkinson bar specimen, which was subjected to mechanical shock tests. For additional details on the results of the dynamic evaluation of these two specimens, refer to 7.1.7.

For information pertaining to performance with respect to gage factor, apparent strain, drift, zero-shift, and resistance to ground, refer to Sec. 7.1.2 through 7.1.6.

7.2 Joint Evaluations

Table 8 summarizes the results from the mechanical (tensile) strength evaluations of joint specimens prepared by means of the NASA butt-weld, pulse arc, and laser joining processes. It is noted that (a) the average breaking load for the NASA BCL-3 to BCL-5 butt-welds was 0.73 N (2.63 oz.). This compares with a breaking load of 0.79 N (2.83 oz.) for the BCL-5 base material. (b) Of the 12 samples, none of the breaks occurred in the weld joint, or in the BCL-3 wire, indicating excellent joint efficiency and higher strength properties for the BCL-3 wire than the BCL-5 wire. (The BCL-3 wire was as-drawn wire, whereas the BCL-5 wire was air annealed.) (c) Of the three joining processes for making the wire to lead tab ribbon joint, the NASA butt-weld process was superior, in terms of breaking load, (0.53 N versus 0.75 N or 1.15N) even though all failures occurred at the joint. The fact that all failures occurred at the joint is not surprising in view of the abrupt change in cross-sectional area at the joint location. (The stress concentration factor due to this abrupt change could be moderated considerably by tapering the ribbon.)

Table 9 summarizes the results of the mechanical strength evaluations for six different joint configurations prepared with the DC parallel gap welding process. It is noted that (a) the perpendicular-folded (9E-F0) joint Configuration 8, with BCL-3 as-drawn wire, had the highest average breaking load (1.58 N). (b) Configuration 1, which is similar to Configuration 8 except that air-annealed rather than as-drawn BCL-3 wire was used, had an average breaking load of only 0.67 N. Similar differences are also noted for Configurations 2 and 5. It is therefore obvious that a large portion of the superior performance of Configurations 5 and 8 can be attributed to the use of as-drawn, rather than air-annealed wire. Had the evaluations been performed at elevated temperatures, however, these differences in strength would have been much less. (c) The use of Cu electrodes results in joints having less strength than those prepared with Mo electrodes and results in a much larger percentage of "no welds", as is evident from a comparison of Configurations 2 and 4. (d) Excluding Configurations 3, 5, and 8, which were all prepared with the as-drawn wire, and Configuration 2, which is for Cu electrodes, which wear rapidly and produce a large percentage of no welds, Configurations 1 and 4 are the only remaining configurations with air-annealed wire and Mo electrodes. The difference in strength between these two configurations is not great; however, none of the failures for Configuration 1 occurred at the joint, whereas 16% of the failures for Configuration 4 occurred at the joint. It is believed that, although Configuration 4 is about 18% stronger than Configuration 1 under static loading, under cyclic mechanical or thermal loading Configuration 1 would prove to be the superior of the two configurations, because of the differences in failure locations and the probable differences in fatigue stress concentration factors at these two locations.

On the basis of the above results, Configuration 1 was selected as the most promising joint geometry to use with BCL-3 wire, as far as mechanical strength and weld uniformity is concerned. (Electrical resistivity

characteristics will be discussed later.)

Table 10 summarizes resistivity changes in 12 BCL-3 to BCL-5 wire specimens NASA butt-welded joints. It is noted that (a) there was approximately 5 ohms variation in initial room temperature resistance. This variation, in part, is due to slightly different specimen lengths and possibly, in the case of Specimens 5 and 7, due to imperfect joints as later evidenced by marked increases in specimen resistance. (b) There was a slight increase in specimen resistance when the temperature was raised to 1144 K (1600 F), and only a slight further increase in resistance during the 3.67 hour soak period at this temperature, as evidenced by the small changes in the three sets of reading during this period, including the set of readings taken at the mid-period. (c) Upon return to room temperature, after completion of the first cycle, it is evident that the specimens experienced a slight permanent increase with respect to the original room temperature, which was probably due to oxidation. During the second cycle at 1144 K for 3.42 hours, the increase in resistance with time were, in general, even less than during the first cycle, except for Specimen 4. (d) There was little increase in resistance in going from 1144 K (1600 F), Cycle 2 to 1311 K (1900 F), Cycle 3, and only a slight change in resistance over the 4.75 hour period at temperature. At this point the changes were both positive and negative, indicating further oxidation or possible initiation of joint deterioration which would cause an increase in specimen resistance or depletion of Al from the wire, which would cause a decrease in specimen resistance. (e) After return to room temperature, all specimens, except 5, 7, and 8, experienced a net decrease in room temperature resistance, probably due to Al depletion, which is also evident during gage prestabilization. This increase in resistivity of these three specimens is believed due to joint degradation. The causes for the slight instability in Specimen 6 is not known.

The last column in Table 10 is a tabulation of the unit changes in specimen resistance, with respect to final room temperatures and room temperature resistances after the first cycle. The positive changes therein indicated represent unit changes of +12.8%, +12.6%, +0.8% for Specimens 5, 7, and 8 and are believed due to joint degradation because they show positive rather than negative changes in resistance. Further, unit resistivity changes as large as those exhibited by Specimens 5 and 7 could not be attributed to metallurgical changes in the wire, even if they were negative. Excluding the three specimens barring a positive change, the range in change in unit resistance is from -4.2×10^{-3} to -23.69×10^{-3} . For a room temperature gage factor of 2.6, this would correspond to a change of $-1619 \mu\epsilon$ to $-9111 \mu\epsilon$, after exposure at 1144 K (1600 F) for 3.42 hours and 4.75 hours at 1311 K (1900 F). For tests of one hour duration, these changes would, of course, be considerably less, and the performance of the NASA butt weld joint is therefore considered a satisfactory joining technique for making gage filament to gage filament joints for self temperature compensating composite strain gages, particularly if the gage "turns ratio" were established to provide minimum apparent strain over the range in temperature of interest.

Table 11 summarizes resistivity changes for 12 BCL-3 wire to Alloy 875 ribbon specimens prepared with the NASA butt-weld technique. The behavior is, in general, similar to that exhibited by the BCL-3 to BCL-5 wire specimens, except that no erratic behavior in any specimen was observed. The average drift rate for Cycle 1 is micro-ohms/hr. (It should be noted that the measurements taken during Cycle 2 were over short periods of time and were taken to provide information on changes in resistivity with temperature and were not intended to provide drift information.) It is further noted that the average difference between the initial room temperature and final room temperature values does not exceed one ohm, and that there were no specimens which exhibited excessively large changes (positive or negative). It is therefore concluded that all specimens performed satisfactorily, and that the NASA butt weld technique produces sound electrical BCL-3 to Alloy 875 ribbon joints.

Table 12 summarizes the electrical resistivity characteristics of the joint specimens, which were prepared by the DC parallel gap welding process, for five of the six joint configurations. Resistivity measurements were not taken for the joint Configuration 2, because of the very poor consistency of weld joints made with the Cu electrodes. To minimize the effects of longitudinal temperature gradients within the miniature furnace, the data for the 12 specimens were paired together to form six groups--each pair comprised of specimens that were closely matched with respect to furnace temperature. Because of the differences from pair to pair due in part to furnace temperature gradients, evaluation of the data was done taking the average of the resistivity changes for all pairs representing each joint configuration. Further, to put all resistivity changes on the same time basis, they were converted to resistivity changes per hour (average drift rate) of exposure at temperature. The following is a tabulation of the drift rates obtained in this manner from the unit resistivity changes and time intervals for each cycle:

<u>Joint Type</u>	Av. Drift Rate during Cycle 1 soak, <u>micro-ohms</u> <u>ohm-hr.</u>	Av. Drift Rate during Cycle 2 soak, <u>micro-ohms</u> <u>ohm-hr.</u>
1	1173	-2045
3	-1607	436
4	9494	-4865
5	776	--
8	24261	-13596

It is noted from the above that (a) on the basis of Cycle 1 results, joint Type 5 was the best in terms of the average resistivity changes. Also, referring back to the individual unit changes, it is evident that they were also small, of the same general magnitude (1.08 to 5.78×10^{-4}) and of the same sign. This was not true of most of the other joints. (b) In terms of

Cycle 2 data, no conclusions can be drawn with respect to Joint Type 5, since difficulties were encountered in taking the Cycle 2 resistivity data for it and, consequently, were omitted from Table 12. Therefore, on the basis of the data obtained for Cycle 2, Joint Type 3 performed the best. (c) For joints prepared with air-annealed BCL-3 wire, it is evident that Joint Type 1 was the best performer, in terms of Cycle 1 and Cycle 2 results. It should be pointed out that this was the joint type used for fabrication of the prototype BCL-3 gages evaluated in this program. (Joint Types 3 and 5 utilize as-drawn BCL-3 wire.)

The following represents the average room temperature unit changes in resistivity, before and after the Cycle 1 soak. They were obtained by averaging the individual values listed in the last column of Table 12.

<u>Joint Type</u>	<u>Av. Unit Chg. in Rm. Temp. Resistance, %</u>
1	1.22
3	0.09
4	-0.81
5	--
8	1.90

It is evident that Joint Type 3 had the lowest average unit change in room temperature resistance. (It also had the best performance in terms of Cycle 2 drift performance.)

In summary, if as-drawn wire is used it appears that, on the basis of the limited data, (Cycle 1 only), Joint Type 5 is the best performer. However, if Cycle 1, Cycle 2, and room temperature unit changes in resistivity are considered, it appears that Joint Type 3 is the best, or at least the next best in performance. If air-annealed wire is used, it appears that Joint Type 1 would be the best, even though its room temperature unit changes in resistivity are greater than that for Joint Type 4, because of its superior Cycle 1 and Cycle 2 drift performance. Since Joint Type 1 was also found superior from the standpoint of mechanical strength, for use with BCL-3 air-annealed wire, it is therefore selected as the best type for use with the DC parallel gap welding process.

7.3 Barrier Coating Evaluation

The three barrier coated Specimens BC-1, BC-2, and BC-3 described in 5.2 and subjected to the evaluation history delineated in Table 3 were monitored periodically, during the 911.6 hours evaluation period with respect to changes in resistance to ground which, initially was infinity as determined with a megger. It was felt that a break-down in the barrier coating, due to exposure at temperature and cyclic straining of Specimens BC-1, BC-2, and BC-3 to

strain levels of 0, 1000 $\mu\epsilon$, and 1500 $\mu\epsilon$, respectively, would provide the most reliable means of determining when moisture penetrated the barrier coating. For further discussion on this point refer to 5.2.

No changes in resistance to ground were observed until after 502.6 hours, which was after the 533 K (500 F) soak which occurred between 363 to 409.3 hours. At that time, while in the 98% humidity environment, the gage on BC-2 dropped to 100 meg-ohms. At the end of 522.6 hours, the gage on Specimen BC-3 also dropped to 100 meg-ohms, with the gage on BC-1 still retaining infinite resistance. This indicated that a slight amount of deterioration of the coating had developed as a result of the combined exposure at temperature and strain.

After removal of the specimens from the 98% humidity chamber, (at 525.2 hours) the resistances to ground of Specimen BC-1, BC-2, and BC-3, while under strains of 0, 1000, and 1500 $\mu\epsilon$, increased to 2000, 170, and 2000 meg-ohms, respectively. The evaluation was continued and it was noted that during the 616 K (650 F) soak (530 to 575 hours) the resistance of the gage on BC-3 dropped to as low as 5 meg-ohms, while the resistances of the other two gages increased. As noted from Table 3, all three gages were under strain during this soak. Upon return to room temperature, ambient conditions (at 575 hours), while still under 0, 1000, and 1500 $\mu\epsilon$ levels, the gage resistances increased to ∞ , 150 kilomeg-ohms, and 55 meg-ohms.

The specimens were then reinstalled in the humidity chamber (at 575.6 hours), under strains of 0, 1000, and 1500 $\mu\epsilon$ and a steady decrease in resistance was observed on Specimens BC-1 and BC-2 until the evaluation was terminated at the end of 911.6 hours. On Specimen BC-3 an interesting pattern was observed:

<u>Elapsed Time, (hr.)</u>	<u>Resistance to Ground, Meg-ohms</u>
575.6 to 583.5	56
583.5 to 642.3	120
642.3 to 642.5	180
642.5 to 651	180
651 to 667.2	105
667.2 to 697.2	70
697.2 to 911.6	7

Apparently, for a period of time, a more favorable moisture balance was established to permit the resistance to increase to 180 meg-ohms, and then decrease to 7 meg-ohms due to pick-up of additional moisture through the cracked barrier coating which was subjected to the highest strain level (1500 $\mu\epsilon$).

7.4 Coated Wire Evaluation

Figure 28 is a plot of the unit resistance versus temperature for platinum coated and uncoated BCL-3, 2 mil diameter wire. The top curve is for BCL-3 wire with a platinum coating which was deposited by sputtering for 20 minutes. The intermediate curve is for BCL-3 wire similarly coated, with a sputtering time of only 10 minutes, which resulted in a coating thickness that provided optimum temperature compensation from room temperature to 1089 K (1500 F).

It is noted that the curve is flat to at least 600 K (620 F), and that at 1089 K (1500 F), the change in resistivity is only about 40% of that for the uncoated wire. More importantly, these curves vividly demonstrate what can be achieved with the "clad-wire" concept in terms of temperature compensation. It is now believed that it should be possible to produce platinum-clad BCL-3 strain gages, which will have considerably reduced apparent strain output, and enhanced oxidation resistance, by utilizing platinum clad wire of the appropriate thickness. This clad-wire could be produced by sputtering or by a co-extrusion process.

CONCLUSIONS

Based on the information obtained in this program, it is concluded that the strain gage system herein developed should perform satisfactorily at temperatures up to at least 1311 K (1900 F) for periods of time up to at least one hour at the maximum temperature. Because of the limited number of specimens evaluated in replica and yielding in the calibration bar, establishment of accuracy limits on a statistical basis was not possible. Nevertheless, sufficient static (gage factor, linearity, apparent strain, drift, zero-shift resistance to ground) and dynamic (thermal and mechanical shock) data on gage performance were obtained to provide an overall characterization of gage system performance.

The tendency of the apparent strain curves to characteristically converge to the maximum evaluation temperature was observed in this program, as well as the previous program carried out under NASA Contract NAS1-11277. (For a detailed discussion on the technical significant of this characteristic, refer to p. 25 of NASA CR-112241). It was shown in this program with actual test data that the heating up portion of the apparent strain cycle retraces the previous cooling down cycle within very close limits, because of the convergence characteristic. It is concluded that this characteristic provides a viable way to obtain the apparent strain calibration curves with high accuracy.

The graded precoat system developed in this program was successful in eliminating the bond failures which occurred in the previous program in the vicinity of 1089 K (1500 F). Although there was evidence of minor separation at the edges of the coating or substrate at 1311 K (1900 F), after many hours of evaluation at various temperatures, it is concluded that, for tests of one hour duration at maximum temperature, the coating system should perform adequately to 1366 K (2000 F), or higher.

Most of the failures that occurred in the gage system during evaluation were attributed to breaks or cracks in the lead tab ribbons. Careful examination revealed that the failures were caused by (1) embrittlement associated with oxidation of the ribbon during evaluation and/or embrittlement caused by the abrading procedure used to clean the lead-tabs, prior to welding, and (2) restraints to free thermal expansion of the test fixture which caused excessive loads to be imposed on the lead tabs, even though expansion loops in the lead-tab ribbons were provided. It is concluded that the new lead-tab ribbon cleaning procedures, utilizing etching rather than abrasion, should eliminate lead-tab ribbon embrittlement from this source, and that tests of one hour duration at maximum temperature should not pose a problem with respect to lead-tab ribbon embrittlement due to oxidation. Greater care in the design of the lead tab and lead wire flexibility loops and in selection of the location of points to "anchor" the lead wire cables, should eliminate failure due to excessive loading of the lead-tab ribbons.

It is concluded that substitution of BCL-3 wire for the Pt-W wire filaments in Ailtech type SG 420 strain gages was only of limited success,

due to excessive draft above 922 K (1200 F). Although the use of BCL-3 alloy increased the static maximum operating temperature from 755 K (900 F) to 922 K (1200 F), it was hoped that the maximum operating temperature could be extended much more. It is believed that this excessive drift is due to migration (at the higher temperatures) of the gold plating on the filament shank, and that this migration could be eliminated by substituting a plating having a much higher melting point.

It was clearly demonstrated in this program that the clad-wire concept provides a viable means of temperature compensating BCL-3 alloy wire to 1033 K (1400 F), when Pt is used as the cladding. Further past work indicates that it should be possible to produce platinum-clad wire of strain gage size with commercially available co-extrusion processes. Above 1033 K (1400 F), the apparent strain for BCL-3 gages installed on Haynes 25 base material becomes positive; thus a cladding material with a negative temperature coefficient of resistivity above this temperature would be required to provide compensation. One alloy, BCL-4 (Fe-20 Cr-10 AL 0.1 Y) developed at Battelle, but not investigated in this program, has a negative temperature coefficient of resistance to at least 1478 K (2200 F). Presumably, this alloy could likewise be sputtered to provide effective temperature compensation to temperatures approaching 1478 K (2200 F).

Evaluation of several different joining processes (NASA Butt welding, pulse-arc, plasma-needle arc, laser, and dc parallel gap welding), revealed that the NASA butt-welding technique, dc parallel gap, and resistance spot welding processes were the best processes for making BCL-3 to BCL-5 wire butt joints, BCL-3 wire to Hoskins Alloy 875 gage filament to lead-tab ribbon joints, and lead-tab ribbon to lead-wire joints, respectively. It was also established that the folded ribbon, with the electrode perpendicular to the wire (Joint Type 1), provided the best configuration for joining with the dc parallel gap welding process.

Finally, it is concluded that the BLH Barrier H Water Proofing offers only limited protection against moisture penetration into the strain gage area after exposure to temperatures of 589 K (600 F) and straining to a maximum of 1500 $\mu\epsilon$. However, it is believed that even this limited protection may be useful in those applications where the gage installation is subjected to relatively high humidity conditions for extended periods of time at ambient temperature, prior to taking strain measurements at temperature.

ACKNOWLEDGEMENTS

Battelle-Columbus Laboratories wishes to express their gratitude to Mr. Chris Gross (Head Sensor Physics Section, Instrument Research Division, NASA Langley Research Center) and his staff for their valuable contributions relating to platinum coating BCL-3 wire specimens with the sputtering process, and to measuring the resistivity versus temperature characteristics of the platinum coated wires. Appreciation is also expressed to Mr. W. M. Haraway, Jr., (Head Materials and Processes Development Section, Fabrication Division, NASA Langley Research Center) and his staff, including Messrs. W. P. Kabana and T. P. Kelly, for preparation of the joint samples, utilizing the NASA butt-weld technique.

Thanks are also expressed to Mr. A. Witzerman, (Supervisor, Explosive Developments Component Section, Mound Laboratory, Miamisburg, Ohio) and his staff, including Messrs. G. Nesslage and D. Kaser, for use of percussive welding equipment, and for preparation of the joint samples utilizing the laser welding technique.

TABLE 1. HAYNES 25 SPECIMEN MATERIAL PROPERTIES

Mechanical Properties							Chemical Composition	
Temperature		Ultimate Tensile Strength		Yield Strength (0.2% Offset)		% Elongation (in 4 Diameters)	Element	%
^o K	^o F	N/m ²	psi	N/m ²	psi			
R.T.	R.T.	9.786 x 10 ⁸	141,950	4.622 x 10 ⁸	67,050	61	Cr	19.17
922	1200	7.100 x 10 ⁸	103,000	2.412 x 10 ⁸	35,000	35	W	14.91
1089	1500	3.447 x 10 ⁸	50,000	2.482 x 10 ⁸	36,000	16	Ni	10.50
1255	1800	2.343 x 10 ⁸	34,000	1.586 x 10 ⁸	23,000	41	Fe	2.68
1366	2000	1.448 x 10 ⁸	21,000	0.47 x 10 ⁸	11,000	19	Mn	1.48
							Si	0.36
							C	0.10
							P	0.010
							S	0.002
							Co	balance

TABLE 2. TEST MATRIX

Specimen Number	Description of Static Calibration Specimen	Max. Run Eval. Temp.		Step										
		°K	°F	1	2	3	4	5	6	7	8	9		
H-21R	Four Ailtech SG 420 gages with BCL-3, 1 mil dia. vacuum annealed wire. Gages resistance spot-welded to calibration bar.	922	1200	x	x	x	x	x	x	x				
H-25R2	One Ailtech SG 420 gage with BCL-3, 1 mil dia. vacuum annealed wire. Gages resistance spot-welded to calibration bar.	866	1100											x
		922	1200											x
		977	1300											x
		1033	1400											x
		1089	1500											
H-26R2	Four BCL-3 gages. Standard installation ⁽¹⁾	1366	2000	x	x	x	x ⁽²⁾			x				
H-28	Four BCL-3 gages. Standard installation ⁽¹⁾	1200	1700	x			x	x	x	x				x
		1255	1800	x	x		x	x						
		1311	1900	x			x	x	x	x				
H-29	Four BCL-3 gages. Standard installation ⁽¹⁾	1311	1900	x	x	x	x	x ⁽³⁾	x	x				
		1366	2000	x	x		x	x						
H-32	Four BCL-3 gages. Standard installation ⁽¹⁾	1311	1900	x		x	x	x	x	x				x
		1366	2000	x	x					x				

(1) Precoats:

Layer 1 - Nichrome, 3 mils thick
 Layer 2 - 50%-50% mixture of Nichrome and alumina, 3 mils thick

Note: 1 mil = .025 mm

Substrate:

Rokide - 5 mils thick

(2) Room Temperature precycling only.

(3) Gage factor to 700 $\mu\epsilon$ only because of excessive yielding in bar.

TABLE 3. BARRIER COATING EVALUATION HISTORY

Elapsed Time, hr.	Exposure Increment, hr.	Nominal Temperature °K (°F)	Imposed strain, $\mu\epsilon$	Humidity, %
0 to 73.3	73.3	RT	0,0,0	98
73.3 to 145.0	71.7	"	0,1000,1500	"
145.0 to 164.8	19.8	"	" " "	AMB
164.8 to 213.0	48.2	394 (250)	" " "	"
213.0 to 213.5	0.5	RT	" " "	"
213.5 to 311.2	97.7	"	" " "	98
311.2 to 357.5	46.3	"	0,0,0	"
357.5 to 363.0	5.5	"	0,1000,1500	AMB
363.0 to 409.3	46.3	533 (500)	" " "	"
409.3 to 411.0	1.7	RT	" " "	"
411.0 to 480.5	69.5	"	" " "	98
480.5 to 525.2	44.7	"	0,0,0	"
525.2 to 530.0	4.8	"	0,1000,1500	AMB
530.0 to 575.0	45.0	616 (650)	" " "	"
575.0 to 575.6	0.6	RT	" " "	"
575.6 to 642.5	66.9	RT	" " "	98
642.5 to 911.6	269.1	RT	0,0,0	"

TABLE 4. SPECIMEN H-21R (AILTECH) GAGE FACTOR CHARACTERISTICS (ROOM TEMPERATURE)

True Strain, $\mu\epsilon$	Measured Strain, $\mu\epsilon$			
	-Cycle 2-			
	Gage 1	Gage 2	Gage 3	Gage 4
0	0	0	0	0
244.5	264	268	-223	-231
644.5	643	640	-565	-581
1044.5	966	961	-893	-910
1444.5	1273	1268	-1222	-1239
1844.5	1567	1560	-1546	-1565
0	2	3	-7	-7
	-Cycle 3-			
0	0	0	0	0
244.5	256	260	-217	-226
644.5	636	632	-560	-574
1044.5	959	954	-866	-902
1444.5	1268	1262	-1217	-1234
1844.5	1566	1557	-1542	-1562
0	1	-2	-2	-4

TABLE 5. GAGE FACTOR SUMMARY

Specimen	Temperature		Tension	Compression
	^o K	^o F		
H-21R (Ailtech Gages)	RT	RT	2.04	-1.68
	589	600	1.70	-1.75
	922	1200	1.84	-1.90
H-28	RT	RT	2.80	-2.82
	755	900	1.95	-1.96
	1200	1700	1.72	-1.68
	1255	1800	1.36	-1.36
H-29	RT	RT	2.47	-2.46
	811	1000	1.84	-1.92
	1311	1900	1.54	-1.48
	1366	2000	1.18	-1.29
H-32	RT	RT	2.16	-2.32
	811	1000	1.84	-1.85
	1311	1900	1.64	-1.58

Note: The above gage factors are nominal values. They have not been corrected for "stand-off", or lead-wire resistance. At room temperature, the combined correction factor for which the above values should be multiplied by is 1.049. The correction factor for stand-off above which is applicable at all temperatures, is 1.067.

TABLE 6. ZERO-SHIFTS

Spec. No.	Nominal Temperature		Type of Loading	Cycle No.	Maximum Calibration Strain, $\mu\epsilon$	Specimen Permanent Set, Mils	Correction Factor, $\mu\epsilon$	Zero-Shift, $\mu\epsilon$			
	$^{\circ}\text{K}$	$^{\circ}\text{F}$						Gage 1	Gage 2	Gage 3	Gage 4
H-21R	RT	RT	S ⁽¹⁾	1(T) ⁽³⁾	2000	23.6	155.	+70	+69	-74	-81
				2(T)	2000	24.7	163.	+72	+72	-81	-88
	589	600	S	1(T)	2000	53.7	354.	+277	+287	-308	-316
				2(T)	2000	54.3	358.	+274	+305	-306	-316
	922	1200	S	1(T)	2000	47.5	313.	+91	+163	-100	-108
				2(T)	2000	48.3	318.	+76	+193	-84	-79
H-28	RT	RT	S	1(T)	2000	32.1	212.	+220	+213	+343	+486
				2(T)	2000	34.0	224.	+236	+227	+348	+503
	811	1000	S	1(T)	1600	59.2	390.	-306	-318	+302	+303
				2(T)	1600	26.5	175.	-54	-50	+110	+107
	1255	1800	S	1(T)	1500	92.6	610.	--	-410	+347	+403
				2(T)	1500	96.6	636.	--	-424	+394	+409
H-29	RT	RT	R ⁽²⁾	1(T)	2000	25.5	168.	-205	-204	+217	+216
				1(C) ⁽⁴⁾	2000	26.5	175.	+36	+13	+8	+8
	811	1000	R	1(T)	1500	9.0	59.	-77	-62	+75	+82
				1(C)	1500	13.4	88.	+135	+142	+21	-15
				2(T)	1500	11.1	73.	-32	-17	+159	+116
				2(C)	1500	11.2	74.	+164	+169	+152	+30
				3(T)	1500	10.9	72.	+17	+28	+277	+157
				3(C)	1500	10.9	72.	+220	+226	+214	+74
	1311	1900	S	1(T)	800	36.5	241.	+291	+180	-292	-199
				2(T)	800	43.5	287.	+216	+201	-237	-245
				3(T)	800	45.8	302.	+215	+190	-257	-269
	1311	1900	S	1(C)	700	39.0	257.	-184	-187	217	187
				2(C)	700	44.2	291.	-216	-217	236	200
				3(C)	700	47.8	315.	-246	-248	237	195

(1) Load applied in same direction

(2) Reversed loading; load applied in one direction; then applied in opposite direction

(3) First cycle tension (Gages 1 and 2 in tension; Gages 3 and 4 in compression)

(4) First cycle compression (Gages 1 and 2 in compression; Gages 3 and 4 in tension)

TABLE 6. (Continued)

Spec. No.	Nominal Temperature		Type of Loading	Cycle No.	Maximum Calibration Strain, $\mu\epsilon$	Specimen Permanent Set, Mils	Correction Factor, $\mu\epsilon$	Zero-Shift, $\mu\epsilon$			
	$^{\circ}K$	$^{\circ}F$						Gage 1	Gage 2	Gage 3	Gage 4
H-32	RT	RT	R	1(T)	2000	34.5	227	-254	-259	+273	+265
				1(C)	2000	34.2	225	+3	+5	+13	+11
				2(T)	2000	33.9	223	-252	-258	+279	+272
			R	2(C)	2000	34.9	230	+2	+7	+17	+15
				3(T)	2000	34.1	225	-247	-251	+281	+273
				3(C)	2000	33.3	219	+2	+6	+20	+20
	811	1000	R	1(T)	2000	59.3	291	+14	+28	+41	+4
				1(C)	2000	61.1	403	+67	+76	+40	+33
				2(T)	2000	59.1	389	+69	+945	+77	+56
				2(C)	2000	59.4	391	+28	+22	+25	+26
3(T)	2000	58.3	384	-20	-13	+47	+41				
	3(C)	2000	58.3	384	+39	+39	+45	+23			
H-32	1311	1900	R	1(T)	2000	204	1344	+1252	+1213	-1174	--
				1(C)	2000	208	1371	+32	-1	+54	--
				2(T)	2000	202	1331	+1165	+1166	-1104	--
				2(C)	2000	211	1390	-14	-44	+130	--
				3(T)	2000	222	1463	+1204	+1223	-1133	--
				3(C)	2000	212	1397	+9	+3	+86	--

TABLE 7. PERFORMANCE HISTORY

Specimen No.	Gage No.	Gage Performance
H-21R (Ail-Tech)	1	No failure
	2	No failure
	3	No failure
	4	No failure
H-25R2 (Ail-Tech)	1	OK to 922 K (1200 F). Excessive drift noted above 977 K (1300 F)
H-26R2	1	During room temperature precycling (Step 4) of 1366 K (2000 F) run, some separation, between precoat and specimen, occurred. This partial failure precluded gage factor evaluation (Step 5), but did not weaken the bond sufficiently to preclude apparent strain evaluation (Step 6)
	2	
	3	
	4	
H-28	1	No failure
	2	Failure due to break in lead tab ribbon next to lead wire joint, during first apparent strain cycle to 1311 K (1900 F)
	3	No failure
	4	No failure
H-29	1	No failure
	2	No failure
	3	Failed due to 16 ohms increase in gage lead wire resistance, during second gage factor run to 1311 K (1900 F); probably due to bad joint or minute crack in ribbon
	4	No failure
H-32	1,2,3	Lead tab ribbons broke during four hour drift evaluation at 1311 K (1900 F). Repairs made on Gages 2 and 4 used for evaluation at 1366 K (2000 F). Slight separation of substrate near edges, after room temperature gage factor evaluation of 1366 K (2000 F) run.
	4	Lead tab ribbon broke again during cool-down from gage factor evaluation at 1311 K (1900 F)

TABLE 8. SUMMARY OF NASA BUTT-WELD, PULSE ARC, AND LASER JOINTS,
MECHANICAL (TENSILE) STRENGTH EVALUATIONS

Specimen Number	NASA Butt-Weld, BCL-3 to BCL-5 Wire			NASA Butt-Weld BCL-3 Wire to Alloy 875 Ribbon			Pulse Arc BCL-3 to Alloy 875 Wire			Laser, BCL-3 to Alloy 875 Wire		
	Breaking Load Newtons	Oz. of Break	Location	Breaking Load Newtons	Oz. of Break	Location	Breaking Load Newtons	Oz. of Break	Location	Breaking Load Newtons	Oz. of Break	Location
1	0.76	2.75	A	1.50	5.40	E	0.90	3.25	E	1.25	4.51	F
2	0.76	2.75	A	1.56	5.60	E	0.28	1.00	E	-0-	-0-	C
3	0.72	2.60	A	1.44	5.20	E	0.56	2.00	E	0.85	3.06	F
4	0.72	2.60	B	1.72	6.20	E	0.76	2.75	E	1.34	4.83	F
5	0.69	2.50	B	1.33	4.80	E	0.62	2.25	E	-0-	-0-	C
6	0.69	2.50	B	1.44	5.20	E	1.39	5.00	E	-0-	-0-	C
7	0.72	2.60	B	1.50	5.40	E	--	--	--	-0-	-0-	C
8	-0-	-0-	C	1.67	6.00	E	--	--	--	1.16	4.19	F
9	0.76	2.75	A	1.61	5.80	E	--	--	--	-0-	-0-	C
10	0.72	2.60	A	1.39	5.00	E	--	--	--	1.21	4.35	F
11	0.75	2.70	A	2.06	7.40	E	--	--	--	1.08	3.87	F
12	-0-	-0-	D	1.11	4.00	E	--	--	--	-0-	-0-	C
Average*	0.73	2.63		1.53	5.5		0.75	2.71		1.15	4.13	

Legend:

A - indicates break in BCL-5 wire remote from weld
 B - indicates break in BCL-5 wire near weld
 C - indicates joint broken during normal handling

D - indicates joint broken while installing in fixture
 E - indicates failure at joint
 F - indicates failure occurred in heat-affected zone

* - excluding zero breaking loads

TABLE 9. SUMMARY OF DC PARALLEL GAP JOINT MECHANICAL (TENSILE) STRENGTH EVALUATIONS

Joint Type	Joint Description			Electrode Material	Av breaking load		% of failures at joint location	% of "no weld"
	Joint Configuration	Material A	Material B		Newtons	Oz.		
1	PE-FO	Air-Annealed BCL-3 Wire	Alloy 875 ribbon	Mo	0.67	2.42	0	0
2	PE-UN	"	"	Cu	0.72	2.60	0	8
3	PA-FO	As drawn, BCL-3 Wire	"	Mo	0.77	2.77	0	16
4	PE-UN	Air-Annealed BCL-3 Wire	"	Mo	0.82	2.97	16	0
5	PE-UN	As-Drawn, BCL-3 Wire	"	Mo	1.09	3.92	100	0
8	PE-FO	"	"	Mo	1.58	5.68	100	0

Legend:

PE-FO indicates perpendicular weld-folded ribbon configuration (Configuration 2, Figure 3d)
PE-UN indicates perpendicular weld-unfolded ribbon configuration (Configuration 3, Figure 3d)
PA-FO indicates parallel weld-folded ribbon configuration (Configuration 1, Figure 3d)

TABLE 10. NASA BUTT-WELD RESISTIVITY MEASUREMENTS,
(BCL-3 TO BCL-5 WIRE)

Spec. No.	Resistance, ohms												$(\Delta R/R)$ R.T.
	Cycle 1				Cycle 2				Cycle 3				
	R.T.	At 1144 K (1600 F) for 3.67 hr.			R.T.	At 1144 K (1600 F) for 3.42 hr.			R.T.	At 1311 K (1900 F) for 4.75 hr.			
1	152.99	153.11	153.37	153.34	155.44	153.81	153.79	153.83	153.86	153.70	153.78	154.17	-8.17 x 10 ⁻³
2	151.26	151.31	151.62	151.73	153.35	151.99	152.04	152.06	152.05	151.71	151.70	150.20	-20.54
3	150.37	150.43	150.81	150.85	153.04	152.23	152.33	152.37	152.04	152.33	152.56	149.96	-20.12
4	151.00	151.15	151.84	152.03	152.48	153.49	157.70	155.56	155.82	153.83	154.92	150.45	-13.31
5	153.02	153.19	153.78	153.55	154.14	154.55	154.63	154.53	154.44	154.70	153.99	173.85*	+127.87
6	150.67	150.77	150.82	150.83	151.25	151.05	151.07	151.10	151.10	151.05	151.14	148.62**	-17.39
7	154.94	155.15	155.29	155.37	157.62	157.22	157.36	157.42	157.50	156.97	157.19	177.44*	+125.75
8	151.18	151.31	152.13	152.60	155.28	155.76	156.34	156.76	156.99	157.32	158.41	156.46	+7.60
9	152.19	152.25	152.64	152.77	153.63	153.28	153.27	153.33	153.35	153.20	153.41	149.99	-23.69
10	153.34	153.43	153.85	154.00	156.09	155.08	155.08	155.12	155.17	154.67	154.70	153.33	-17.68
11	152.87	152.95	153.19	153.28	155.47	154.33	154.45	154.51	154.55	154.19	154.25	154.04	-9.20
12	149.87	150.04	150.26	150.33	151.84	150.74	150.76	150.77	150.80	150.61	150.53	151.20	-4.21 x 10 ⁻³

* unstable

** slightly unstable

TABLE 11. NASA BUTT-WELD RESISTIVITY MEASUREMENTS
(BCL-3 TO ALLOY 875 RIBBON)

Specimen No.	Resistance, ohms						R.T.
	R.T.	Cycle 1		Cycle 2			
		At 1144 K (1600 F) for 7.75 hr.	R.T.	1144 K (1600 F)	1311 K (1900 F)		
1	77.294	77.373	77.545	78.638	77.09	77.03	77.549
2	79.379	79.382	79.590	79.214	78.09	78.13	78.796
3	77.485	77.499	77.530	78.643	77.47	77.46	77.867
4	79.279	79.319	79.368	80.169	79.54	79.60	79.047
5	80.777	80.745	81.600	79.437	78.96	79.05	77.837
6	78.650	78.587	78.450	79.059	78.80	78.84	76.986
7	79.534	79.494	80.202	79.608	79.66	79.72	77.753
8	77.679	77.682	77.810	78.384	77.66	77.70	76.875
9	78.669	78.659	78.814	79.626	79.13	79.36	78.714
10	77.529	77.272	77.616	79.044	77.12	77.73	77.110
11	81.975	82.073	82.184	83.520	81.84	81.71	80.740
12	79.810	79.980	80.308	80.736	80.10	80.29	80.865

TABLE 12. DC PARALLEL GAP WELD JOINTS, RESISTIVITY CHARACTERISTICS

Joint Type	Joint Configuration	Spec. Pair	Initial Resist. (R_0) at rm. temp., ohms	Cycle 1 at 1144 K (1600 F)				Rm. Temp. Resist. R_0^1 , Cycle 1 soak, ohms	Cycle 2 at 1311 K (1900 F)				Unit Chg. in Rm. Temp. Resist. ($R_0^1 - R_0$)/ R_0 , %
				Resist. R_0^1 beginning of Cycle 1, ohms	Resist. at end of Cycle 1, ohms	Unit chg. in resist. ($\Delta R_1/R_0$)	Time Interval (Δt), hr.		Resist. R_0^2 beginning of Cycle 2, ohms	Resist. at end of Cycle 2, ohms	Unit chg. in resist. ($\Delta R_2/R_0^2$)	Time Interval (Δt), hr.	
1	PE-FO	12-1	79.27	77.68	77.72	5.149×10^{-4}	7	81.98	75.08	75.03	-6.660×10^{-4}	5.17	3.42
		11-2	78.21	76.66	76.63	-3.913	"	78.46	76.66	76.38	-36.52	"	0.32
		10-3	80.87	79.17	79.31	17.680	"	81.26	78.97	78.88	-11.40	"	0.48
		9-4	79.65	77.46	77.98	67.130	"	79.32	77.95	77.73	-28.22	"	-0.41
		8-5	80.25	78.53	78.44	-11.460	"	82.07	78.41	78.23	-22.96×10^{-4}	5.17	2.27
		7-6	80.94	79.19	79.25	7.577×10^{-4}	7	--	--	--	--	--	--
3	PA-FO	12-1	--	--	--	--	--	--	--	--	--	--	--
		11-2	84.18	82.50	82.54	4.848×10^{-4}	9.25	85.60	74.07	83.92	$1330. \times 10^{-4}$	3.75	1.69
		10-3	83.00	81.27	80.21	-130.700	"	80.88	79.58	79.44	-17.59	"	-2.55
		9-4	83.19	81.47	81.39	-9.820	"	83.00	81.73	81.63	-12.24	"	-0.23
		8-5	82.33	80.55	80.44	-13.660×10^{-4}	9.25	82.78	82.48	82.85	14.86×10^{-4}	3.75	0.55
		7-6	--	--	--	--	--	--	--	--	--	--	--
4	PE-UN	12-1	81.17	79.66	79.65	-1.255×10^{-4}	3.83	81.48	80.02	79.74	-34.99×10^{-4}	4.0	0.38
		11-2	80.30	78.71	78.64	-8.893	"	80.09	78.28	78.17	-14.05	"	-0.26
		10-3	80.91	79.33	79.26	-8.824	"	80.84	79.25	78.91	-42.90	"	-0.09
		9-4	81.34	79.73	78.70	-129.200	"	80.89	79.63	80.10	59.02	"	-0.55
		8-5	81.37	80.07	84.27	524.50	"	78.33	77.13	76.98	-19.45	"	-3.74
		7-6	80.36	78.65	78.55	-12.71×10^{-4}	3.83	79.88	78.47	78.28	-24.21×10^{-4}	4.0	-0.60
5	PE-UN	1-12	94.88	95.22	95.27	5.250×10^{-4}	2.0						
		2-11	97.75	88.33	88.35	2.264	"						
		3-10	87.55	87.73	87.74	1.140	"						
		4-9	85.94	86.40	86.45	5.878	"						
		5-8	91.78	92.56	92.57	1.080×10^{-4}	2.0						
8	PE-FO	1-12	80.89	80.93	81.31	46.95×10^{-4}	5.0	81.53	79.85	78.78	-134.0×10^{-4}	4.0	0.70
		2-11	80.82	80.72	80.82	12.39	"	84.20	82.71	82.29	-50.78	"	4.18
		3-10	82.50	80.67	82.82	266.5	"	83.80	82.71	81.32	-168.1	"	1.58
		4-9	80.98	82.16	89.77	926.2	"	83.34	82.13	80.93	-146.1	"	2.51
		5-8	81.10	80.93	80.85	-9.885	"	83.51	82.08	82.05	-3.655	"	2.97
		6-7	81.31	81.16	81.07	-11.09×10^{-4}	5.0	80.86	80.09	79.76	-41.2×10^{-4}	4.0	-0.55

* See Legend for Table 9 for description of joint configuration.

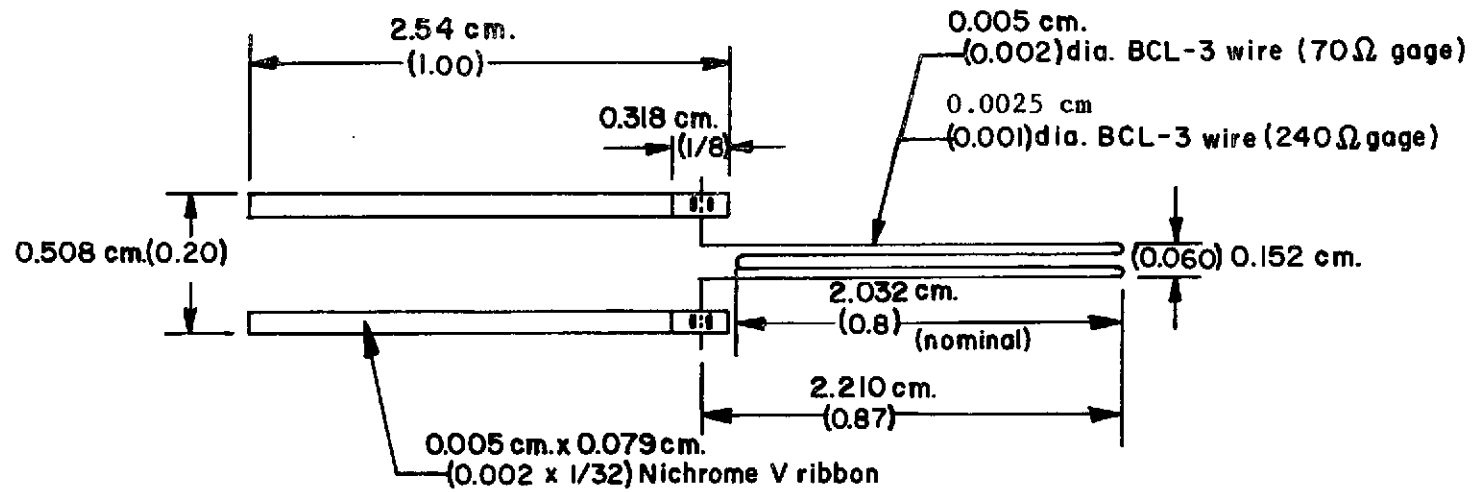


FIGURE 1. GAGE GEOMETRY

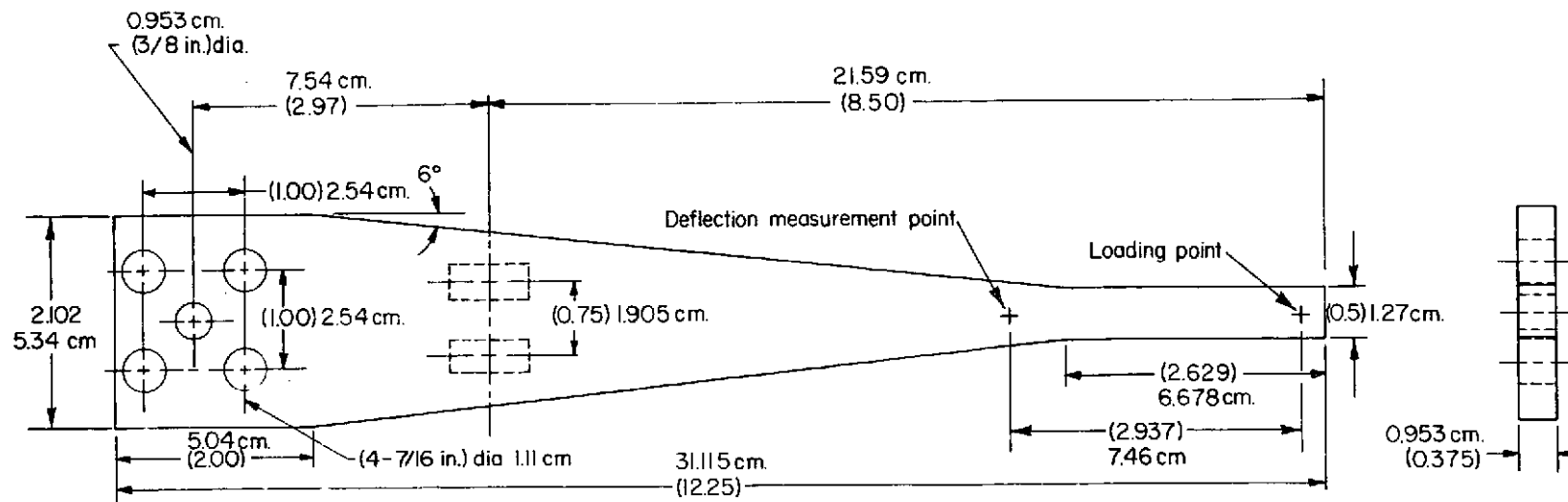
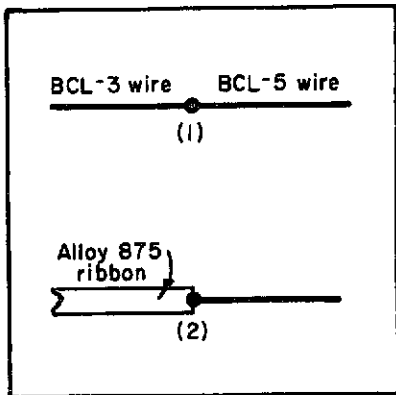
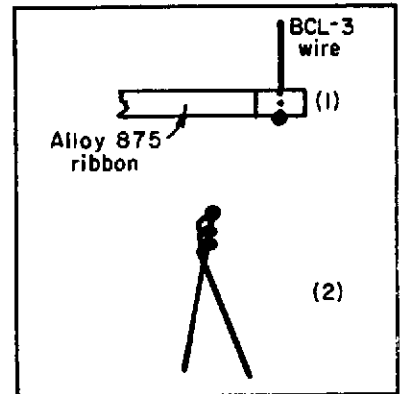


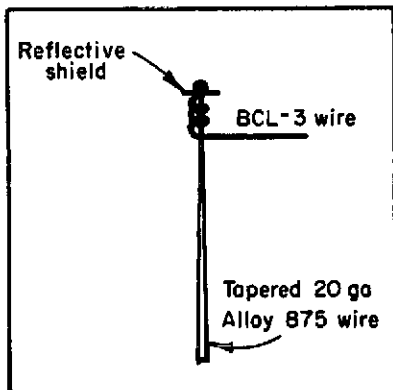
FIGURE 2. STATIC CALIBRATION SPECIMEN GEOMETRY AND GAGE LOCATIONS



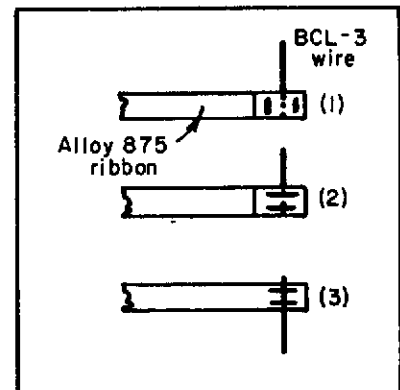
a. NASA BUTT



b. PULSE ARC



c. PULSE ARC PLASMA NEEDLE
ARC, AND LASER



d. DC PARALLEL GAP

FIGURE 3. JOINT GEOMETRIES

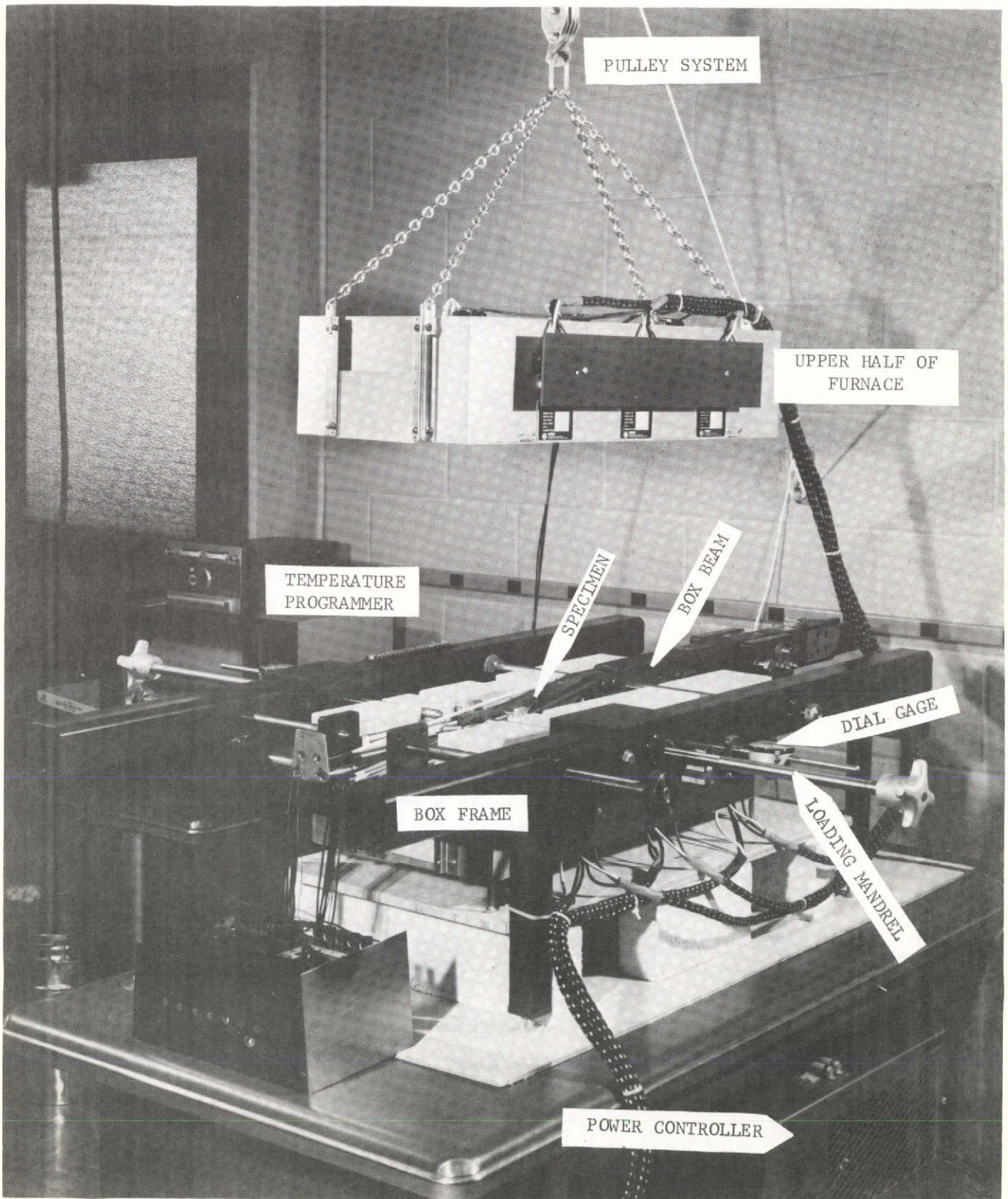


FIGURE 4. OVERALL VIEW OF GAGE EVALUATION FACILITY

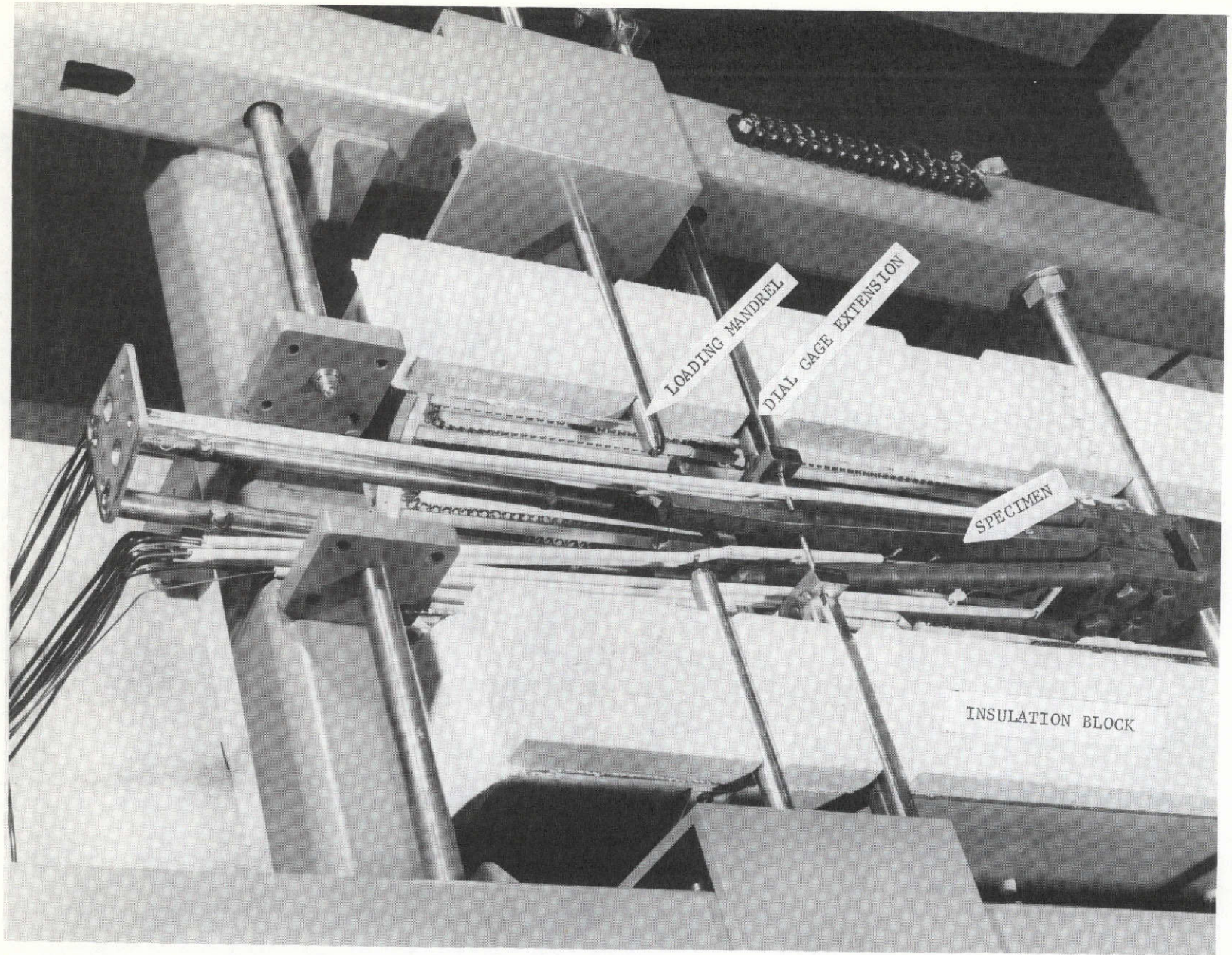


FIGURE 5. CLOSE-UP OF SPECIMEN INSTALLED IN EVALUATION FACILITY

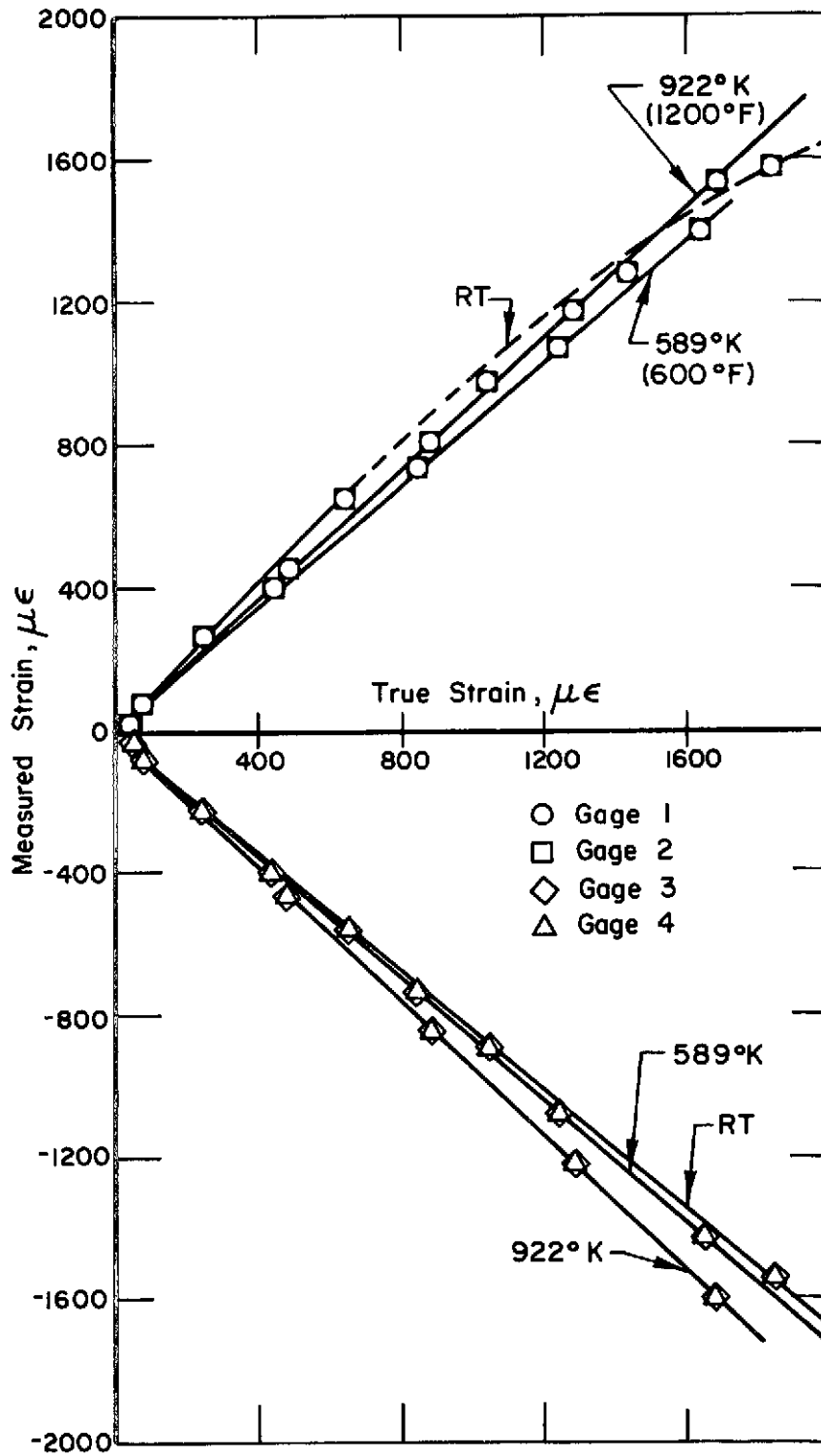


FIGURE 6. SPECIMEN H-21R (ALLTECH), GAGE FACTOR, RT
 589 K (600 F), 922 K (1200 F)

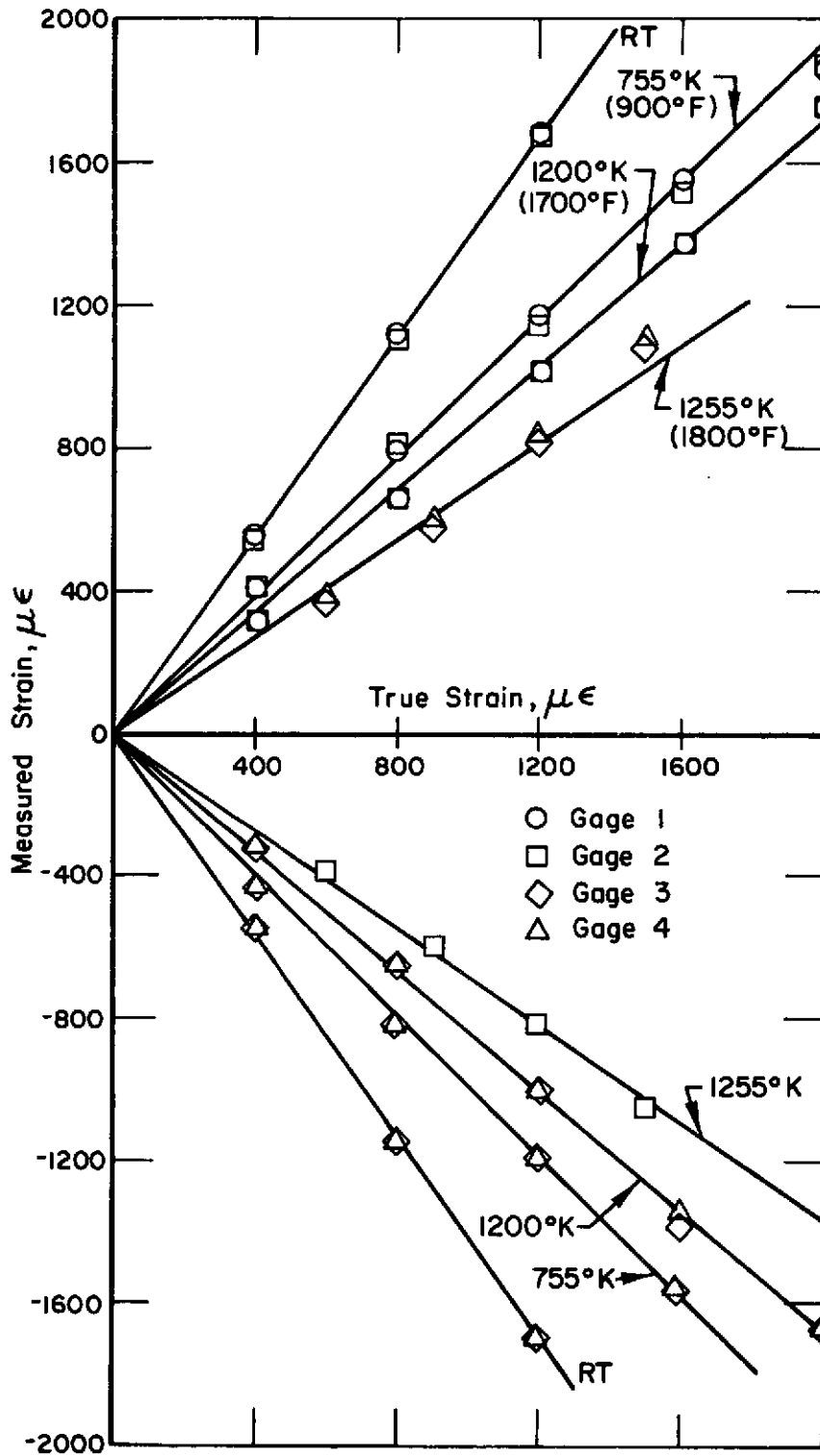


FIGURE 7. SPECIMEN H-28, GAGE FACTOR R.T., 755 K (900 F), 1200 K (1700 F), 1255 K (1800 F)

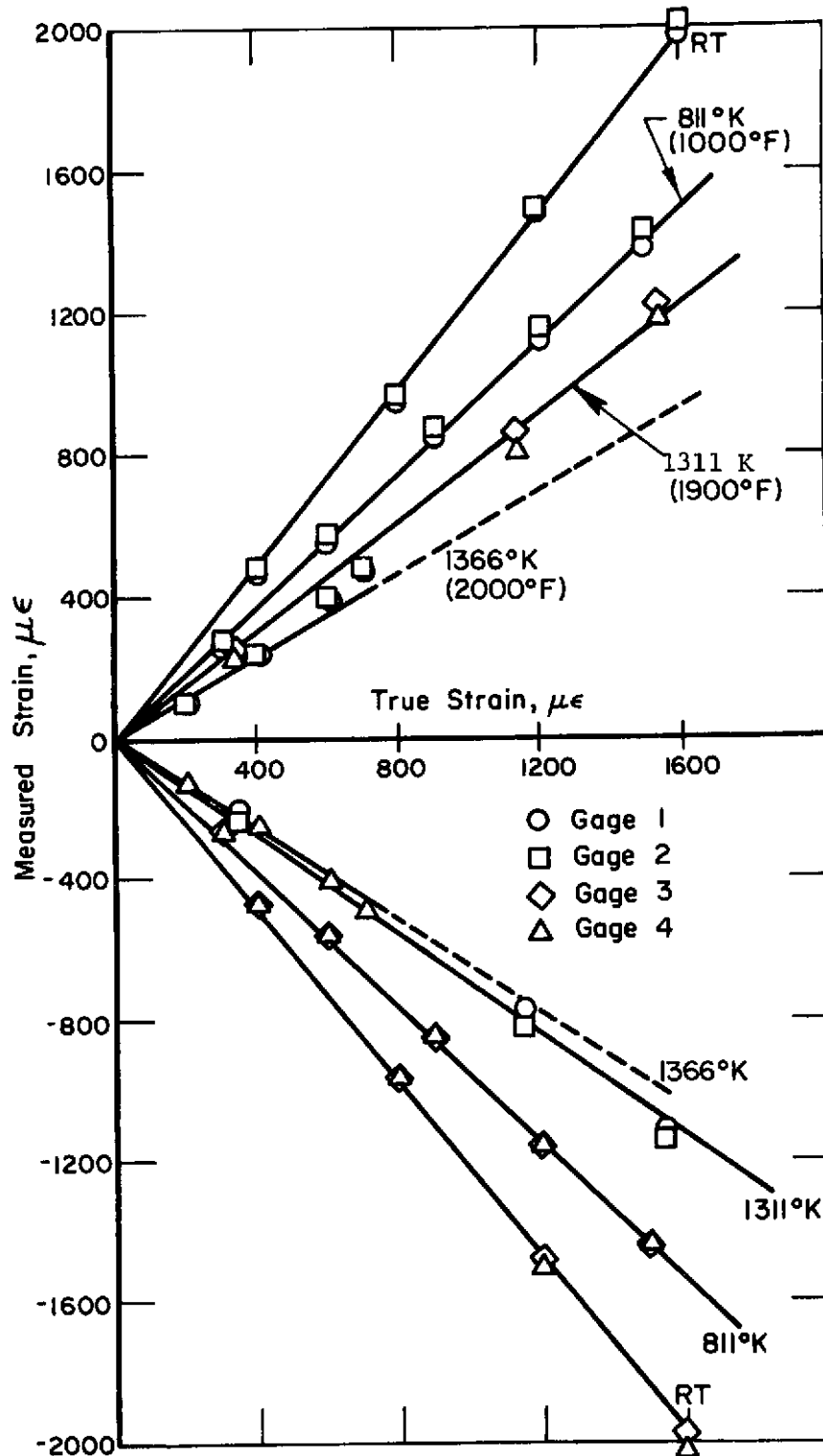


FIGURE 8. SPECIMEN H-29, GAGE FACTOR, R.T., 811 K (1000 F), 1311 K (1900 F), 1366 K (2000 F)

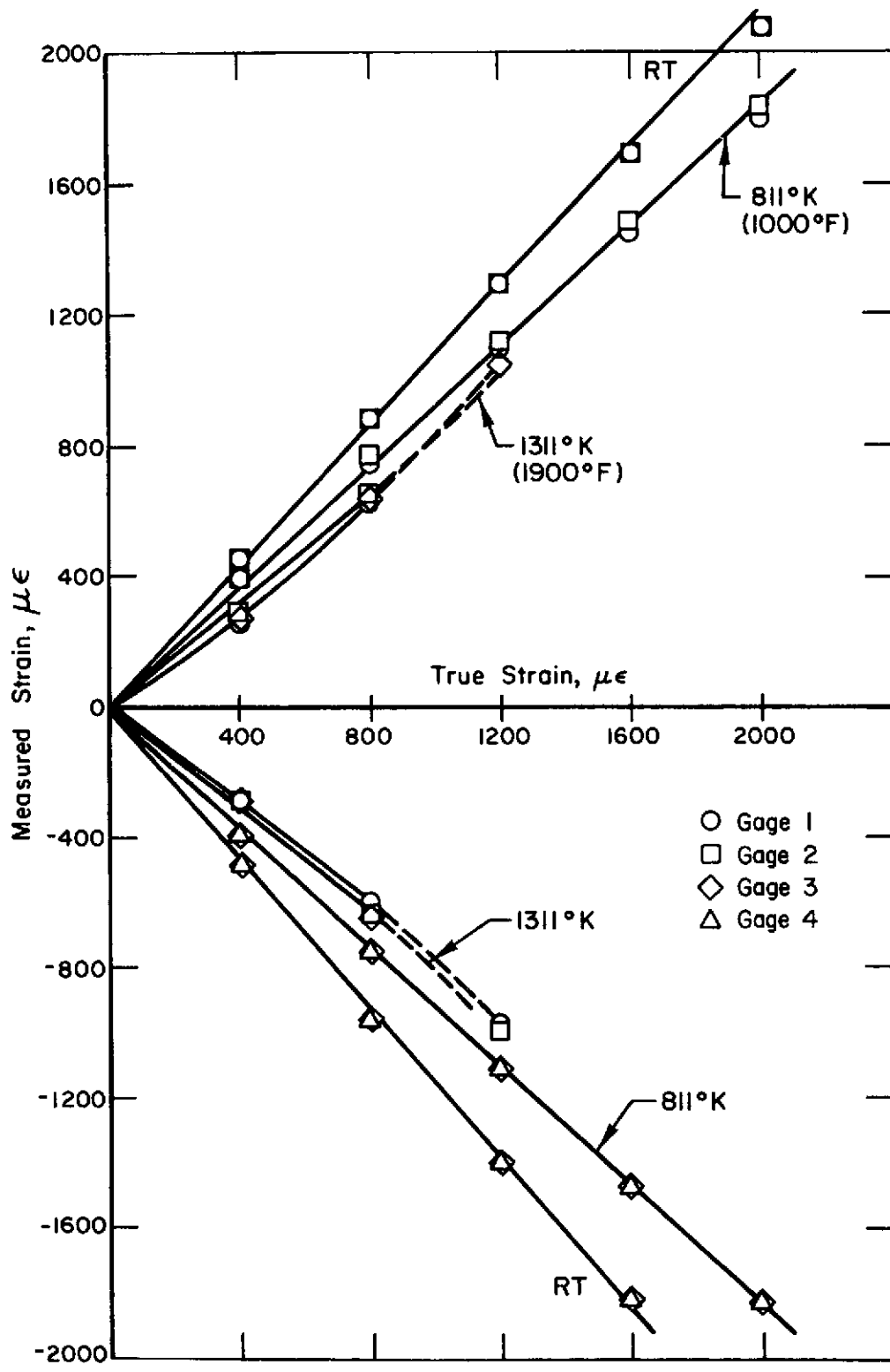


FIGURE 9. SPECIMEN H-32, GAGE FACTOR, R.T., 811 K (1000 F), 1311 K (1900 F)

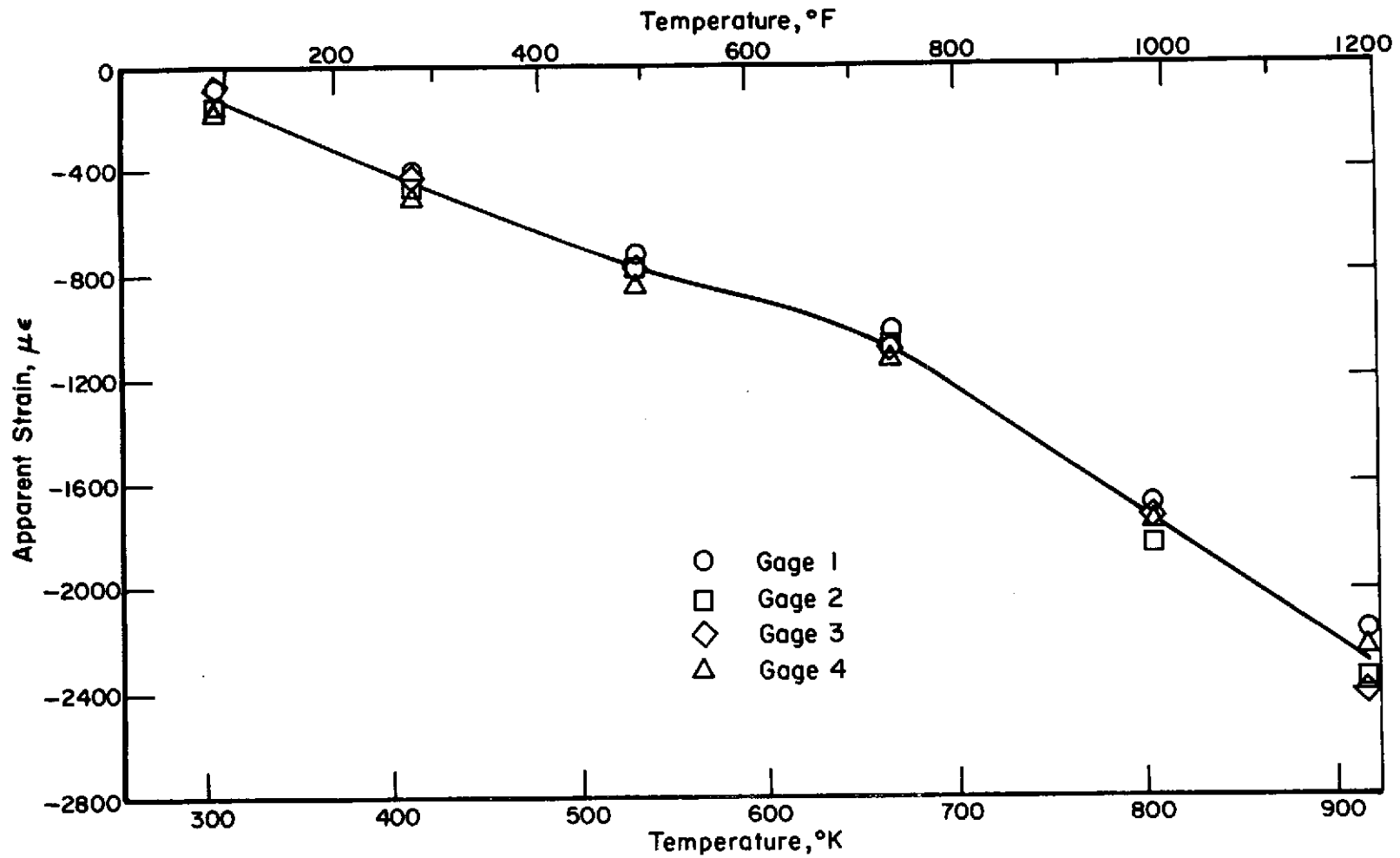


FIGURE 10. SPECIMEN H-21R (AILTECH GAGES) APPARENT STRAIN TO 922 K (1200 F)

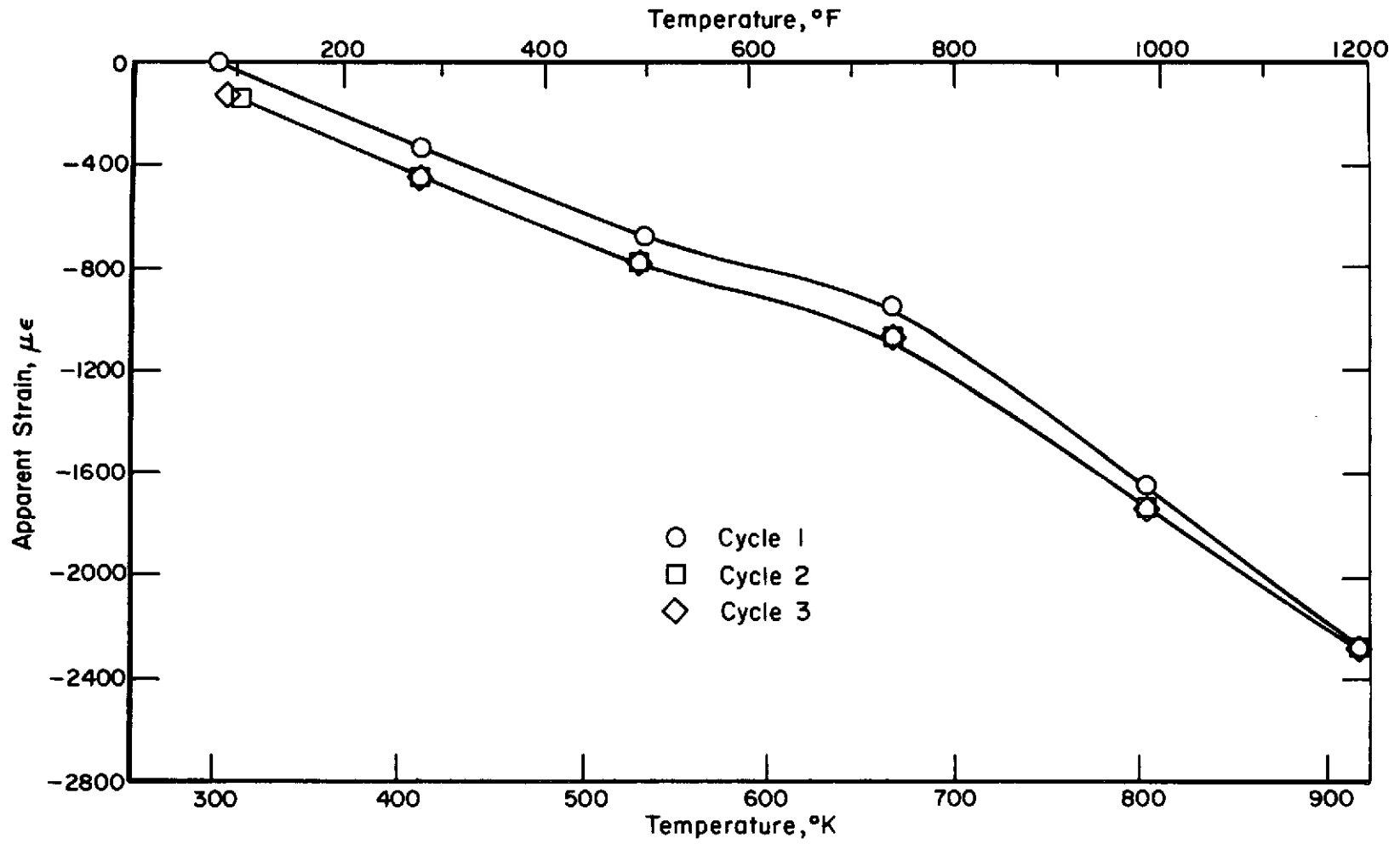


FIGURE 11. SPECIMEN H-21R (AILTECH GAGES) APPARENT STRAIN TO 922 K (1200 F), 3 CYCLES

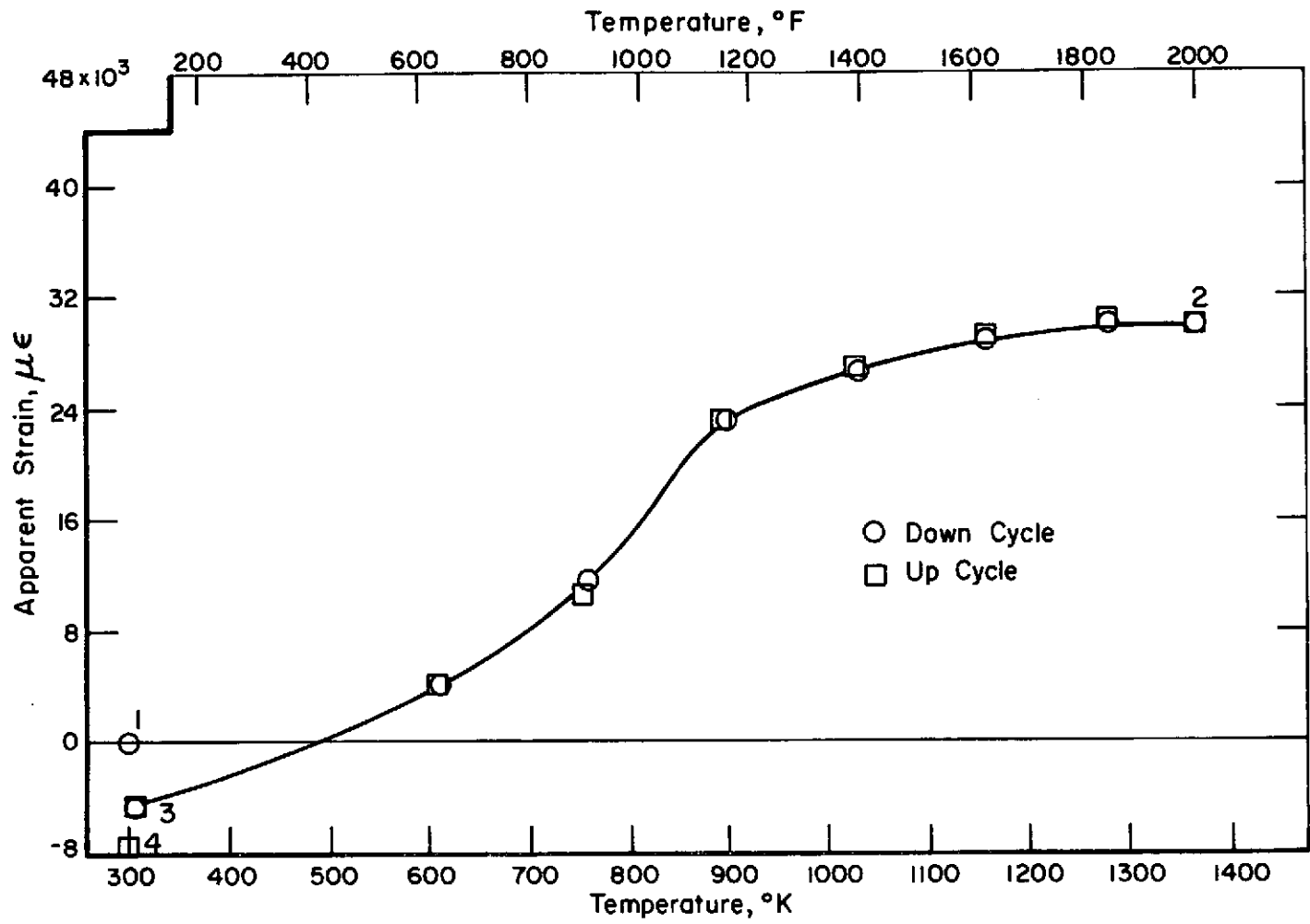


FIGURE 12. SPECIMEN H-26R2, APPARENT STRAIN TO 1366 K (2000 F)

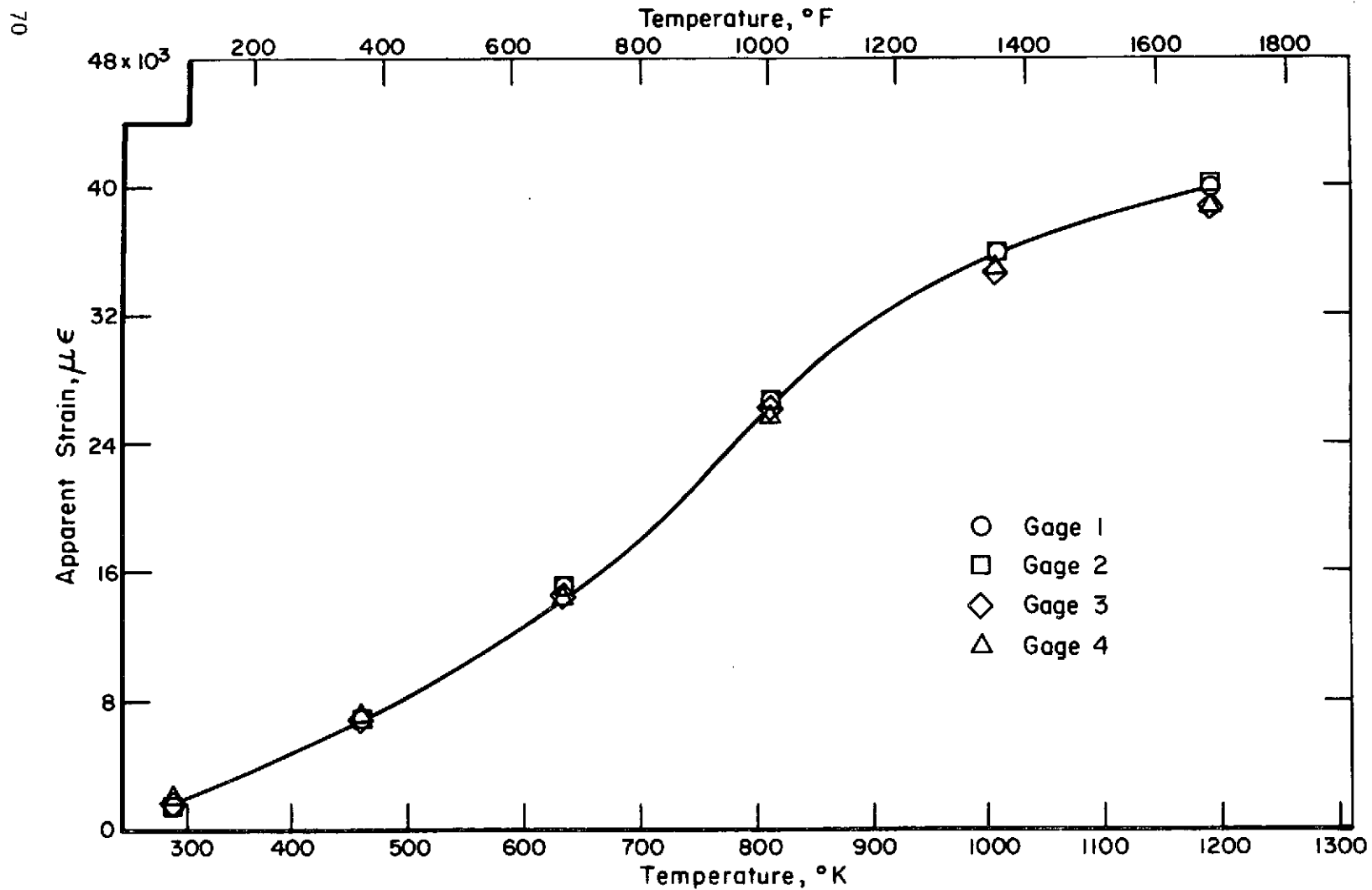


FIGURE 13. SPECIMEN H-28, APPARENT STRAIN TO 1200 K (1700 F)

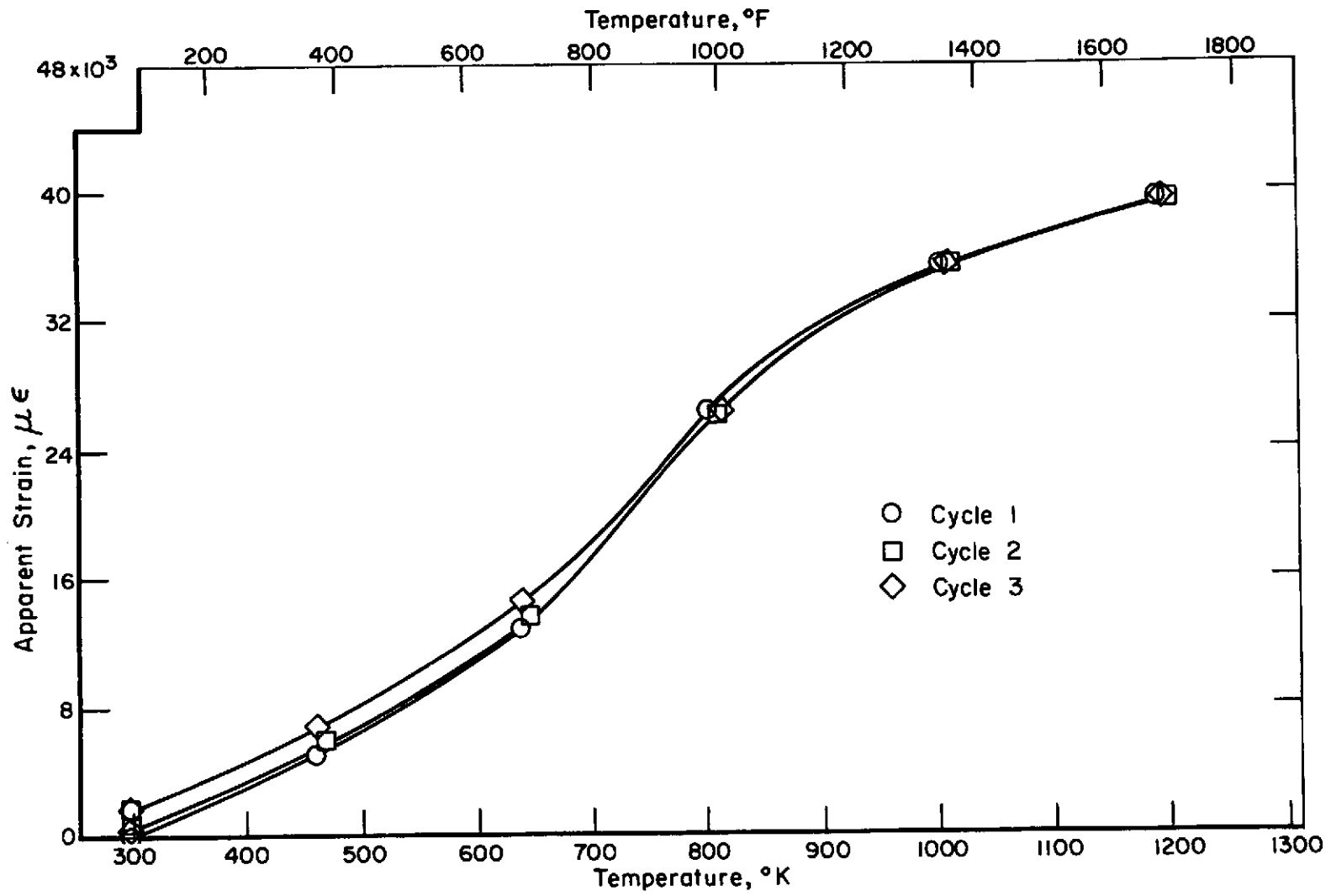


FIGURE 14. SPECIMEN H-28, APPARENT STRAIN TO 1200 K (1700 F), 3 CYCLES

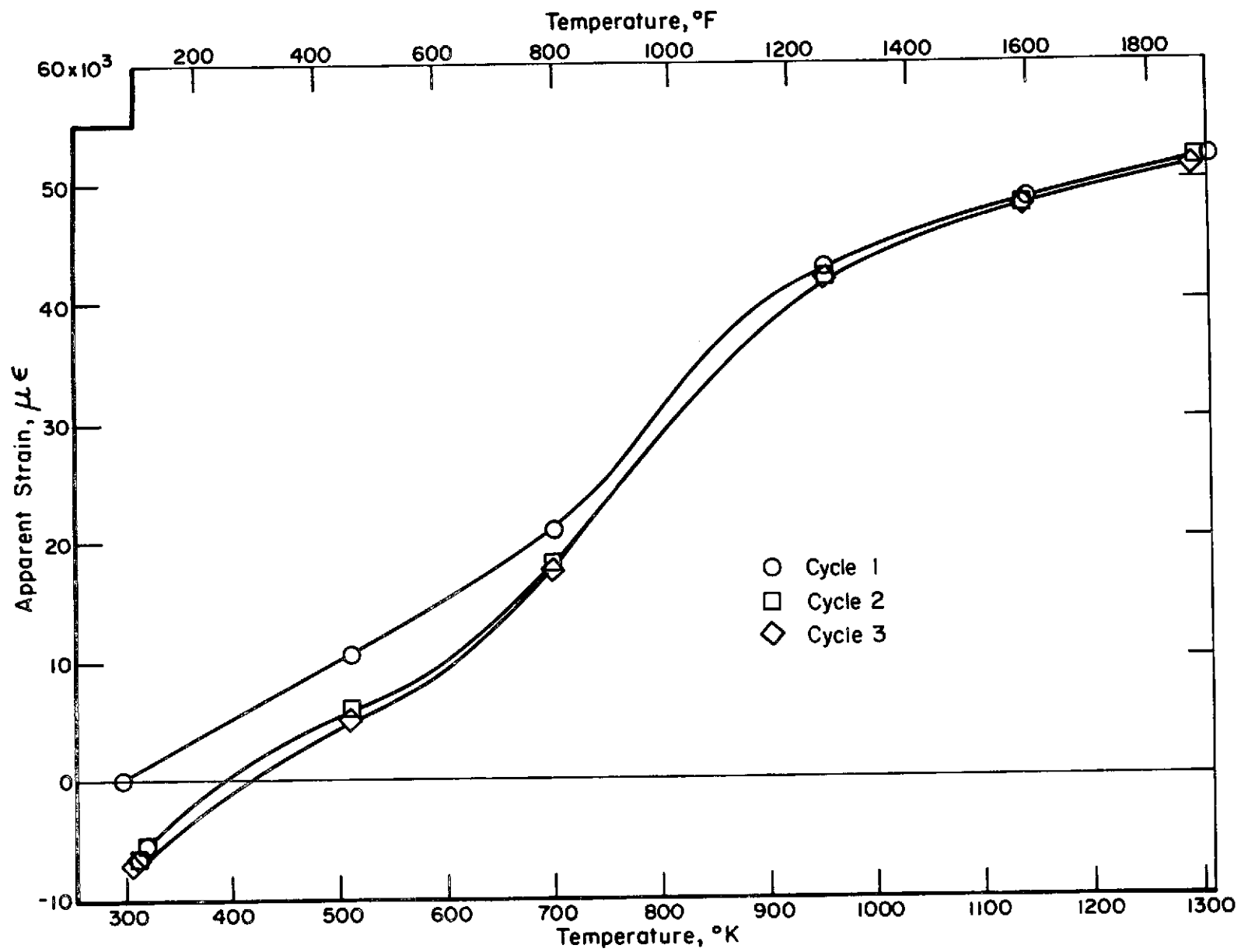


FIGURE 15. SPECIMEN H-28, APPARENT STRAIN TO 1311 K (1900 F), 3 CYCLES

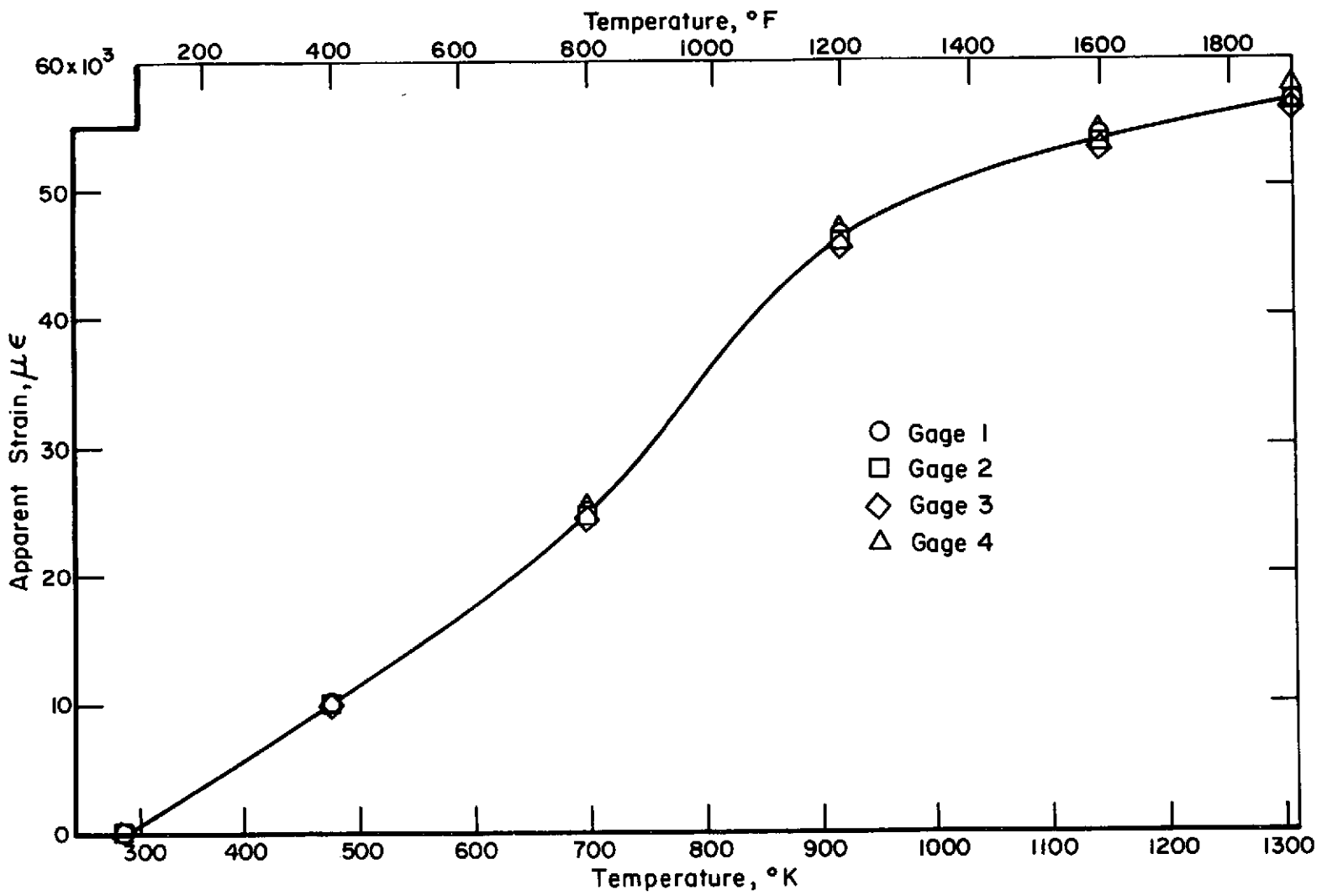


FIGURE 16. SPECIMEN H-29, APPARENT STRAIN TO 1311 K (1900 F)

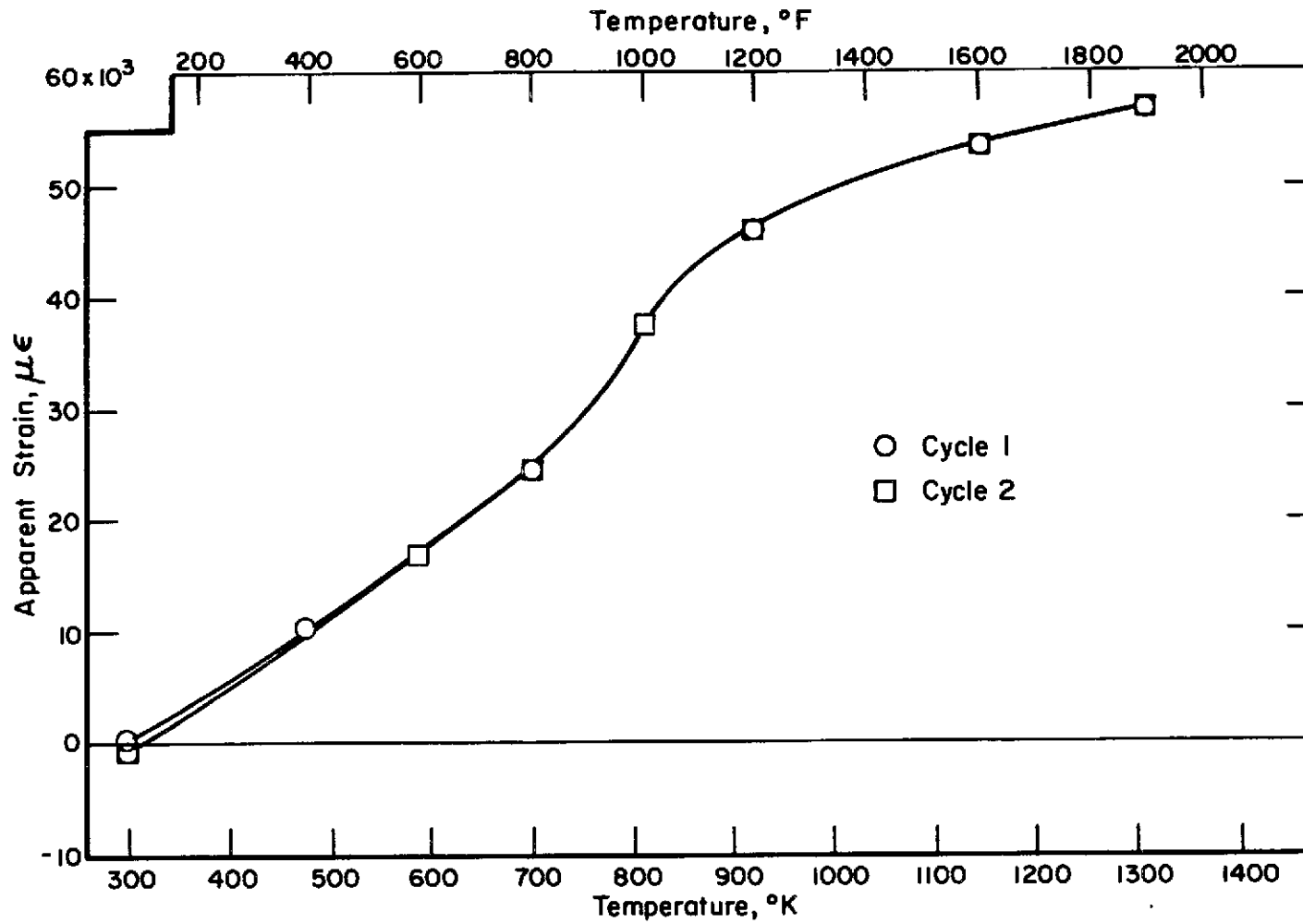


FIGURE 17. SPECIMEN H-29 APPARENT STRAIN TO 1311 K (1900 F), 2 CYCLES

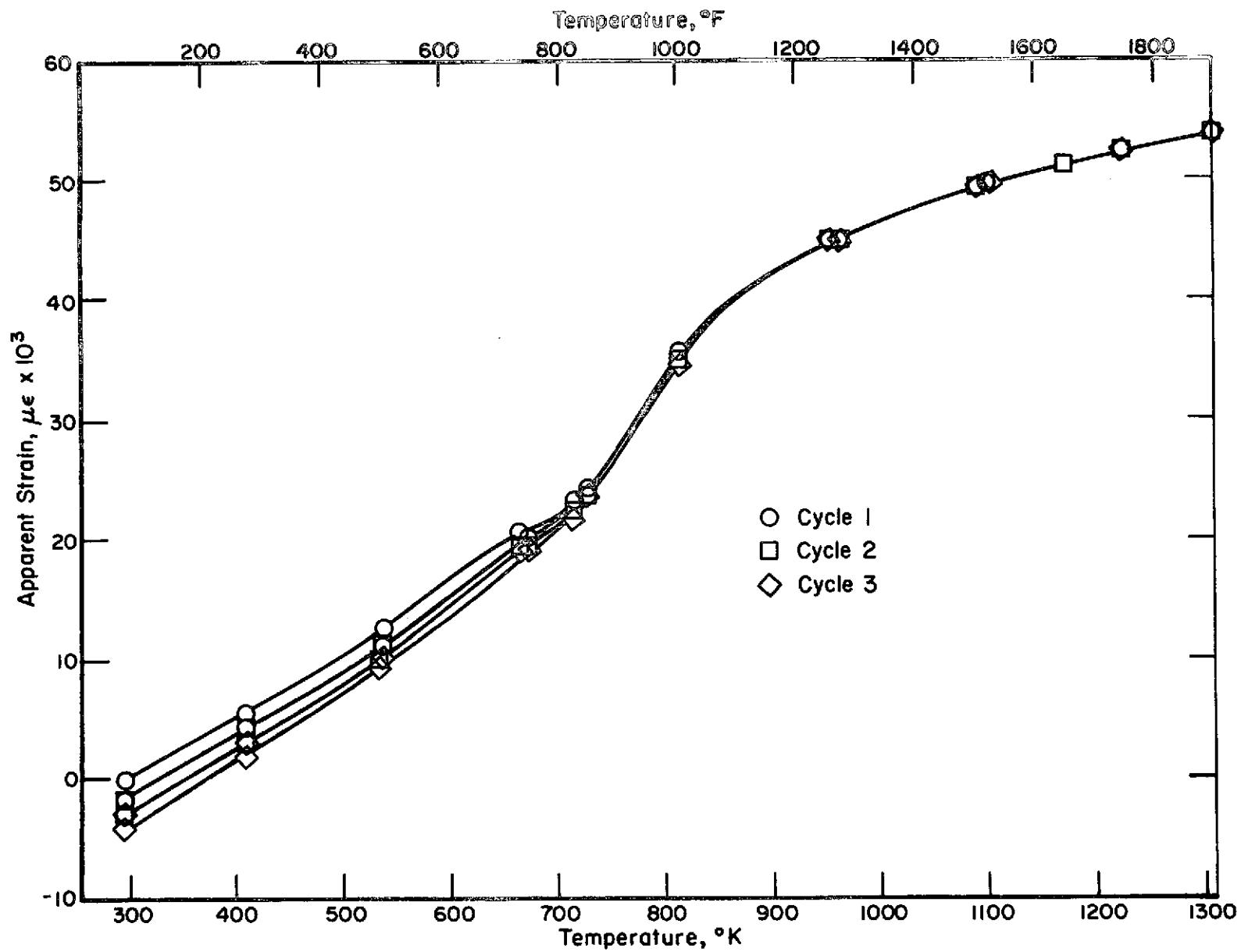


FIGURE 18. SPECIMEN H-32, APPARENT STRAIN TO 1311 K (1900 F), 4 CYCLES

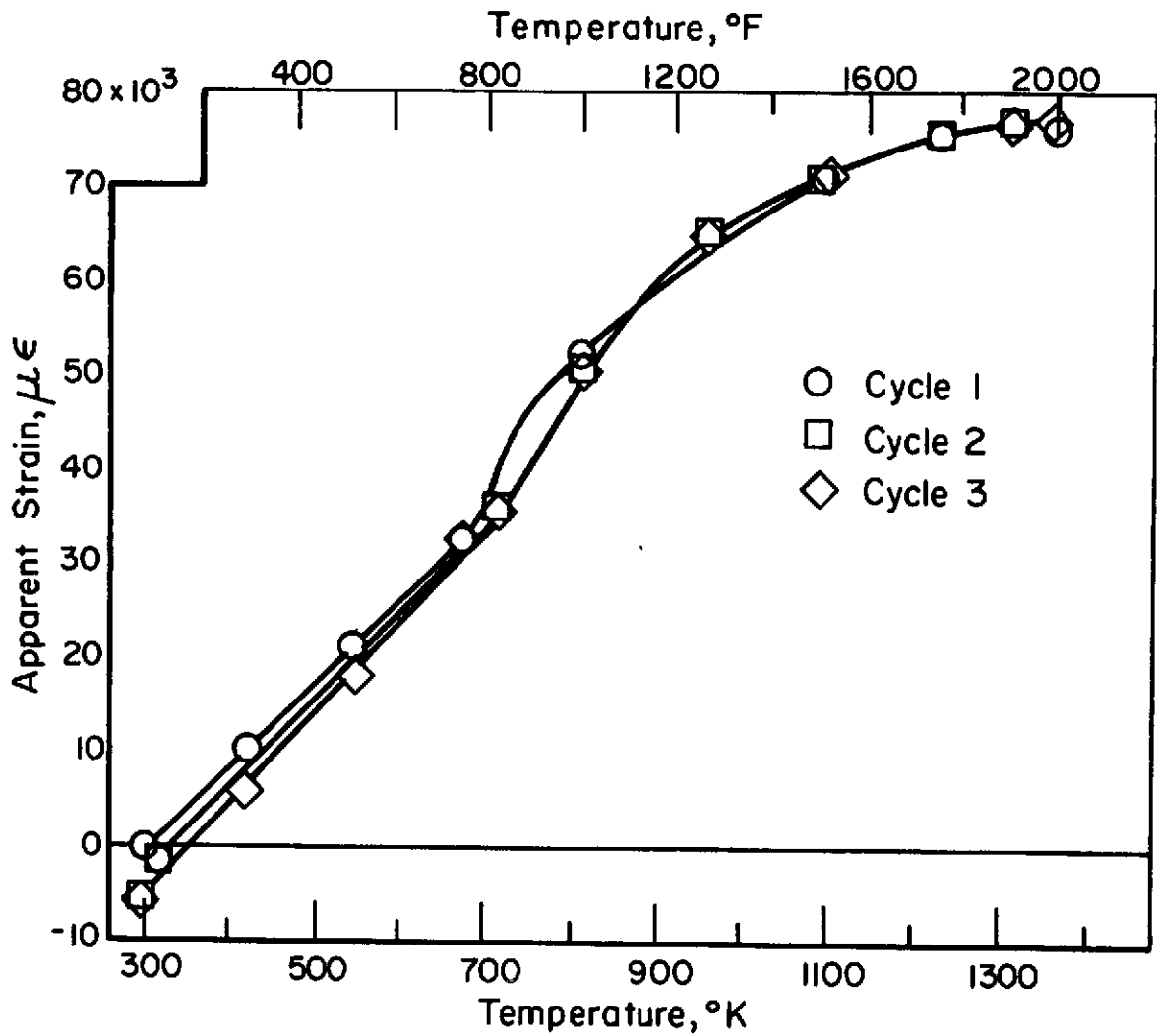


FIGURE 19. SPECIMEN H-32, APPARENT STRAIN TO 1366 K (2000 F), 3 CYCLES

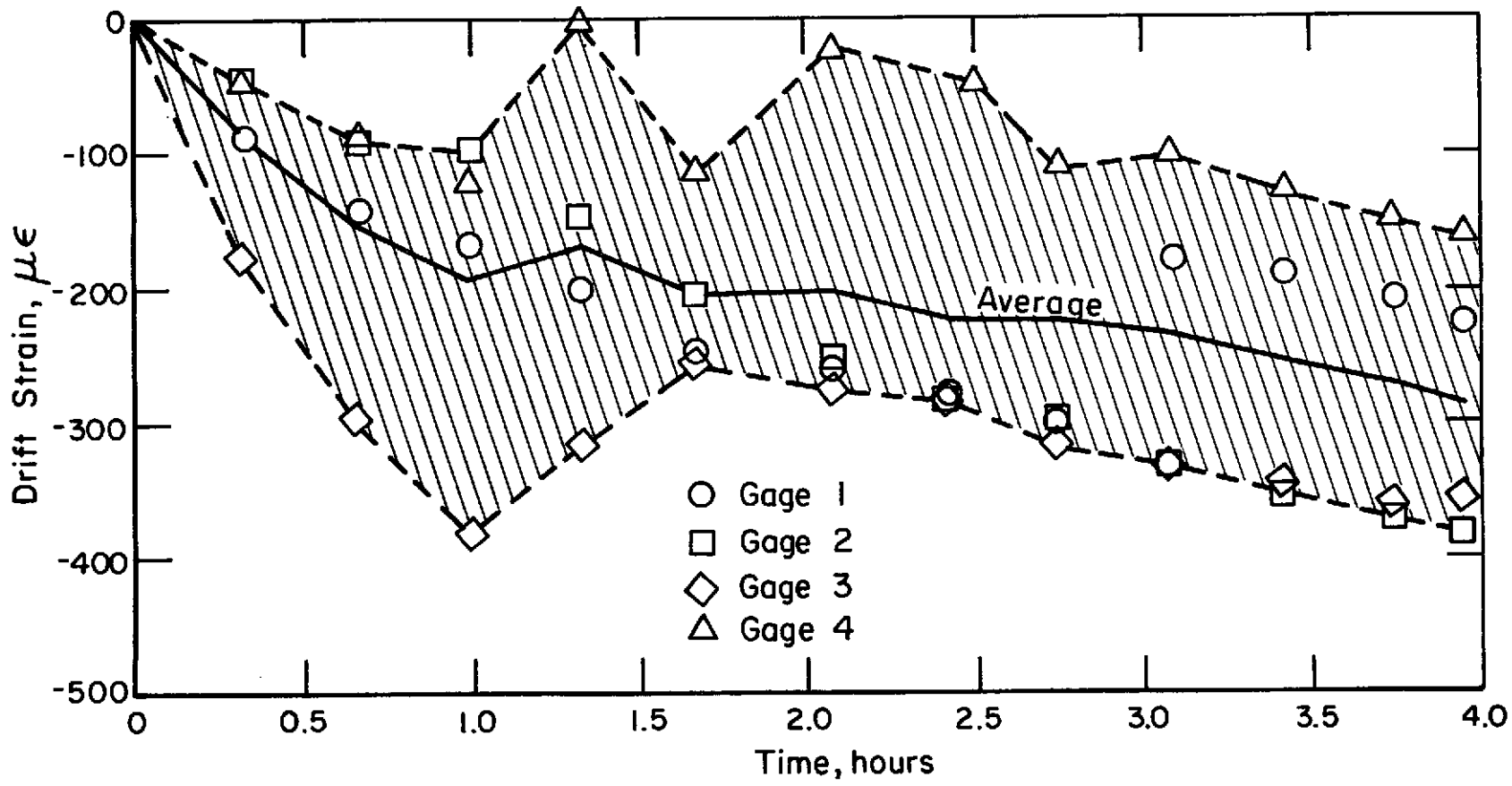


FIGURE 20. SPECIMEN H-21R (ALLTECH GAGES), DRIFT AT 922 K (1200 F)

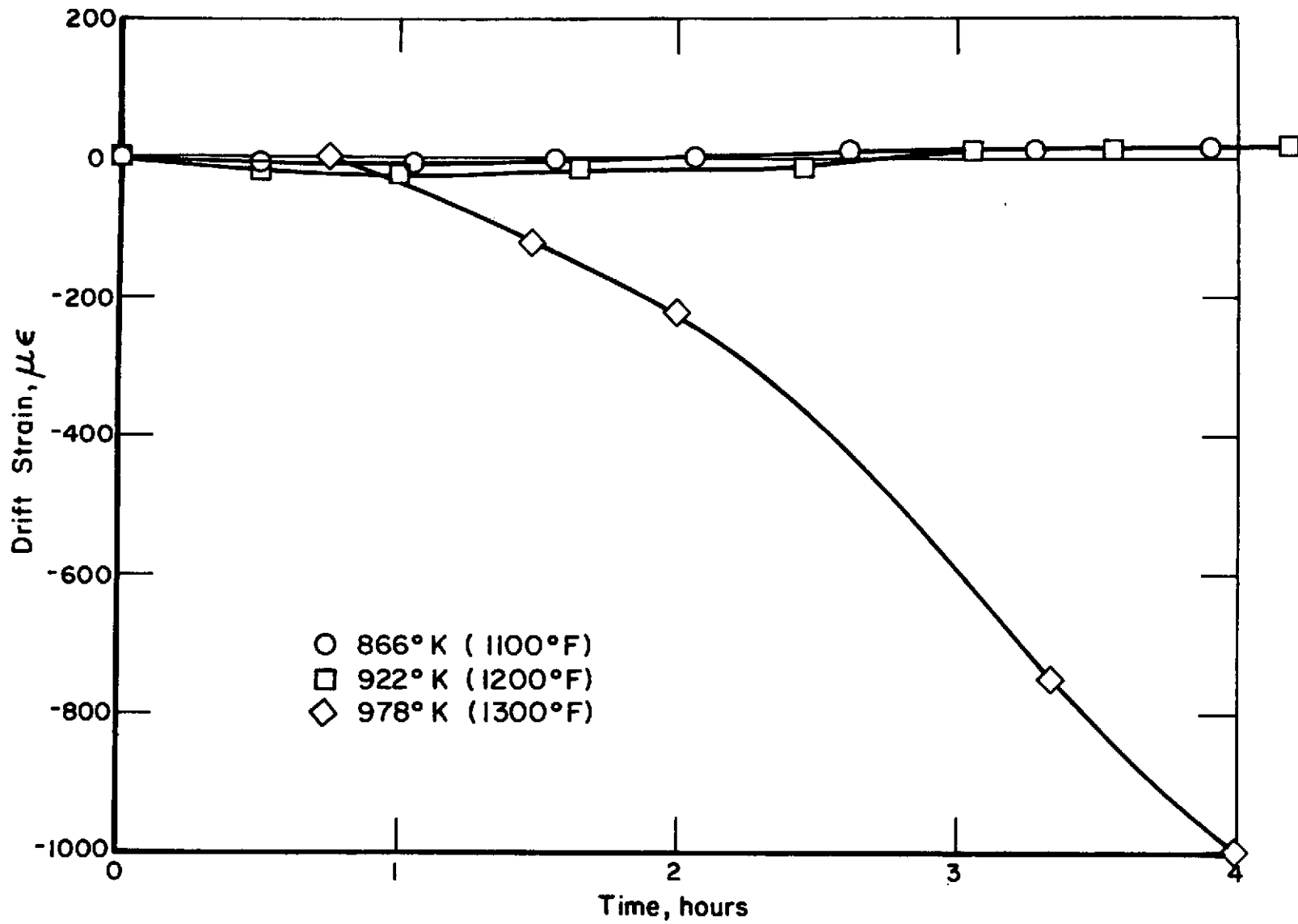


FIGURE 21. SPECIMEN H-25R2 (ALLTECH GAGES) DRIFT AT 866 K (1100 F), 922 K (1200 F), and 978 K (1300 F)

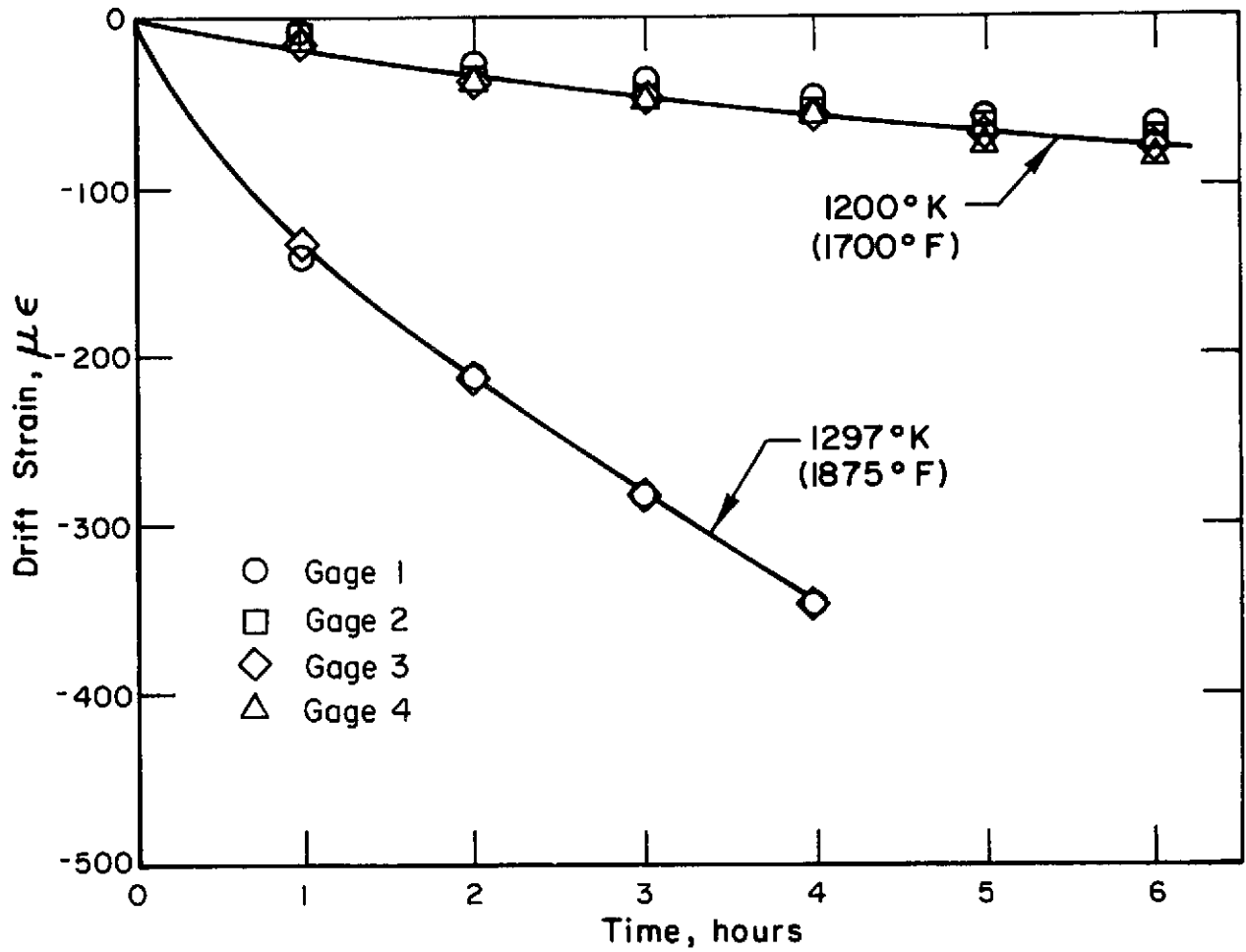


FIGURE 22. SPECIMEN H-28, DRIFT AT 1200 K (1700 F) AND 1297 K (1875F)

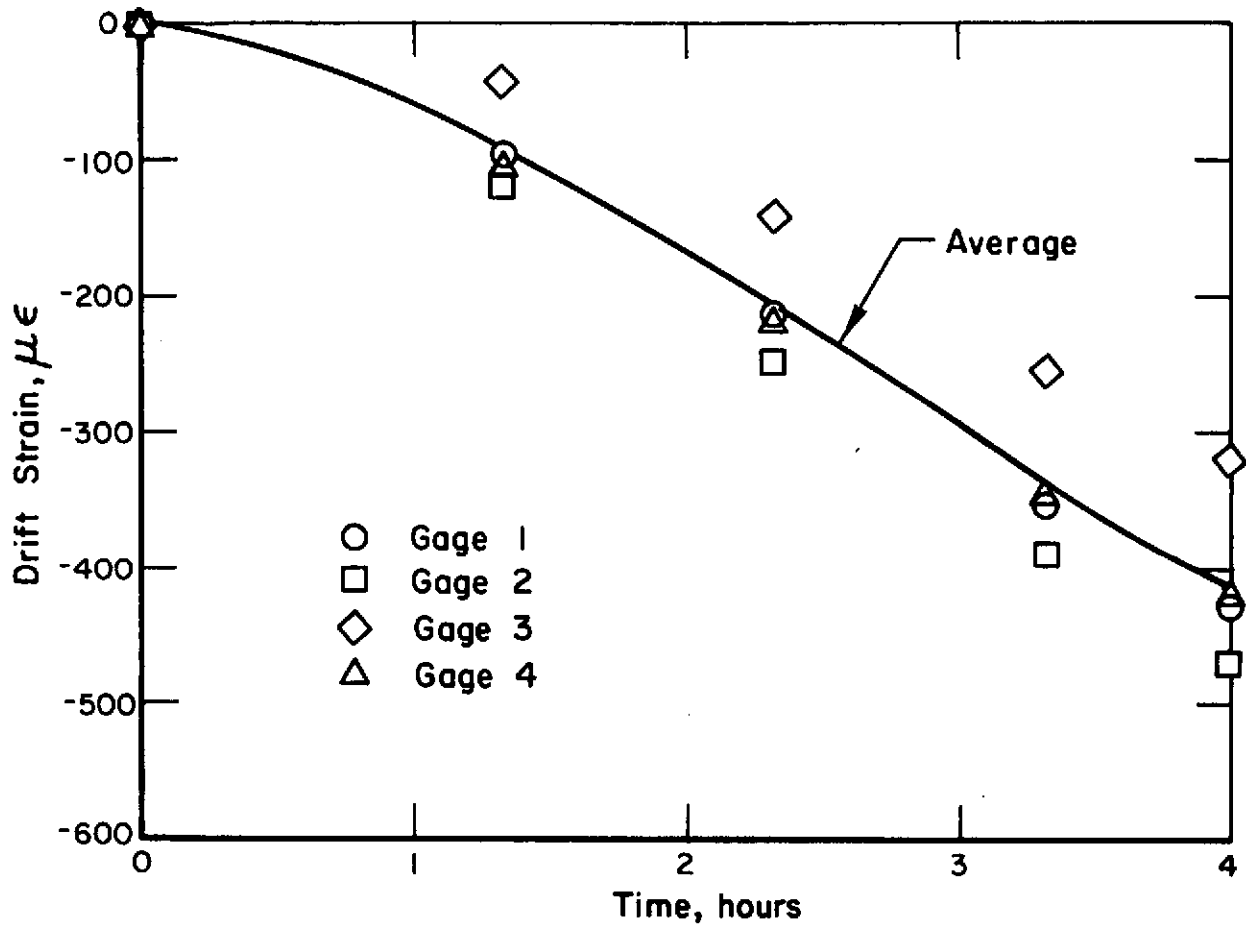


FIGURE 23. SPECIMEN H-29, DRIFT AT 1311 K (1900 F)

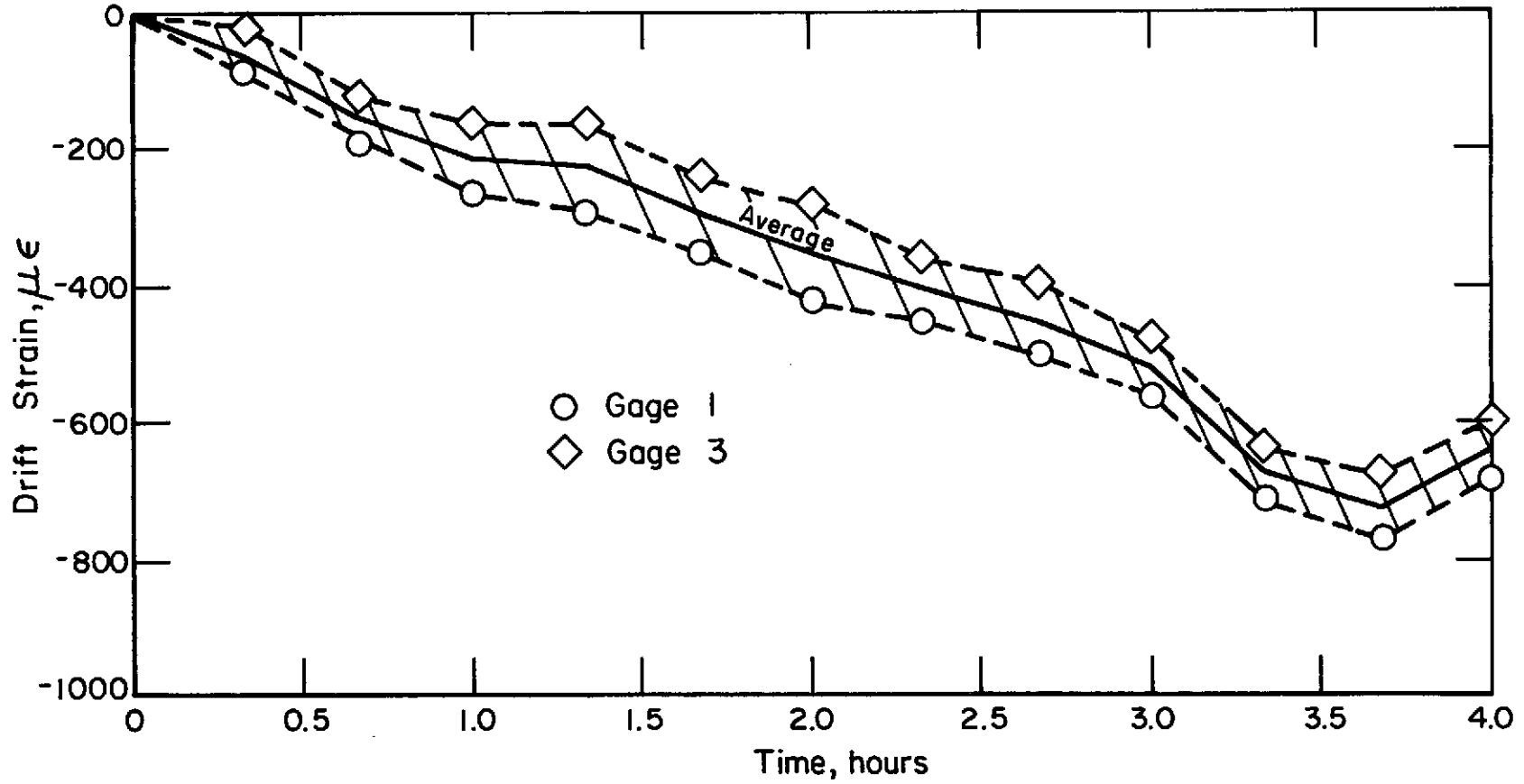


FIGURE 24. SPECIMEN H-32, DRIFT AT 1311 K (1900 F)

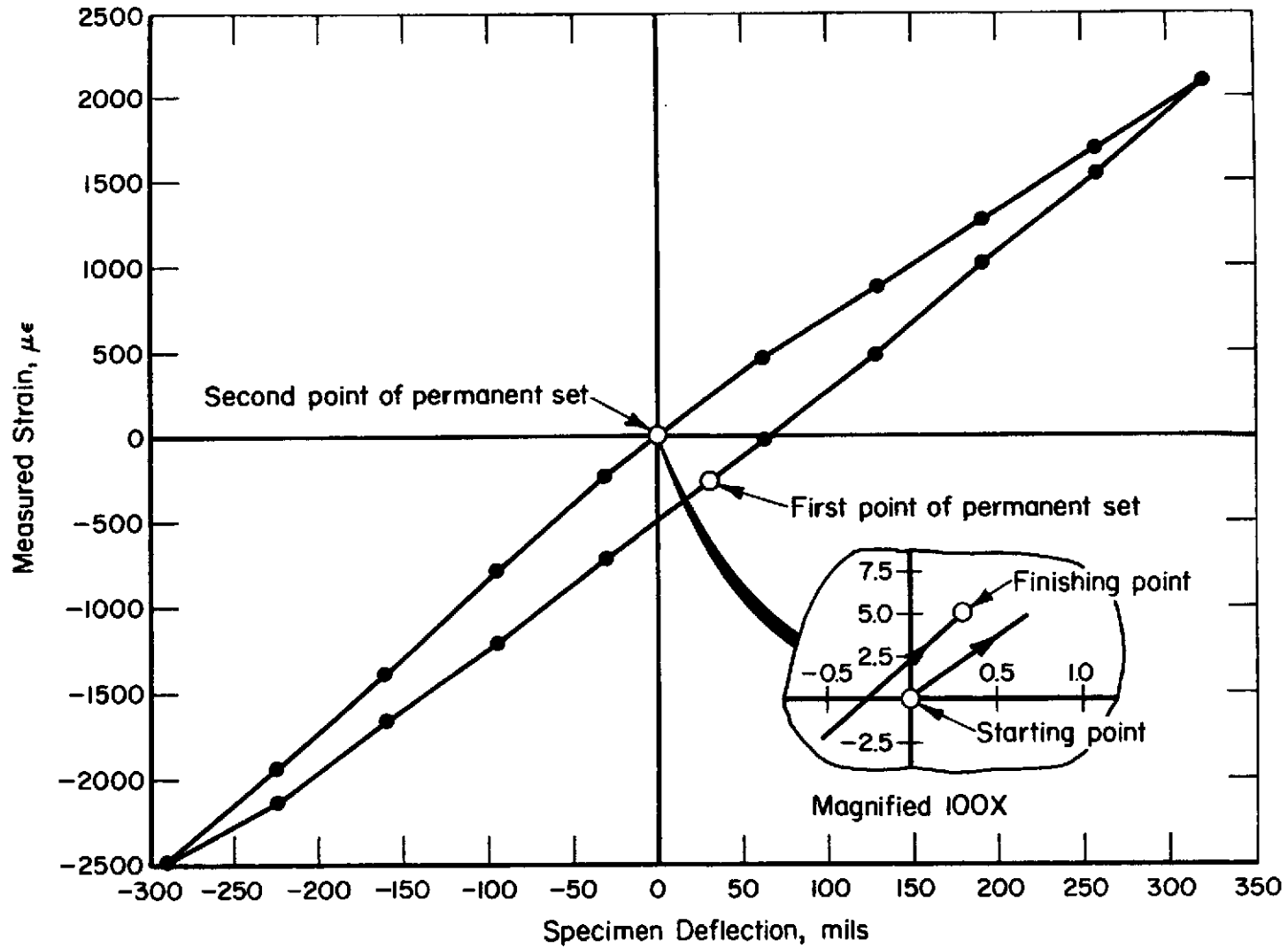


FIGURE 25. SPECIMEN H-32, STRAIN-DEFLECTION LOOP UNDER REVERSED LOADING, ROOM TEMPERATURE

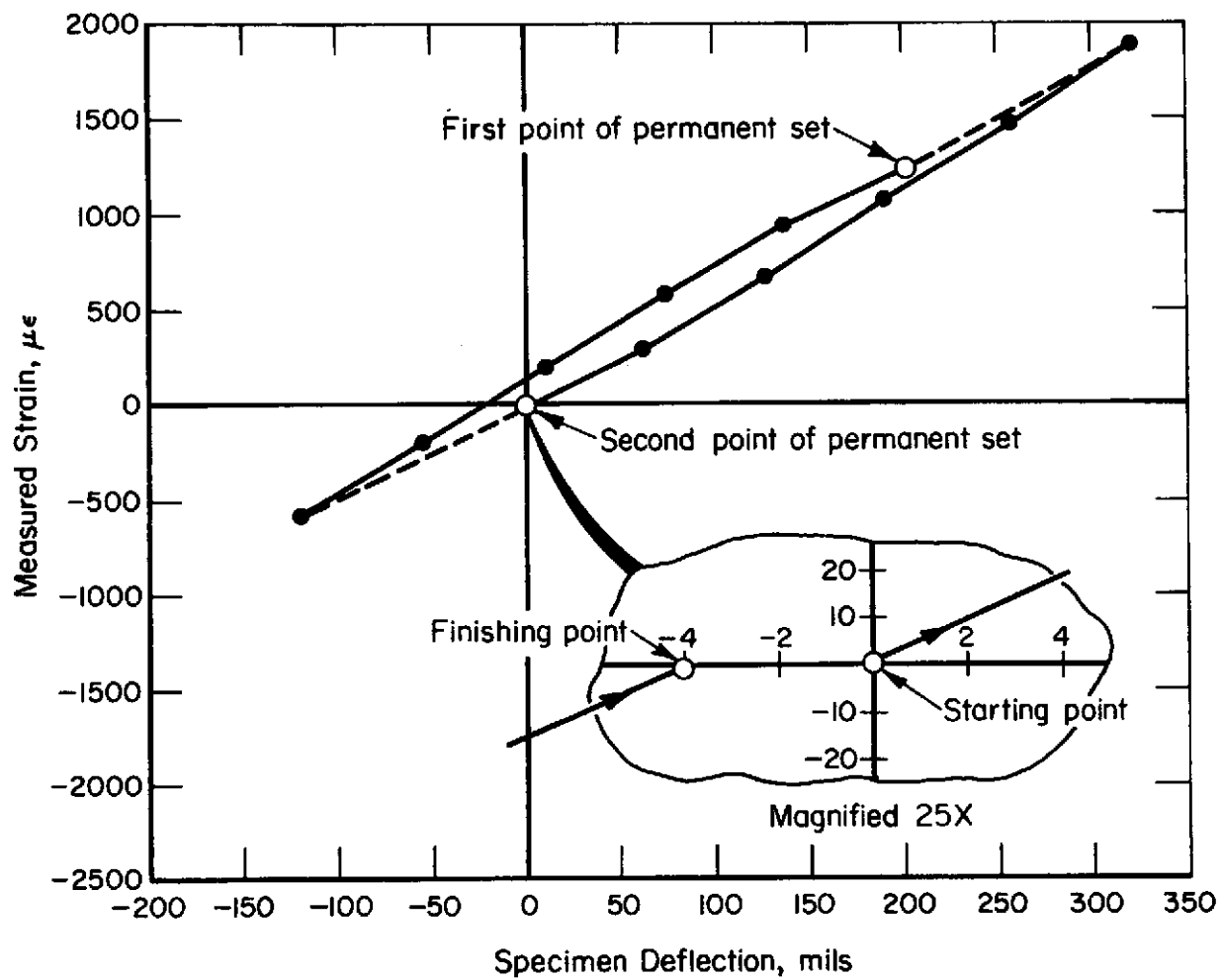


FIGURE 26. SPECIMEN H-32, STRAIN-DEFLECTION LOOP UNDER REVERSED LOADING, 1311 K (1900 F)

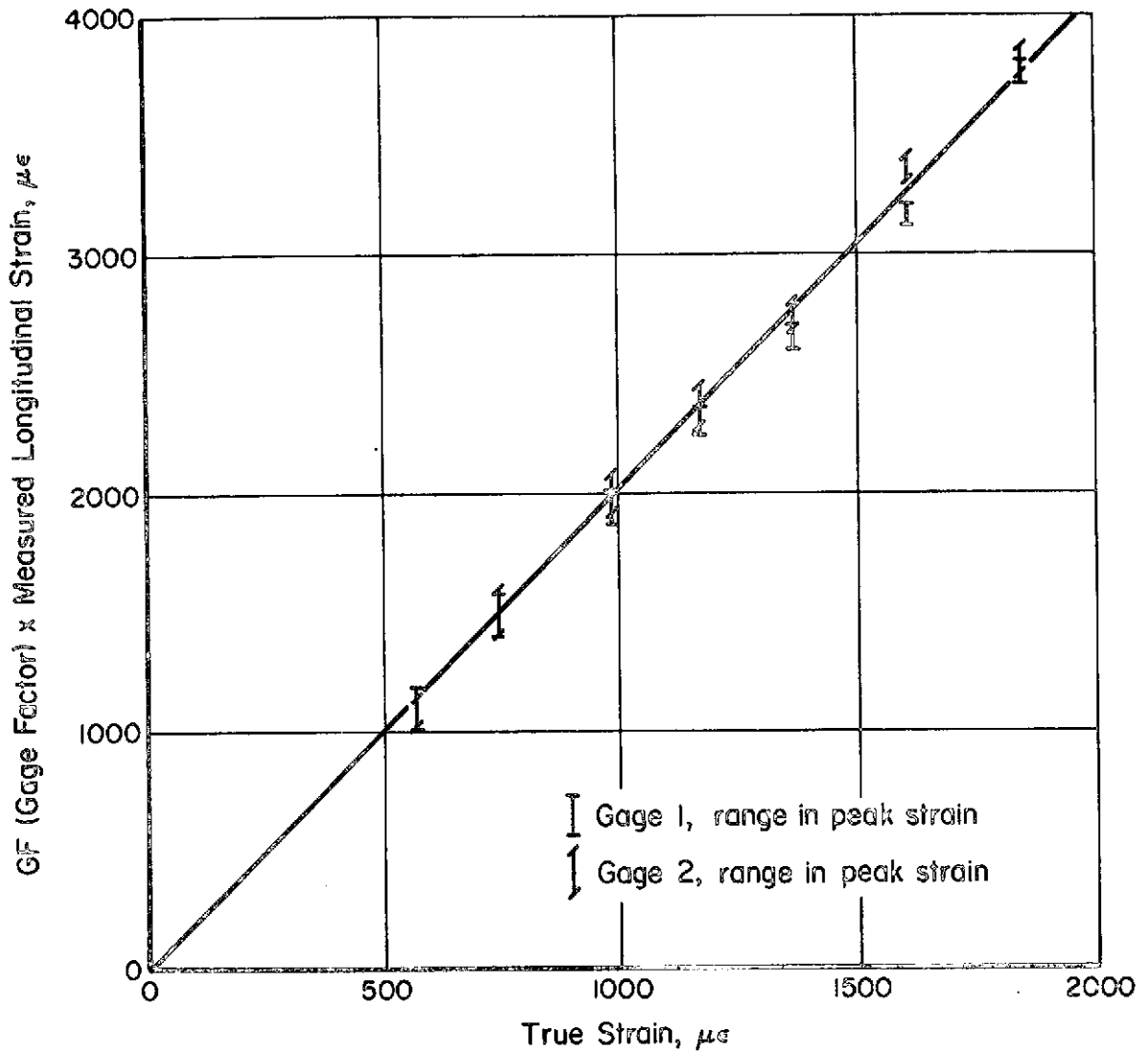


FIGURE 27. HOPKINSON BAR, (GF) x MEASURED STRAIN VERSUS TRUE STRAIN, ROOM TEMPERATURE

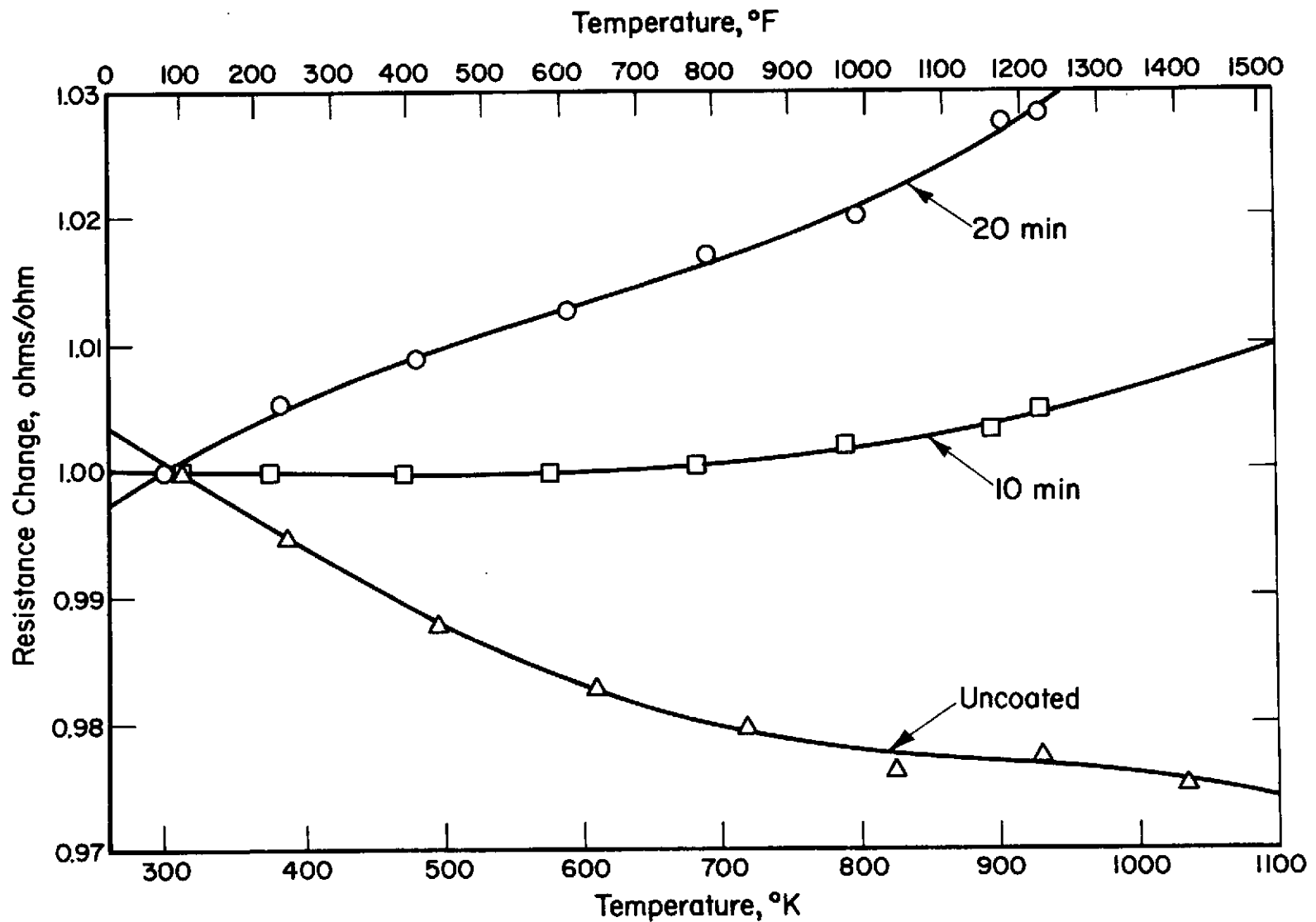


FIGURE 28. UNIT RESISTIVITY CHANGES VERSUS TEMPERATURE, COATED AND UNCOATED BCL-3 WIRE

APPENDIX A

RESISTANCE TO GROUND MEASUREMENTS

TABLE A-1. RESISTANCE TO GROUND MEASUREMENTS

Spec. No.	Max. Run Temp.		Step No.	Cycle No.	Gage Temp.		Gage No.	Resistance to
	°K	°F			°K	°F		Ground, ohms
								VTVM Megger
H-21R	936	1225	2	1	936	1225	1	>20M
							2	>20M
							3	>20M
							4	19M
H-26R2	1366	2000	2	1	RT	RT	1	∞
							2	∞
							3	∞
							4	∞
	1366	2000	2	1	1381	2027	1	2.3M
							2	1.7M
							3	1.7M
							4	1.7M
	1366	2000	3	2	1366	1999	1	100K
							2	60K
							3	80K
							4	60K
H-28	1311	1900	6	1	RT	RT	1	∞
							2	∞
							3	∞
							4	∞
	1311	1900	7	1	1316	1909	1	70K
							2	60K
							3	500K
							4	<600K
	1311	1900	6	2	1296	1874	1	331K
							2	--
							3	255K
							4	360K

Legend

- ∞ - indicates infinity
- K - indicates kilo-ohms
- M - indicates Meg-ohms

TABLE A-1. (Continued)

Spec. No.	Max. Run Temp.		Step No.	Cycle No.	Gage Temp.		Gage No.	Resistance to Ground, ohms	
	°K	°F			°K	°F		VTVM	Megger
H-29	1325	1925	2	1	1326	1928	1	140K	
							2	120K	
							3	130K	
							4	140K	
	1311	1900	3	3	1312	1902	1	90K	
							2	85K	
							3	70K	
							4	70K	
	1311	1900	4	3	1312	1902	1	300K	200K
							2	220K	80K
							3	300K	100K
							4	300K	30K
H-32	RT	RT	1	1	RT	RT	1	∞	
							2	∞	
							3	∞	
							4	∞	
	1311	1900	3	3	1319	1915	1	115K	
							2	70K	
							3	100K	
							4	60K	
	1311	1900	4	1	811	1000	1	16M	
							2	15M	
							3	16M	
							4	16M	
	1380	2025	2	1	1380	2025	1	--	
							2	2M	
							3	--	
							4	2M	
	1366	2000	6	1	1368	2002	1	--	
							2	2M	
							3	--	
							4	2M	

LIST OF REFERENCES

1. Lemcoe, M. M., "Development of High Temperature Strain Gages", NASA CR-112241, 1973.
2. Kabana, W. B., "Butt Welder for Fine Gage Wire, NASA Tech Brief 70-10136, 1970.